



Measurement of the transverse momentum distribution of Drell–Yan lepton pairs in proton–proton collisions at $\sqrt{s} = 13$ TeV with the ATLAS detector

ATLAS Collaboration*

CERN, 1211 Geneva 23, Switzerland

Received: 9 December 2019 / Accepted: 4 May 2020 / Published online: 10 July 2020
 © CERN for the benefit of the ATLAS collaboration 2020

Abstract This paper describes precision measurements of the transverse momentum $p_T^{\ell\ell}$ ($\ell = e, \mu$) and of the angular variable ϕ_η^* distributions of Drell–Yan lepton pairs in a mass range of 66–116 GeV. The analysis uses data from 36.1 fb^{-1} of proton–proton collisions at a centre-of-mass energy of $\sqrt{s} = 13$ TeV collected by the ATLAS experiment at the LHC in 2015 and 2016. Measurements in electron-pair and muon-pair final states are performed in the same fiducial volumes, corrected for detector effects, and combined. Compared to previous measurements in proton–proton collisions at $\sqrt{s} = 7$ and 8 TeV, these new measurements probe perturbative QCD at a higher centre-of-mass energy with a different composition of initial states. They reach a precision of 0.2% for the normalized spectra at low values of $p_T^{\ell\ell}$. The data are compared with different QCD predictions, where it is found that predictions based on resummation approaches can describe the full spectrum within uncertainties.

1 Introduction

In high-energy hadron–hadron collisions, the vector bosons W and Z/γ^* are produced via quark–antiquark annihilation [1], and can be observed with very small backgrounds by using their leptonic decay modes. The vector bosons have non-zero momentum transverse to the beam direction due to the emission of quarks and gluons from the initial-state partons as well as to the intrinsic transverse momentum of the initial-state partons in the proton. Phenomenologically, the spectrum at low transverse momentum of the Z boson, $p_T^{\ell\ell}$, reconstructed through the decay into a pair of charged leptons, can be described using soft-gluon resummation [2–7] and non-perturbative models to account for the intrinsic transverse momentum of partons. At high $p_T^{\ell\ell}$ the spectrum can be calculated by fixed-order perturbative quantum chromodynamics (QCD) predictions [8–12], and next-to-leading-order electroweak (NLO EW) effects are expected to be important [13–15]. Parton-shower models [16–18] or resummation may be matched to fixed-order calculations to describe the full spectrum.

A precise measurement of the $p_T^{\ell\ell}$ spectrum provides an important input to the background prediction in searches for beyond the Standard Model (SM) processes, e.g. in the monojet signature [19], as well as to SM precision measurements. In particular, the measurement of the mass of the W boson [20] relies on the measurement of the $p_T^{\ell\ell}$ distribution to constrain the transverse momentum spectrum of the W boson, p_T^W , since a direct measurement of the transverse momentum distribution of W bosons is experimentally challenging [21]. The $p_T^{\ell\ell}$ spectrum was measured previously in proton–proton (pp) collisions at the Large Hadron Collider (LHC) by the ATLAS Collaboration at centre-of-mass energies of $\sqrt{s} = 7$ TeV and 8 TeV [22, 23], including several mass regions near and away from the Z -boson resonance. Related measurements were also made by the CMS [24–28] and the LHCb [29–31] collaborations at the LHC and by the

Contents

1 Introduction	1
2 The ATLAS detector	2
3 Analysis methodology	2
3.1 Description of the measurements	2
3.2 Simulated event samples	3
3.3 Event selection	3
3.4 Estimation of backgrounds	3
3.5 Correction for detector effects	4
4 Statistical and systematic uncertainties	5
5 Results and discussion	7
5.1 Combination	7
5.2 Comparison with predictions	8
6 Conclusion	12
References	13

* e-mail: atlas.publications@cern.ch

CDF [32] and D0 [33,34] collaborations in $p\bar{p}$ collisions at the TeVatron.

Compared to measurements at lower \sqrt{s} , Z -boson production at 13 TeV is characterized by a smaller parton momentum fraction of the colliding protons, leading to a different flavour composition and a larger phase space for hard QCD radiation. A precise measurement will test this energy dependence and play an important role in future studies of the W -boson mass using the 13 TeV data.

The granularity of the measurement in the low- $p_T^{\ell\ell}$ domain is limited by the lepton momentum resolution. To overcome this limitation, the ϕ_η^* observable was introduced [35] as an alternative probe of $p_T^{\ell\ell}$. It is defined as

$$\phi_\eta^* = \tan\left(\frac{\pi - \Delta\phi}{2}\right) \times \sin(\theta_\eta^*),$$

where $\Delta\phi$ is the azimuthal angle in radians between the two leptons. The angle θ_η^* is a measure of the scattering angle of the leptons relative to the proton beam direction in the rest frame of the dilepton system and is defined by $\cos(\theta_\eta^*) = \tanh[(\eta^- - \eta^+)/2]$, where η^- and η^+ are the pseudorapidities¹ of the negatively and positively charged lepton, respectively. Therefore, ϕ_η^* depends exclusively on the directions of the two leptons, which are measured more precisely than their momenta.

In this paper, measurements of the $p_T^{\ell\ell}$ and the ϕ_η^* spectra are presented using pp collision data at $\sqrt{s} = 13$ TeV collected in 2015 and 2016 with the ATLAS detector, corresponding to an integrated luminosity of 36.1 fb^{-1} . Both the dielectron and dimuon final states $Z/\gamma^* \rightarrow \ell\ell$ ($\ell = e$ or μ) are analysed in a dilepton mass window of $m_{\ell\ell} = 66\text{--}116$ GeV. The measurement is performed in a fiducial phase space that is close to the detector acceptance for leptons in transverse momentum p_T^ℓ and pseudorapidity η_ℓ .

2 The ATLAS detector

The ATLAS experiment uses a multipurpose detector [36–38] with a cylindrical geometry and almost 4π coverage in solid angle. The collision point is surrounded by tracking detectors, collectively referred to as the inner detector (ID), followed by a superconducting solenoid providing a 2 T

axial magnetic field, a calorimeter system and a muon spectrometer. The ID provides precise measurements of charged-particle tracks in the pseudorapidity range $|\eta| < 2.5$. It consists of three subdetectors arranged in a coaxial geometry around the beam axis: a silicon pixel detector, a silicon microstrip detector and a transition radiation tracker.

The electromagnetic calorimeter covers the region $|\eta| < 3.2$ and is based on a high-granularity, lead/liquid-argon (LAr) sampling technology. The hadronic calorimeter uses a steel/scintillator-tile detector in the region $|\eta| < 1.7$ and a copper/LAr detector in the region $1.5 < |\eta| < 3.2$. The forward calorimeter (FCAL) covers the range $3.2 < |\eta| < 4.9$ and also uses LAr as the active material and copper or tungsten absorbers for the EM and hadronic sections, respectively.

The muon spectrometer (MS) consists of separate trigger and high-precision tracking chambers to measure the deflection of muons in a magnetic field generated by three large superconducting toroids arranged with an eightfold azimuthal coil symmetry around the calorimeters. The high-precision chambers cover a range of $|\eta| < 2.7$. The muon trigger system covers the range $|\eta| < 2.4$ with resistive-plate chambers in the barrel and thin-gap chambers in the endcap regions.

A two-level trigger system is used to select events in real time [39]. It consists of a hardware-based first-level trigger and a software-based high-level trigger. The latter employs algorithms similar to those used offline and is used to identify electrons and muons.

3 Analysis methodology

3.1 Description of the measurements

The Z -boson differential cross-sections are measured as a function of $p_T^{\ell\ell}$ and ϕ_η^* separately for the dielectron and dimuon decay channels. Only small background contributions are expected. The results are reported within a fiducial phase space chosen to be close to the experimental acceptance defined by the lepton transverse momenta $p_T^\ell > 27$ GeV, the absolute lepton pseudorapidity $|\eta_\ell| < 2.5$ and the dilepton invariant mass $m_{\ell\ell} = 66\text{--}116$ GeV.

The lepton kinematics can be described at different levels regarding the effects of final-state photon radiation (QED FSR). Cross-sections at *Born* level employ the lepton kinematics before QED FSR, while the *bare* level is defined by leptons after emission of QED FSR. A *dressed* lepton is defined by combining the bare four-momenta of each lepton with that of QED FSR photons radiated from the lepton within a cone of size $\Delta R = 0.1$ around the lepton. The results in this paper are reported at the dressed and Born levels.

The differential cross-sections in $p_T^{\ell\ell}$ and ϕ_η^* are measured and their normalized spectra derived. The total systematic

¹ ATLAS uses a right-handed coordinate system with its origin at the nominal interaction point (IP) in the centre of the detector and the z -axis along the beam pipe. The x -axis points from the IP to the centre of the LHC ring, and the y -axis points upwards. Cylindrical coordinates (r, ϕ) are used in the transverse plane, ϕ being the azimuthal angle around the z -axis. The pseudorapidity is defined in terms of the polar angle θ as $\eta = -\ln \tan(\theta/2)$. Angular distance is measured in units of $\Delta R = \sqrt{(\Delta\eta)^2 + (\Delta\phi)^2}$.

uncertainty of the latter is significantly reduced due to large correlations in many sources of uncertainty between the measurement bins.

3.2 Simulated event samples

Events simulated by Monte Carlo (MC) generators are used to predict the detector response to the signal process in order to correct the data for detector inefficiencies and resolution as well as to estimate most of the background from processes other than $Z/\gamma^* \rightarrow \ell\ell$ in the selected data sample.

The $Z/\gamma^* \rightarrow \ell\ell$ signal process was generated with the POWHEG-BOX V1 MC event generator [40–43] at next-to-leading order in α_s interfaced to PYTHIA 8.186 [17] for the modelling of the parton shower, hadronization, and underlying event, with parameters set according to the AZNLO tune [22]. The CT10 (NLO) set of parton distribution functions (PDF) [44] was used for the hard-scattering processes, whereas the CTEQ6L1 PDF set [45] was used for the parton shower. The effect of final-state photon radiation was simulated with Photos++ v3.52 [46,47]. The EVTGEN v1.2.0 program [48] was used to decay bottom and charm hadrons.

POWHEG+PYTHIA8 was also used to simulate the majority of the background processes considered. The $Z \rightarrow \tau\tau$ and the diboson processes WW , WZ and ZZ [49] (requiring $m_{\ell\ell} > 4$ GeV for any pair of same-flavour opposite-charge leptons) used the same tune and PDF as the signal process. The $t\bar{t}$ and single-top-quark [50,51] backgrounds to the dielectron channel were simulated with POWHEG+PYTHIA6 [52] with the P2012 tune [53] and CT10 PDF, while for the dimuon channel POWHEG+PYTHIA8 with the A14 tune [54] and the NNPDF3.0 PDF [55] was used. It was found that the prediction of the $t\bar{t}$ background is in very good agreement for both generators. The photon-induced background $\gamma\gamma \rightarrow \ell\ell$ was generated with PYTHIA8 using the NNPDF2.3 QED PDF [56].

The effect of multiple interactions in the same and neighbouring bunch crossings (pile-up) was modelled by overlaying the hard-scattering event with simulated minimum-bias events generated with PYTHIA 8.186 using the MSTW2008LO set of PDFs [57] and the A2 tune [58]. The simulated event samples were reweighted to describe the distribution of the number of pile-up interactions in the data, and further reweighted such that the distribution of the longitudinal position of the primary pp collision vertex matches that in data. The primary vertex is defined as the vertex with at least two reconstructed tracks with $p_T > 0.4$ GeV and with the highest sum of squared transverse momenta of associated tracks. The GEANT4 program was used to simulate the passage of particles through the ATLAS detector [59,60]. The simulated events are reconstructed with the same analysis procedure as the data. The reconstruction, trigger and isolation efficiencies as well as lepton momentum scale and resolution in the

MC simulation are corrected to match those determined in data [61–63].

3.3 Event selection

Candidate $Z \rightarrow ee$ events are triggered requiring at least one identified electron with $p_T > 24$ GeV in 2015 and $p_T > 26$ GeV in 2016 data [64]. In addition to the increased p_T threshold, the electron also has to satisfy isolation criteria in the 2016 data. Candidate $Z \rightarrow \mu\mu$ events were recorded with triggers that require at least one isolated muon with $p_T > 20$ GeV in 2015 and $p_T > 26$ GeV in 2016 data.

Electron candidates are reconstructed from clusters of energy in the electromagnetic calorimeter matched to ID tracks [62]. They are required to have $p_T > 27$ GeV and $|\eta| < 2.47$ (excluding the transition regions between the barrel and the endcap electromagnetic calorimeters, $1.37 < |\eta| < 1.52$). Electron candidates are required to pass the ‘medium’ identification requirement, and are also required to be isolated according to the ‘gradient’ isolation criterion [62].

Muon candidates are reconstructed by combining tracks reconstructed in the inner detector with tracks reconstructed in the MS [61]. They are required to have $p_T > 27$ GeV and $|\eta| < 2.5$ and satisfy identification criteria corresponding to the ‘medium’ working point [61]. Track quality requirements are imposed to suppress backgrounds, and the muon candidates are required to be isolated according to the ‘gradient’ isolation criterion [61], which is p_T - and η -dependent and based on the calorimeter and track information.

Electron and muon candidates are required to originate from the primary vertex. Thus, the significance of the track’s transverse impact parameter calculated relative to the beam line, $|d_0/\sigma_{d_0}|$, must be smaller than 3.0 for muons and less than 5.0 for electrons. Furthermore, the longitudinal impact parameter, z_0 (the difference between the z -coordinate of the point on the track at which d_0 is defined and the longitudinal position of the primary vertex), is required to satisfy $|z_0 \cdot \sin(\theta)| < 0.5$ mm.

Events are required to contain exactly two same-flavour leptons passing the lepton selection. The two leptons must be of opposite electric charge and their invariant mass must satisfy $66 < m_{\ell\ell} < 116$ GeV. No additional veto on the presence of leptons of different flavour is applied. Table 1 shows the number of events satisfying the above selection criteria in the electron channel and the muon channel. Also given are the estimated contributions from the background sources described below in Sect. 3.4.

3.4 Estimation of backgrounds

The backgrounds from all sources other than multijet processes are estimated using the MC samples detailed in Sect. 3.2. The number and properties of the background

Table 1 Selected signal candidate events in data for both decay channels as well as the expected background contributions including their total uncertainties

	$Z/\gamma^* \rightarrow ee$	$Z/\gamma^* \rightarrow \mu\mu$
Two reconstructed leptons within fiducial volume	13 649 239	18 162 641
Electroweak background ($Z \rightarrow \tau\tau, WW, WZ, ZZ$)	$40\,000 \pm 2000$	$50\,000 \pm 2500$
Photon-induced background	2900 ± 140	4100 ± 200
Top-quark background	$38\,000 \pm 1900$	$45\,400 \pm 2200$
Multijet background	8500 ± 4900	1000 ± 200
Total background	$89\,400 \pm 5600$	$100\,500 \pm 3300$

events where one or two reconstructed lepton candidates originate from hadrons or hadron decay products, i.e. multijet processes as well as W +jets, are estimated using the data-driven techniques described in the following for both decay channels.

In the electron channel, a multijet-dominated sample is selected from data with two same-charge electron candidates satisfying the ‘loose’ identification criteria, but not the ‘medium’ criteria [62], i.e. they are more likely to be caused by misidentified jets. This sample is collected by a dielectron trigger without isolation criteria [64]. In the muon channel, a multijet sample is obtained by selecting two same-charge muons. The residual contamination from processes with prompt leptons is estimated using the simulation and subtracted.

The normalization of the multijet template in the electron channel is determined in a fit to the distribution of the electron isolation using all event-selection criteria except those for the isolation variables. Systematic uncertainties in the normalization are estimated by varying the fit range on the electron isolation distribution.

In the muon channel, the normalization is obtained using the ratio of number of opposite-charge dimuon events to the number of same-charge dimuon events where the muons fail to satisfy the isolation criterion. Assuming no correlation between the isolation of muons in multijet events and their charge, this ratio can be applied to a control sample, defined by pairs of isolated same-charge muons passing the signal-kinematic selection, to determine the multijet contamination in the signal region. The systematic uncertainty in the estimate is obtained by varying the isolation criterion for the muons.

The total fraction of selected data events originating from background processes is about 0.6% in both the electron and muon channels. The background is dominated by contributions from diboson and $t\bar{t}$ processes. An overview of the estimated number of background events is given in Table 1, together with the corresponding total uncertainties.

Figure 1 shows the dilepton invariant mass and the lepton pseudorapidity distribution, for the electron and muon channels separately. The predictions are in fair agreement with the data. The impact of the residual differences between

these distributions on the $p_T^{\ell\ell}$ and ϕ_η^* measurements is estimated by reweighting the MC signal sample to data and then repeating the measurement procedure. Figure 2 compares the measured $p_T^{\ell\ell}$ and ϕ_η^* distributions for both channels with the signal MC predictions. The disagreement between the data and the predictions for large values of $p_T^{\ell\ell}$ and ϕ_η^* is expected because POWHEG+PYTHIA8 is effectively a computation at leading-order in α_S in this region.

3.5 Correction for detector effects

The production cross-section times the branching ratio for decays into a single lepton flavour are measured in fiducial volumes as defined in Sect. 3.1. Integrated fiducial cross-sections in the electron and muon channels are computed following the equation

$$\sigma_{Z/\gamma^* \rightarrow \ell\ell}^{\text{fid}} = \frac{N_{\text{Data}} - N_{\text{Bkg}}}{C_Z \cdot L},$$

where N_{Data} is the number of observed signal candidates and N_{Bkg} is the number of background events expected in the selected sample. The integrated luminosity of the sample is $L = 36.1 \text{ fb}^{-1}$. A correction for the event detection efficiency is applied with the factor C_Z , which is obtained from the simulation of signal events as the ratio of the sum of event weights after simulation, reconstruction and selection, to the sum of MC event weights for events satisfying the fiducial requirements. The factor C_Z is affected by experimental uncertainties, described in Sect. 4, while theory and modelling uncertainties are negligible.

The differential distributions within the fiducial volume are corrected for detector effects and bin-to-bin migrations using an iterative Bayesian unfolding method [65–67]. First, the data are corrected for events that pass the detector-level selection but not the particle-level selection. Then, the iterative Bayesian unfolding technique is used as a regularized way to correct for the detector resolution in events that pass both the detector-level and particle-level selections. The method is applied with four iterations implemented in the RooUnfold framework [67]. After the application of the response matrix, a final correction is applied to account for events that pass the particle-level but not detector-level selec-

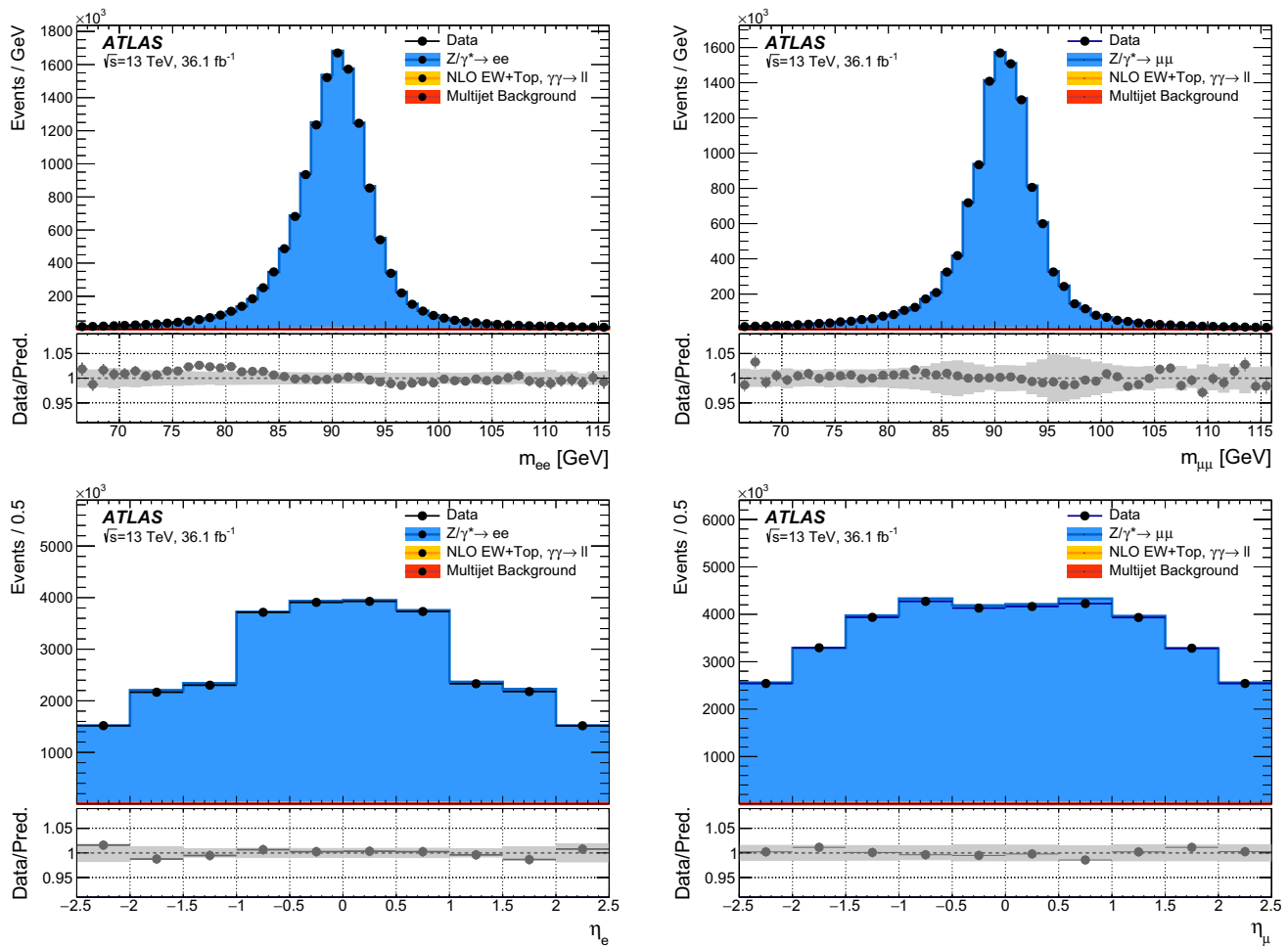


Fig. 1 The distribution of events passing the selection requirements in the electron channel (left) and muon channel (right) as a function of dilepton invariant mass $m_{\ell\ell}$ (upper row) and lepton pseudorapidity η (lower row), the latter with one entry for each lepton per event. The MC signal sample is simulated using POWHEG+PYTHIA8. The statistical

uncertainties of the data points are generally smaller than the size of the markers. The predictions of the MC signal sample together with the MC background samples are normalized to the integral of the data and the total experimental uncertainty of the predicted values is shown as a grey band in the ratio of the prediction to data

tion, resulting in unfolded distributions on Born and dressed particle level. The response matrices, which connect the distributions at reconstruction and particle level, as well as the correction factors are derived using the POWHEG+PYTHIA signal MC sample.

4 Statistical and systematic uncertainties

Uncertainties in the measurement are assessed for each aspect of the analysis, including the background subtraction, event detection efficiencies, response matrix, and unfolding method. The entire analysis procedure is repeated for each systematic uncertainty. Each source of uncertainty is varied to estimate the effect on the final result.

The effect on the measurement from the size of the data and MC samples is estimated by generating pseudo-experiment variations of the respective samples. The resulting statistical uncertainties are considered as uncorrelated between bins and between channels.

Uncertainties in the scale and resolution of the electron energy scale [63] and muon momentum scale [61] are among the dominant uncertainties in the $p_T^{\ell\ell}$ measurement. Furthermore, uncertainties related to lepton reconstruction and selection efficiencies are considered [39, 61, 62, 64], covering the lepton identification, reconstruction, isolation, triggering and track-to-vertex matching processes. The lepton related systematic uncertainties have only a small statistical component. There is an additional uncertainty in the muon channel to cover charge-dependent biases in the muon momentum measurement. The majority of these experimental uncertain-

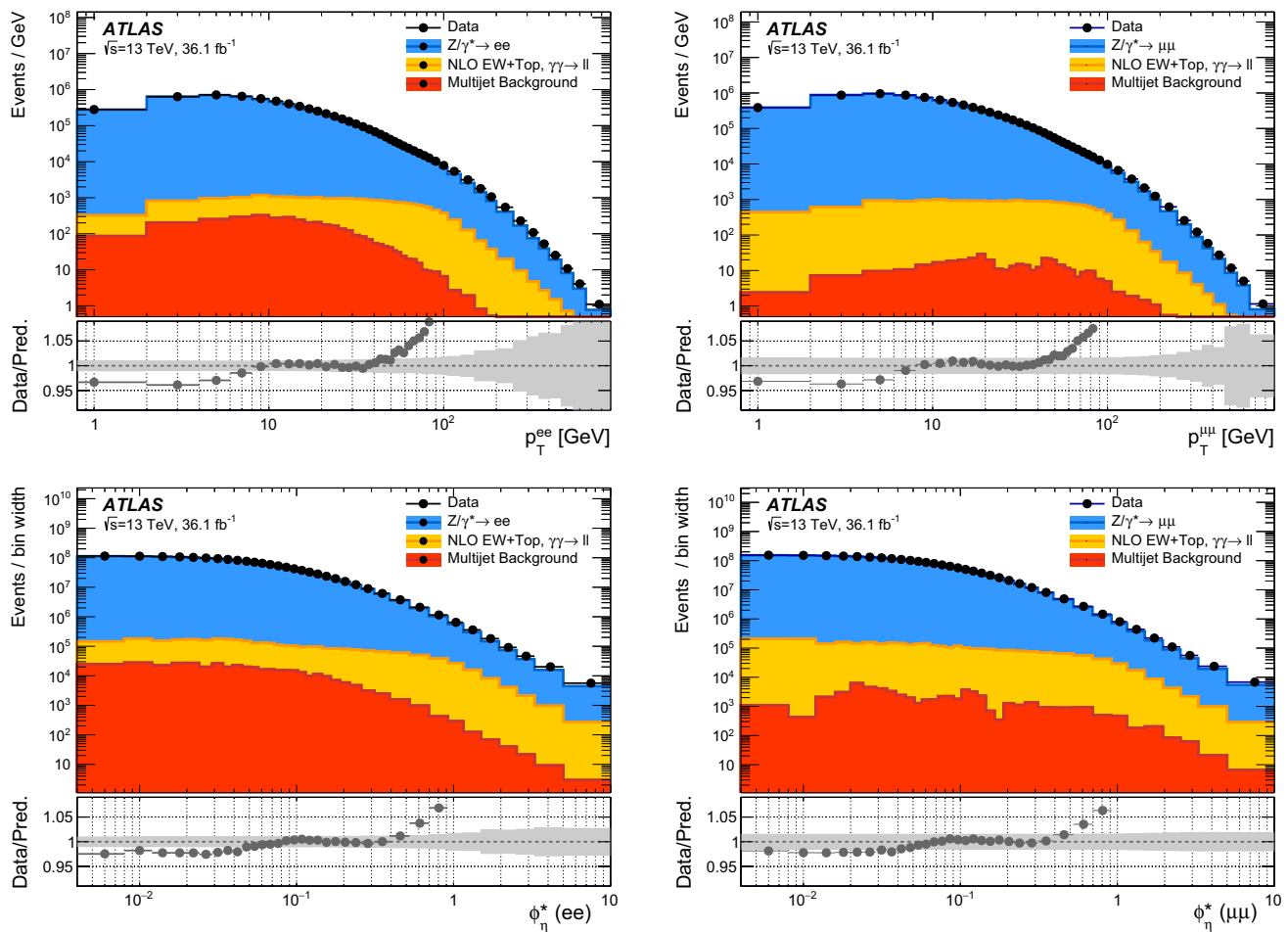


Fig. 2 The distribution of events passing the selection requirements in the electron channel (left) and muon channel (right) as a function of dilepton transverse momentum (upper row) and ϕ_{η}^* (lower row). The MC signal sample is simulated using POWHEG+PYTHIA8. The statistical

uncertainties of the data points are generally smaller than the size of the markers. The predictions are normalized to the integral of the data and the total experimental uncertainty of the predicted values is shown as a grey band in the ratio of the prediction to data

ties are considered correlated between bins of $p_T^{\ell\ell}$ and ϕ_{η}^* . An exception are the components of the reconstruction and identification efficiencies which have a significant statistical component due to the limited number of events in the data samples used to derive the efficiency corrections. Uncertainties related to electron or muon reconstruction and identification are always assumed to be uncorrelated with each other. They dominate the uncertainty in the fiducial cross-section measurement.

The uncertainties in the MC background estimates are obtained by independently varying the theory cross-sections used to normalize the corresponding samples and observing the effect on the measured $p_T^{\ell\ell}$ and ϕ_{η}^* cross-sections. These background uncertainties are considered correlated between bins of $p_T^{\ell\ell}$ and ϕ_{η}^* and between the electron and muon channels. As described in Sect. 3.4, the uncertainty in the multijet background in the electron channel is obtained by changing the input range of the template used to estimate the multijet

background. For the muon channel, the measurement is performed again with a modified isolation variable used in the normalization procedure. The differences between the nominal and modified measurements are used as uncertainty. The estimated multijet backgrounds are assumed to be uncorrelated between the channels.

An uncertainty is derived to cover the mis-modelling of the simulated pile-up activity following the measurement of the cross-section of inelastic pp collisions [68]. Also, the uncertainty in modelling the distribution of the longitudinal position of the primary vertex is considered. These uncertainties are treated as correlated between the electron channel and muon channel.

The uncertainty from the unfolding method is determined by repeating the procedure with a different simulation where the nominal particle-level spectrum is reweighted so that the simulated detector-level spectrum is in good agreement with the data. The modified detector-level distribution is unfolded

Table 2 Overview of the detector efficiency correction factors, C_Z , for the electron and muon channels and their systematic uncertainty contributions

	Electron channel		Muon channel	
	Born	Dressed	Born	Dressed
C_Z	0.509 ± 0.005	0.522 ± 0.005	0.685 ± 0.011	0.702 ± 0.011
Trigger efficiencies		± 0.0004		± 0.0004
Identification & reconstruction efficiencies		± 0.0049		± 0.0102
Isolation efficiencies		± 0.0009		± 0.0029
Energy/momentum scale and resolution		± 0.0014		± 0.0010
Pile-up		± 0.0011		± 0.0019
Model uncertainties		± 0.0001		± 0.0001

with the nominal response matrix and the difference between the result and the reweighted particle-level spectrum is taken as the bias of the unfolding method due to the choice of prior. The closure of the unfolding procedure is also tested using the generator-level distributions of the SHERPA MC sample described in Sect. 5.2, where consistent results within the assigned unfolding uncertainties are found.

The uncertainty from the choice of PDF used in the signal MC generator is evaluated by reweighting the signal MC simulation to the 52 error sets of the CT10 PDF set and computing the resulting variation of the results [44, 69]. The differences found in this way are negligible, similar to scale-choice uncertainties. The uncertainty in the combined 2015–2016 integrated luminosity is 2.1% [70], obtained using the LUCID-2 detector [71] for the primary luminosity measurements. This uncertainty only applies to the absolute cross-section measurements.

The experimental uncertainties of C_Z for the integrated fiducial cross-section measurements in the electron and muon channels are summarized in Table 2. The electron identification efficiency and muon reconstruction efficiency contribute a large fraction of the total systematic uncertainty for both the integrated and absolute differential measurements. These uncertainties are greatly reduced for the normalized measurement of differential distributions. A summary of the uncertainties in the normalized differential cross-section measurements is provided in Fig. 3 as a function of $p_T^{\ell\ell}$ and ϕ_η^* for both decay channels. The statistical uncertainties for the electron and muon channel measurements are a combination of the uncertainties due to limited data and MC sample sizes. The systematic uncertainties are divided into categories and originate from lepton scales and resolutions, reconstruction and identification efficiencies, as well as the MC signal modelling in the unfolding procedure and further smaller uncertainty sources such as the subtraction of background contributions. These smaller contributions are summarized as “other” uncertainties.

5 Results and discussion

5.1 Combination

The fiducial cross-sections measured in the $Z/\gamma^* \rightarrow ee$ and $Z/\gamma^* \rightarrow \mu\mu$ channels are presented in Table 3 including statistical, systematic and luminosity uncertainties. When correcting for the more restrictive fiducial volume definition, these results are in good agreement with the previous ATLAS measurements at 13 TeV [72]. The electron- and muon-channel cross-sections are combined using χ^2 minimization, following the best linear unbiased estimator prescription (BLUE) [73–75]. The combination is performed on Born level, resulting in a combined cross-section of $\sigma_{\text{fid}}(pp \rightarrow Z/\gamma^* \rightarrow \ell\ell) = 736.2 \pm 0.2(\text{stat}) \pm 6.4(\text{sys}) \pm 14.7(\text{lumi})$ pb (Table 3).² There is a reduction of the uncertainty compared to individual electron- and muon-channel measurements since the dominant detector-related systematic uncertainty sources are largely uncorrelated. The uncertainties due to pile-up, physics modelling and luminosity are treated as correlated between the two decay channels.

The normalized differential cross-sections $1/\sigma_{\text{fid}} \times d\sigma_{\text{fid}}/dp_T^{\ell\ell}$ and $1/\sigma_{\text{fid}} \times d\sigma_{\text{fid}}/d\phi_\eta^*$ measured in the two decay channels as well as their combination are illustrated in Fig. 4. When building the χ^2 for combination procedure, the measurement uncertainties are separated into those from bin-to-bin uncorrelated sources and those from bin-to-bin correlated sources, the latter largely reduced due to the normalization by the fiducial cross-section. The normalized differential measurements are combined at Born level following the BLUE prescription. The resulting $\chi^2/N_{\text{dof}} = 47/44$ for the combination for $p_T^{\ell\ell}$ and the $\chi^2/N_{\text{dof}} = 32/36$ for ϕ_η^* indicate good agreement between the two chan-

² The results on dressed level are about 2.4% lower compared to the Born level definition

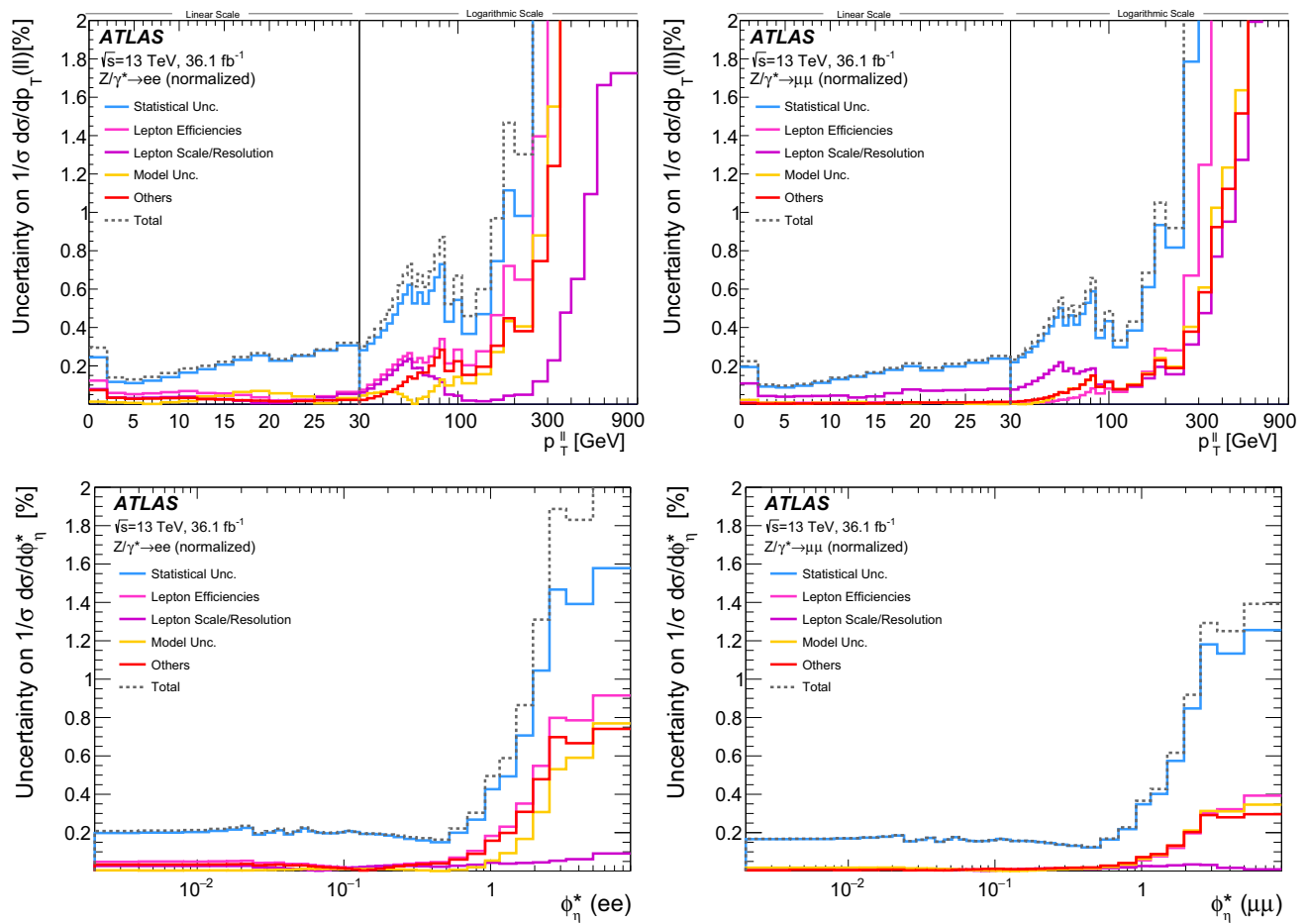


Fig. 3 The systematic uncertainties for the electron channel measurement (left) and muon channel measurement (right) for the normalized $p_T^{\ell\ell}$ (upper row) and normalized ϕ_η^* (lower row). The statistical uncertainties are a combination of the uncertainties due to limited data and

MC sample sizes. The $p_T^{\ell\ell}$ distribution is split into linear and logarithmic scales at 30 GeV. Some uncertainties are larger than 2% for $p_T^{\ell\ell} > 200$ GeV and hence cannot be displayed. The corresponding uncertainties are also summarized in Table 4

Table 3 Measured integrated cross-section in the fiducial volume in the electron and muon decay channels at Born level and their combination as well as the theory prediction at NNLO in α_S using the CT14 PDF set

Channel	Measured cross-section $\times \mathcal{B}(Z/\gamma^* \rightarrow \ell\ell)$ (value \pm stat. \pm syst. \pm lumi.)	Predicted cross-section $\times \mathcal{B}(Z/\gamma^* \rightarrow \ell\ell)$ (value \pm PDF \pm α_S \pm scale \pm intrinsic)
$Z/\gamma^* \rightarrow ee$	$738.3 \pm 0.2 \pm 7.7 \pm 15.5$ pb	
$Z/\gamma^* \rightarrow \mu\mu$	$731.7 \pm 0.2 \pm 11.3 \pm 15.3$ pb	
$Z/\gamma^* \rightarrow \ell\ell$	$736.2 \pm 0.2 \pm 6.4 \pm 15.5$ pb	$703_{-24}^{+19} {}_{-8}^{+6} {}_{-6}^{+4} {}_{-5}^{+5}$ pb [72]

nels.³ The combined precision is between 0.1% and 0.5% for $p_T^{\ell\ell} < 100$ GeV, rising to 10% towards the high end of the spectrum, where the overall precision is limited by the data and MC sample size. The combined results for both distributions are presented in Table 4 including statistical and bin-to-bin uncorrelated and correlated systematic uncertainties. The measurement results are reported at Born level and factors k_{dr} , the binwise ratio of dressed and

born level results, are given to transfer to the dressed particle level.

5.2 Comparison with predictions

The integrated fiducial cross-section is compared with a fixed-order theory prediction that is computed in the same way as in Ref. [76]. The speed-optimized DYTURBO [77] version of the DYNLO 1.5 [10] program with the CT14 NNLO set of PDFs [78] is used to obtain a prediction at next-to-next-to-leading order (NNLO) in α_S in the G_μ EW

³ The χ^2/N_{dof} is still good when taking into account only bins with $p_T^{\ell\ell} > 50$ GeV.

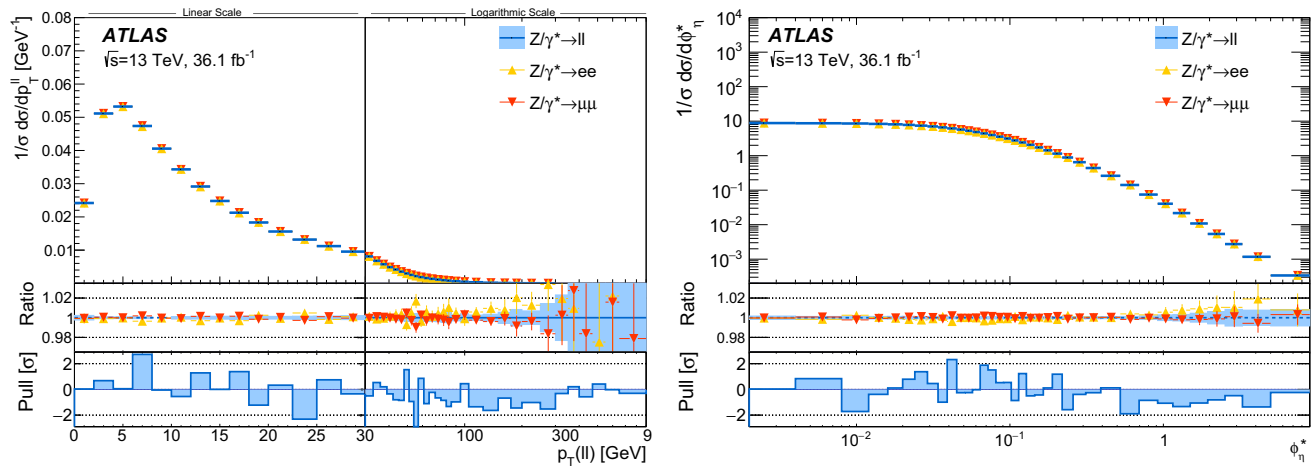


Fig. 4 The measured normalized cross section as a function of $p_T^{\ell\ell}$ (left) and ϕ_η^* (right) for the electron and muon channels and the combined result as well as their ratio together with the total uncertainties, shown as a blue band. The pull distribution between the electron and

muon channels, defined as the difference between the two channels divided by the combined uncorrelated uncertainty, is also shown. The $p_T^{\ell\ell}$ distribution is split into linear and logarithmic scales at 30 GeV

Table 4 The measured combined normalized differential cross-sections, divided by the bin-width, in the fiducial volume at Born level as well as a factor k_{dr} to translate from the Born particle level to the dressed particle level

Bin [GeV]	$1/\sigma_{fid} \times d\sigma/dp_T^{\ell\ell}$ [1/GeV]	Corr. uncert.	Uncorr. uncert.	k_{dr}	Bin	$1/\sigma_{fid} \times d\sigma/d\phi_\eta^*$	Corr. uncert.	Uncorr. uncert.	k_{dr}
0–2	0.024189	$\pm 0.15\%$	$\pm 0.18\%$	0.978	0–0.004	8.8053	$\pm 0.03\%$	$\pm 0.13\%$	0.992
2–4	0.051144	$\pm 0.06\%$	$\pm 0.08\%$	0.985	0.004–0.008	8.6969	$\pm 0.03\%$	$\pm 0.13\%$	0.993
4–6	0.053232	$\pm 0.05\%$	$\pm 0.08\%$	0.994	0.008–0.012	8.5624	$\pm 0.02\%$	$\pm 0.13\%$	0.993
6–8	0.047383	$\pm 0.05\%$	$\pm 0.08\%$	1.000	0.012–0.016	8.3378	$\pm 0.02\%$	$\pm 0.13\%$	0.994
8–10	0.040568	$\pm 0.04\%$	$\pm 0.09\%$	1.010	0.016–0.02	8.0881	$\pm 0.03\%$	$\pm 0.14\%$	0.994
10–12	0.034317	$\pm 0.06\%$	$\pm 0.11\%$	1.010	0.02–0.024	7.7920	$\pm 0.03\%$	$\pm 0.14\%$	0.995
12–14	0.029157	$\pm 0.07\%$	$\pm 0.12\%$	1.010	0.024–0.029	7.4174	$\pm 0.02\%$	$\pm 0.12\%$	0.995
14–16	0.024804	$\pm 0.06\%$	$\pm 0.14\%$	1.010	0.029–0.034	7.0360	$\pm 0.02\%$	$\pm 0.13\%$	0.996
16–18	0.021268	$\pm 0.05\%$	$\pm 0.15\%$	1.010	0.034–0.039	6.5989	$\pm 0.02\%$	$\pm 0.13\%$	0.998
18–20	0.018325	$\pm 0.04\%$	$\pm 0.16\%$	1.010	0.039–0.045	6.1608	$\pm 0.02\%$	$\pm 0.12\%$	0.998
20–22.5	0.015605	$\pm 0.03\%$	$\pm 0.14\%$	1.010	0.045–0.051	5.7085	$\pm 0.01\%$	$\pm 0.13\%$	0.999
22.5–25	0.013180	$\pm 0.03\%$	$\pm 0.15\%$	1.000	0.051–0.057	5.2791	$\pm 0.02\%$	$\pm 0.14\%$	1.000
25–27.5	0.011207	$\pm 0.04\%$	$\pm 0.17\%$	1.000	0.057–0.064	4.8488	$\pm 0.02\%$	$\pm 0.13\%$	1.000
27.5–30	0.0095568	$\pm 0.05\%$	$\pm 0.19\%$	0.999	0.064–0.072	4.4139	$\pm 0.01\%$	$\pm 0.12\%$	1.000
30–33	0.0081029	$\pm 0.06\%$	$\pm 0.17\%$	0.998	0.072–0.081	3.9705	$\pm 0.01\%$	$\pm 0.12\%$	1.000
33–36	0.0067881	$\pm 0.08\%$	$\pm 0.19\%$	0.996	0.081–0.091	3.5515	$\pm 0.01\%$	$\pm 0.12\%$	1.000
36–39	0.0057563	$\pm 0.09\%$	$\pm 0.21\%$	0.994	0.091–0.102	3.1421	$\pm 0.02\%$	$\pm 0.13\%$	1.000
39–42	0.0048769	$\pm 0.12\%$	$\pm 0.23\%$	0.993	0.102–0.114	2.7659	$\pm 0.01\%$	$\pm 0.13\%$	1.000
42–45	0.0041688	$\pm 0.12\%$	$\pm 0.25\%$	0.992	0.114–0.128	2.4125	$\pm 0.01\%$	$\pm 0.13\%$	1.000
45–48	0.0035213	$\pm 0.14\%$	$\pm 0.28\%$	0.993	0.128–0.145	2.0648	$\pm 0.01\%$	$\pm 0.12\%$	1.000
48–51	0.0029751	$\pm 0.17\%$	$\pm 0.31\%$	0.991	0.145–0.165	1.7299	$\pm 0.02\%$	$\pm 0.13\%$	1.000
51–54	0.0025433	$\pm 0.18\%$	$\pm 0.35\%$	0.992	0.165–0.189	1.4282	$\pm 0.02\%$	$\pm 0.13\%$	1.000
54–57	0.0021832	$\pm 0.20\%$	$\pm 0.38\%$	0.994	0.189–0.219	1.1469	$\pm 0.02\%$	$\pm 0.12\%$	1.000
57–61	0.0018779	$\pm 0.15\%$	$\pm 0.31\%$	0.994	0.219–0.258	0.8848	$\pm 0.02\%$	$\pm 0.12\%$	1.000
61–65	0.0015932	$\pm 0.17\%$	$\pm 0.35\%$	0.994	0.258–0.312	0.6470	$\pm 0.03\%$	$\pm 0.11\%$	1.000
65–70	0.0013519	$\pm 0.16\%$	$\pm 0.32\%$	0.995	0.312–0.391	0.4387	$\pm 0.03\%$	$\pm 0.11\%$	1.000
70–75	0.0011323	$\pm 0.17\%$	$\pm 0.37\%$	0.995	0.391–0.524	0.2610	$\pm 0.03\%$	$\pm 0.10\%$	1.000

Table 4 continued

Bin [GeV]	$1/\sigma_{\text{fid}} \times d\sigma/dp_T^{\ell\ell}$ [1/GeV]	Corr. uncert.	Uncorr. uncert.	k_{dr}	Bin	$1/\sigma_{\text{fid}} \times d\sigma/d\phi_\eta^*$	Corr. uncert.	Uncorr. uncert.	k_{dr}
75–80	0.0009574	$\pm 0.20\%$	$\pm 0.43\%$	0.995	0.524–0.695	0.1414	$\pm 0.04\%$	$\pm 0.13\%$	1.000
80–85	0.0008150	$\pm 0.22\%$	$\pm 0.49\%$	0.995	0.695–0.918	0.07462	$\pm 0.07\%$	$\pm 0.17\%$	1.000
85–95	0.0006537	$\pm 0.14\%$	$\pm 0.29\%$	0.996	0.918–1.153	0.04047	$\pm 0.12\%$	$\pm 0.27\%$	1.000
95–105	0.0004849	$\pm 0.18\%$	$\pm 0.37\%$	0.995	1.153–1.496	0.02167	$\pm 0.14\%$	$\pm 0.30\%$	1.000
105–125	0.0003291	$\pm 0.12\%$	$\pm 0.25\%$	0.996	1.496–1.947	0.01084	$\pm 0.18\%$	$\pm 0.42\%$	1.000
125–150	0.0001861	$\pm 0.16\%$	$\pm 0.32\%$	0.994	1.947–2.522	0.005386	$\pm 0.23\%$	$\pm 0.59\%$	1.000
150–175	0.0001050	$\pm 0.24\%$	$\pm 0.51\%$	0.993	2.522–3.277	0.002738	$\pm 0.31\%$	$\pm 0.79\%$	1.000
175–200	$6.1279 \cdot 10^{-5}$	$\pm 0.30\%$	$\pm 0.78\%$	0.992	3.277–5.000	0.0011730	$\pm 0.29\%$	$\pm 0.72\%$	1.000
200–250	$3.0584 \cdot 10^{-5}$	$\pm 0.22\%$	$\pm 0.66\%$	0.995	5.000–10.00	0.0003372	$\pm 0.30\%$	$\pm 0.78\%$	0.997
250–300	$1.2211 \cdot 10^{-5}$	$\pm 0.34\%$	$\pm 1.4\%$	0.997					
300–350	$5.9026 \cdot 10^{-6}$	$\pm 0.56\%$	$\pm 2.3\%$	0.994					
350–400	$2.7742 \cdot 10^{-6}$	$\pm 0.90\%$	$\pm 3.8\%$	0.991					
400–470	$1.2513 \cdot 10^{-6}$	$\pm 0.82\%$	$\pm 4.9\%$	0.991					
470–550	$5.5219 \cdot 10^{-7}$	$\pm 1.2\%$	$\pm 7.9\%$	0.994					
550–650	$2.0165 \cdot 10^{-7}$	$\pm 1.5\%$	$\pm 13\%$	0.995					
650–900	$5.1153 \cdot 10^{-8}$	$\pm 1.8\%$	$\pm 16\%$	0.990					
900–2500	$1.5735 \cdot 10^{-9}$	$\pm 6.3\%$	$\pm 60\%$	0.964					

scheme [79]. The FEWZ 3.1 [9] program is used to compute next-to-leading-order (NLO) electroweak corrections and to cross-check the DNNLO calculation. The prediction is shown in Table 3 together with its uncertainties estimated as follows. The dominant uncertainty is from limited knowledge of the proton PDFs and is estimated using the eigenvectors of the respective CT14 PDF set, rescaled from 90% to 68% confidence level. The uncertainties due to the strong coupling constant are estimated by varying α_S by ± 0.001 . Missing higher-order QCD corrections are estimated by variations of the renormalization (μ_R) and factorization (μ_F) scales by factors of two with an additional constraint of $0.5 \leq \mu_R/\mu_F \leq 2$ around the nominal value of $m_{\ell\ell}$. The deviation from the FEWZ calculation is taken as an intrinsic uncertainty in the NNLO QCD calculation. A more detailed discussion of the agreement with theory predictions using different PDF sets is given in Ref. [72].

The differential measurements are compared with a variety of predictions of the $p_T^{\ell\ell}$ and ϕ_η^* spectra that are based on different theoretical approaches to take into account both the soft and hard emissions from the initial state (ISR). Unless stated otherwise, the predictions do not consider NLO EW effects. The comparisons between the combined result corrected to QED Born level and the various predictions are shown in Figs. 5 and 6. Systematic uncertainties in the theoretical predictions are evaluated for this comparison where feasible.

The first prediction is obtained from PYTHIA8 with matrix elements at LO in α_S supplemented with a parton shower with

the AZ set of tuned parameters [22]. The AZ tune optimized the intrinsic k_T and parton shower ISR parameters to optimally describe the ATLAS 7 TeV $p_T^{\ell\ell}$ and ϕ_η^* data [22, 80]. It was later used in the measurement of the W -boson mass using 7 TeV data [20], which requires a high-precision description of the W -boson transverse momentum spectrum at low p_T .

The second prediction is based on POWHEG+PYTHIA8 using NLO matrix elements with the PYTHIA8 parton shower parameters set according to the AZNLO tune [22] derived using the same data as the PYTHIA8 AZ tune. The predictions using the AZ and AZNLO tunes describe the 13 TeV data to within 2–4% in the region of low $p_T^{\ell\ell} < 40$ GeV and $\phi_\eta^* < 0.5$, and in this region the prediction using the PYTHIA8 AZ tune is the one that agrees best with the data. This shows that predictions based on tunes to 7 TeV collision data can also provide a good description at significantly higher centre-of-mass energies for low $p_T^{\ell\ell}$. At high $p_T^{\ell\ell}$ these predictions are well below the data due to missing higher-order matrix elements, similar to the situation observed at lower \sqrt{s} .

The third prediction is simulated with the SHERPA v2.2.1 [18] generator. In this set-up, NLO-accurate matrix elements for up to two partons, and LO-accurate matrix elements for up to four partons are calculated with the Comix [81] and OpenLoops [82, 83] libraries. The default SHERPA parton shower [84] based on Catani–Seymour dipole factorisation and the cluster hadronization model [85] is used with the dedicated set of tuned parameters developed by the authors for the NNPDF3.0nnlo PDF set [55]. The NLO matrix elements of a given parton multiplicity are matched to the parton

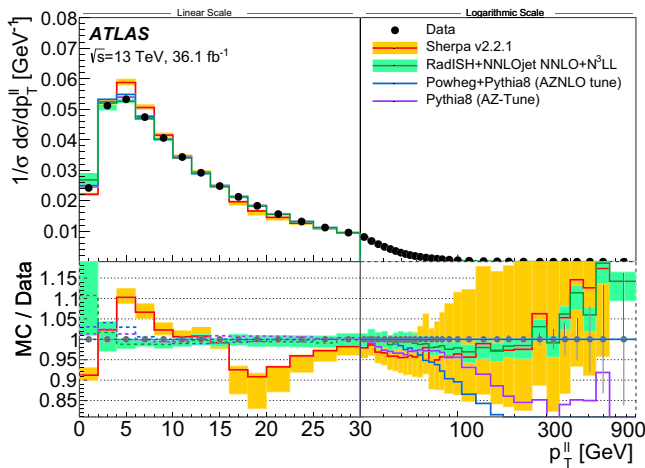
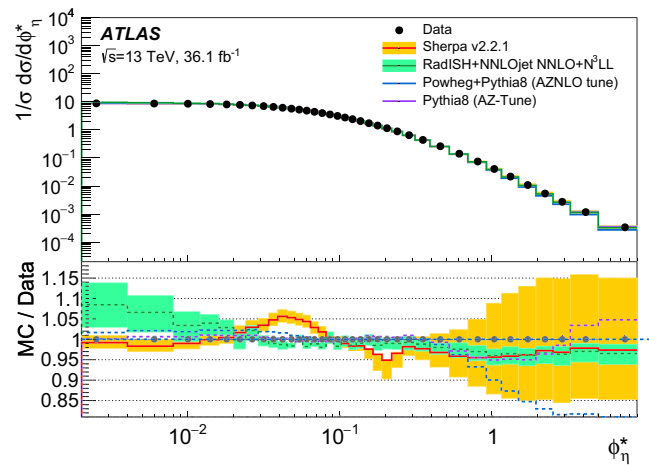


Fig. 5 Comparison of the normalized $p_T^{\ell\ell}$ (left) and ϕ_η^* (right) distributions predicted by different computations: PYTHIA8 with the AZ tune, POWHEG+PYTHIA8 with the AZNLO tune, SHERPA v2.2.1 and RADISH



with the Born level combined measurement. The uncertainties of the measurement are shown as vertical bars and uncertainties of the SHERPA and RADISH predictions are indicated by the coloured bands

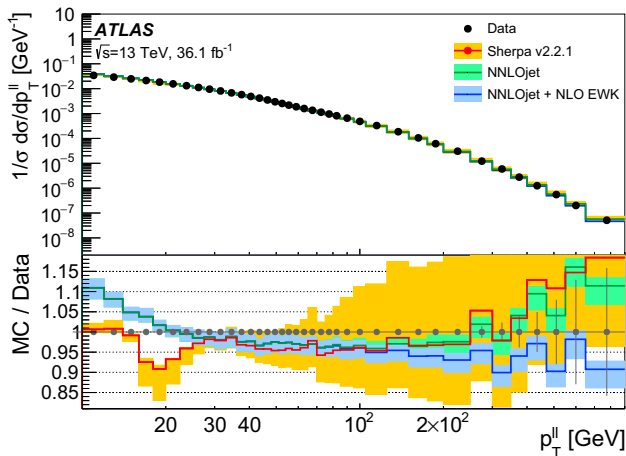


Fig. 6 Comparison of the normalized $p_T^{\ell\ell}$ distribution in the range $p_T^{\ell\ell} > 10$ GeV. The Born level combined measurement is compared with predictions by SHERPA v2.2.1, fixed-order NNLOJET and NNLOJET supplied with NLO electroweak corrections. The uncertainties in the measurement are shown as vertical bars and the uncertainties in the predictions are indicated by the coloured bands

shower using a colour-exact variant of the MC@NLO algorithm [86]. Different parton multiplicities are then merged into an inclusive sample using an improved CKKW matching procedure [87, 88] which is extended to NLO accuracy using the MEPS@NLO prescription [89]. The merging threshold is set to 20 GeV. Uncertainties from missing higher orders are evaluated [90] using seven variations of the QCD factorization and renormalization scales in the matrix elements by factors of 0.5 and 2, avoiding variations in opposite directions. For the computation of uncertainties in the normalized spectra the effect of a certain variation is fully correlated across the full spectrum and an envelope of all variations is taken at the end, which results in uncertainties of 3–4% at low

$p_T^{\ell\ell}$ and up to 25% at high $p_T^{\ell\ell}$. The effects of uncertainties in the PDF set are evaluated using 100 replica variations and are found to be very small, typically $< 1\%$ up to $p_T^{\ell\ell} < 100$ GeV and a few percent above. SHERPA does describe the data in the high $p_T^{\ell\ell} > 30$ GeV and $\phi_\eta^* > 0.1$ region to within about 4% up to the point where statistical uncertainties in the data exceed that level, which is better than the uncertainty estimate obtained from scale variations. On the other hand, the SHERPA prediction disagrees with the shape of the data at low $p_T^{\ell\ell} < 25$ GeV and somewhat less with the ϕ_η^* distribution. The data may be useful in improving the parton shower settings in this regime.

Finally a prediction based on the RADISH program [91, 92] is presented that combines a fixed-order NNLO prediction of Z+jet production ($O(\alpha_s^3)$) from NNLOJET [93] with resummation of $\log(m_{\ell\ell}/p_T^{\ell\ell})$ terms at next-to-next-to-next-to-leading-logarithm (N^3LL) accuracy [7]. The NNPDF3.1nnlo set of PDFs [94] is used with QCD scales set to $\mu_R = \mu_F = \sqrt{(m_{\ell\ell})^2 + (p_T^{\ell\ell})^2}$ and the resummation scale set to $Q = m_{\ell\ell}/2$. Uncertainties in this prediction are derived from variations of μ_R and μ_F in the same way as for the SHERPA prediction described above and, in addition, two variations of Q by a factor of two up and down, assuming that the effects of scale variations are fully correlated across the full spectrum. Within the uncertainties of typically 1–3% the RADISH prediction agrees with the data over the full spectrum of $p_T^{\ell\ell}$ and ϕ_η^* , apart from a small tension in the very low $p_T^{\ell\ell}$ and ϕ_η^* region where non-perturbative effects are relevant, highlighting the benefits of this state-of-the-art prediction.

Figure 6 compares the $p_T^{\ell\ell}$ measurement with predictions in the range of $p_T^{\ell\ell} > 10$ GeV. In addition to the SHERPA prediction described above, the data are compared with the

fixed-order NNLOJET prediction described above both with and without NLO EW corrections [13]. The NNLOJET prediction is only expected to describe the data at sufficiently large $p_T^{\ell\ell} \gtrsim 15$ GeV, while deviations for smaller values are expected due to large logarithms $\ln(m_{\ell\ell}/p_T^{\ell\ell})$ [93]. At the highest $p_T^{\ell\ell}$ values probed, the application of NLO EW leads to a suppression of up to 20% due to large Sudakov logarithms. The theoretical uncertainties on these corrections are not shown, but have been elsewhere estimated to be up to 5% for $p_T^{\ell\ell} \approx 1$ TeV [15]. In this region, NNLOJET without NLO EW corrections is generally above the data, and when including these corrections it tends to be lower than the data. However, the difference is not significantly larger than the uncertainties in the measurements.

6 Conclusion

Measurements of the $Z/\gamma^* \rightarrow ee$ and $Z/\gamma^* \rightarrow \mu\mu$ cross-sections, differential in the transverse momentum and ϕ_η^* , have been performed in a fiducial volume defined by $p_T^{\ell\ell} > 27$ GeV, $|\eta_\ell| < 2.5$ and $66 < m_{\ell\ell} < 116$ GeV, using 36.1 fb^{-1} of data from proton–proton collisions recorded in 2015 and 2016 at a centre-of-mass energy of 13 TeV with the ATLAS experiment at the LHC. This data-set allows coverage of a kinematic range up to the TeV-range. The cross-section results from the individual channels were combined and good agreement between the two was observed. The relative precision of the combined result is better than 0.2% for $p_T^{\ell\ell} < 30$ GeV, which provides crucial information to validate and tune MC event generators and will constrain models of vector-boson production in future measurements of the W -boson mass.

The integrated fiducial cross-section measurements are compared with fixed-order perturbative QCD predictions. Differential spectra in $p_T^{\ell\ell}$ and ϕ_η^* are compared with a selection of calculations implementing resummation and non-perturbative effects through parton showers or analytic calculations. The predictions based on the PYTHIA8 parton shower with parameters tuned to 7 TeV data are found to describe the 13 TeV data well at low $p_T^{\ell\ell}$ and ϕ_η^* . The SHERPA prediction based on merging of higher-order, high-multiplicity matrix elements gives an excellent description of the data at high $p_T^{\ell\ell}$, while the very accurate RADISH NNLO+N³LL prediction agrees with data for the full spectrum. The fixed-order NNLOJET prediction with and without NLO EW effects describes the data well for high $p_T^{\ell\ell}$.

Acknowledgements We thank CERN for the very successful operation of the LHC, as well as the support staff from our institutions without whom ATLAS could not be operated efficiently. We acknowledge the support of ANPCyT, Argentina; YerPhI, Armenia; ARC, Australia; BMWFW and FWF, Austria; ANAS, Azerbaijan; SSTC, Belarus; CNPq and FAPESP, Brazil; NSERC, NRC and CFI, Canada; CERN;

CONICYT, Chile; CAS, MOST and NSFC, China; COLCIENCIAS, Colombia; MSMT CR, MPO CR and VSC CR, Czech Republic; DNRF and DNSRC, Denmark; IN2P3-CNRS and CEA-DRF/IRFU, France; SRNSFG, Georgia; BMBF, HGF and MPG, Germany; GSRT, Greece; RGC and Hong Kong SAR, China; ISF and Benoziyo Center, Israel; INFN, Italy; MEXT and JSPS, Japan; CNRST, Morocco; NWO, The Netherlands; RCN, Norway; MNiSW and NCN, Poland; FCT, Portugal; MNE/IFA, Romania; MES of Russia and NRC KI, Russia Federation; JINR; MESTD, Serbia; MSSR, Slovakia; ARRS and MIZŠ, Slovenia; DST/NRF, South Africa; MINECO, Spain; SRC and Wallenberg Foundation, Sweden; SERI, SNSF and Cantons of Bern and Geneva, Switzerland; MOST, Taiwan; TAEK, Turkey; STFC, UK; DOE and NSF, USA. In addition, individual groups and members have received support from BCKDF, CANARIE, Compute Canada and CRC, Canada; ERC, ERDF, Horizon 2020, Marie Skłodowska-Curie Actions and COST, European Union; Investissements d'Avenir Labex, Investissements d'Avenir Idex and ANR, France; DFG and AvH Foundation, Germany; Herakleitos, Thales and Aristeia programmes co-financed by EU-ESF and the Greek NSRF, Greece; BSF-NSF and GIF, Israel; CERCA Programme Generalitat de Catalunya and PROMETEO Programme Generalitat Valenciana, Spain; Göran Gustafssons Stiftelse, Sweden; The Royal Society and Leverhulme Trust, UK. The crucial computing support from all WLCG partners is acknowledged gratefully, in particular from CERN, the ATLAS Tier-1 facilities at TRIUMF (Canada), NDGF (Denmark, Norway, Sweden), CC-IN2P3 (France), KIT/GridKA (Germany), INFN-CNAF (Italy), NL-T1 (Netherlands), PIC (Spain), ASGC (Taiwan), RAL (UK) and BNL (USA), the Tier-2 facilities worldwide and large non-WLCG resource providers. Major contributors of computing resources are listed in Ref. [95].

Data Availability Statement This manuscript has no associated data or the data will not be deposited. [Authors' comment: All ATLAS scientific output is published in journals, and preliminary results are made available in Conference Notes. All are openly available, without restriction on use by external parties beyond copyright law and the standard conditions agreed by CERN. Data associated with journal publications are also made available: tables and data from plots (e.g. cross section values, likelihood profiles, selection efficiencies, cross section limits, ...) are stored in appropriate repositories such as HEPDATA (<http://hepdata.cedar.ac.uk/>). ATLAS also strives to make additional material related to the paper available that allows a reinterpretation of the data in the context of new theoretical models. For example, an extended encapsulation of the analysis is often provided for measurements in the framework of RIVET (<http://rivet.hepforge.org/>). This information is taken from the ATLAS Data Access Policy, which is a public document that can be downloaded from <http://opendata.cern.ch/record/413> [opendata.cern.ch].]

Open Access This article is licensed under a Creative Commons Attribution 4.0 International License, which permits use, sharing, adaptation, distribution and reproduction in any medium or format, as long as you give appropriate credit to the original author(s) and the source, provide a link to the Creative Commons licence, and indicate if changes were made. The images or other third party material in this article are included in the article's Creative Commons licence, unless indicated otherwise in a credit line to the material. If material is not included in the article's Creative Commons licence and your intended use is not permitted by statutory regulation or exceeds the permitted use, you will need to obtain permission directly from the copyright holder. To view a copy of this licence, visit <http://creativecommons.org/licenses/by/4.0/>.
Funded by SCOAP³.

References

1. S.D. Drell, T.-M. Yan, Massive lepton pair production in hadron-hadron collisions at high-energies. *Phys. Rev. Lett.* **25**, 316 (1970)
2. J.C. Collins, D.E. Soper, G.F. Sterman, Transverse momentum distribution in Drell-Yan pair and W and Z boson Production. *Nucl. Phys. B* **250**, 199 (1985)
3. C. Balázs, C.-P. Yuan, Soft gluon effects on lepton pairs at hadron colliders. *Phys. Rev. D* **56**, 5558 (1997). [arXiv:hep-ph/9704258](#)
4. T. Becher, M. Neubert, Drell-Yan production at small q_T , transverse parton distributions and the collinear anomaly. *Eur. Phys. J. C* **71**, 1665 (2011). [arXiv:1007.4005](#) [hep-ph]
5. S. Catani, D. de Florian, G. Ferrera, M. Grazzini, Vector boson production at hadron colliders: transverse-momentum resummation and leptonic decay. *JHEP* **12**, 047 (2015). [arXiv:1507.06937](#) [hep-ph]
6. M.A. Ebert, F.J. Tackmann, Resummation of transverse momentum distributions in distribution space. *JHEP* **02**, 110 (2017). [arXiv:1611.08610](#) [hep-ph]
7. W. Bizon, P.F. Monni, E. Re, L. Rottoli, P. Torrielli, Momentum-space resummation for transverse observables and the Higgs p_\perp at $N^3\text{LL}+N\text{NLO}$. *JHEP* **02**, 108 (2018). [arXiv:1705.09127](#) [hep-ph]
8. K. Melnikov, F. Petriello, Electroweak gauge boson production at hadron colliders through $\mathcal{O}(\alpha_s^2)$. *Phys. Rev. D* **74**, 114017 (2006). [arXiv:hep-ph/0609070](#)
9. Y. Li, F. Petriello, Combining QCD and electroweak corrections to dilepton production in FEWZ. *Phys. Rev. D* **86**, 094034 (2012). [arXiv:1208.5967](#) [hep-ph]
10. S. Catani, L. Cieri, G. Ferrera, D. de Florian, M. Grazzini, Vector Boson production at hadron colliders: a fully exclusive QCD calculation at next-to-next-to-leading order. *Phys. Rev. Lett.* **103**, 082001 (2009). [arXiv:0903.2120](#) [hep-ph]
11. R. Boughezal et al., Z-boson production in association with a jet at next-to-next-to-leading order in perturbative QCD. *Phys. Rev. Lett.* **116**, 152001 (2016). [arXiv:1512.01291](#) [hep-ph]
12. A. Gehrmann-De Ridder, T. Gehrmann, E.W.N. Glover, A. Huss, T.A. Morgan, Precise QCD predictions for the production of a Z boson in association with a hadronic jet. *Phys. Rev. Lett.* **117**, 022001 (2016). [arXiv:1507.02850](#) [hep-ph]
13. A. Denner, S. Dittmaier, T. Kasprzik, A. Mück, Electroweak corrections to dilepton + jet production at hadron colliders. *JHEP* **06**, 069 (2011). [arXiv:1103.0914](#) [hep-ph]
14. S. Kallweit, J.M. Lindert, P. Maierhöfer, S. Pozzorini, M. Schönherr, NLO QCD+EW predictions for V + jets including off-shell vector-boson decays and multijet merging. *JHEP* **04**, 021 (2016). [arXiv:1511.08692](#) [hep-ph]
15. J.M. Lindert et al., Precise predictions for V+jets dark matter backgrounds. *Eur. Phys. J. C* **77**, 829 (2017). [arXiv:1705.04664](#) [hep-ph]
16. J. Bellm et al., Herwig 7.0/Herwig++ 3.0 release note. *Eur. Phys. J. C* **76**, 196 (2016). [arXiv:1512.01178](#) [hep-ph]
17. T. Sjöstrand et al., An introduction to PYTHIA 8.2. *Comput. Phys. Commun.* **191**, 159 (2015). [arXiv:1410.3012](#) [hep-ph]
18. E. Bothmann et al., Event generation with Sherpa 2.2. *Sci. Post Phys.* **7**, 034 (2019). [arXiv:1905.09127](#) [hep-ph]
19. ATLAS Collaboration, Search for dark matter and other new phenomena in events with an energetic jet and large missing transverse momentum using the ATLAS detector. *JHEP* **01**, 126 (2018). [arXiv:1711.03301](#) [hep-ex]
20. ATLAS Collaboration, Measurement of the W-boson mass in pp collisions at $\sqrt{s} = 7$ TeV with the ATLAS detector. *Eur. Phys. J. C* **78**, 110 (2018). [arXiv:1701.07240](#) [hep-ex]. Erratum: *Eur. Phys. J. C* **78** (2018) 898
21. ATLAS Collaboration, Measurement of the transverse momentum distribution of W bosons in pp collisions at $\sqrt{s} = 7$ TeV with the ATLAS detector. *Phys. Rev. D* **85**, 012005 (2012). [arXiv:1108.6308](#) [hep-ex]
22. ATLAS Collaboration, Measurement of the Z/γ^* boson transverse momentum distribution in pp collisions at $\sqrt{s} = 7$ TeV with the ATLAS detector. *JHEP* **09**, 145 (2014). [arXiv:1406.3660](#) [hep-ex]
23. ATLAS Collaboration, Measurement of the transverse momentum and ϕ_η^* distributions of Drell-Yan lepton pairs in proton-proton collisions at $\sqrt{s} = 8$ TeV with the ATLAS detector. *Eur. Phys. J. C* **76**, 291 (2016). [arXiv:1512.02192](#) [hep-ex]
24. CMS Collaboration, Measurements of differential Z boson production cross sections in proton-proton collisions at $\sqrt{s} = 13$ TeV. *JHEP* **12**, 061 (2019). [arXiv:1909.04133](#) [hep-ex]
25. CMS Collaboration, Measurement of differential cross sections in the kinematic angular variable ϕ^* for inclusive Z boson production in pp collisions at $\sqrt{s} = 8$ TeV. *JHEP* **03**, 172 (2018). [arXiv:1710.07955](#) [hep-ex]
26. CMS Collaboration, Measurement of the transverse momentum spectra of weak vector bosons produced in proton-proton collisions at $\sqrt{s} = 8$ TeV. *JHEP* **02**, 096 (2017). [arXiv:1606.05864](#) [hep-ex]
27. CMS Collaboration, Measurement of the Z boson differential cross section in transverse momentum and rapidity in proton-proton collisions at 8 TeV. *Phys. Lett. B* **749**, 187 (2015). [arXiv:1504.03511](#) [hep-ex]
28. CMS Collaboration, Measurement of the rapidity and transverse momentum distributions of Z bosons in pp collisions at $\sqrt{s} = 7$ TeV. *Phys. Rev. D* **85**, 032002 (2012). [arXiv:1110.4973](#) [hep-ex]
29. LHCb Collaboration, Measurement of the forward Z boson production cross-section in pp collisions at $\sqrt{s} = 7$ TeV. *JHEP* **08**, 039 (2015). [arXiv:1505.07024](#) [hep-ex]
30. LHCb Collaboration, Measurement of forward W and Z boson production in association with jets in proton-proton collisions at $\sqrt{s} = 8$ TeV. *JHEP* **05**, 131 (2016). [arXiv:1605.00951](#) [hep-ex]
31. LHCb Collaboration, Measurement of the forward Z boson production cross-section in pp collisions at $\sqrt{s} = 13$ TeV. *JHEP* **09**, 136 (2016). [arXiv:1607.06495](#) [hep-ex]
32. T. Aaltonen et al., Transverse momentum cross section of e^+e^- pairs in the Z-boson region from $p\bar{p}$ collisions at $\sqrt{s} = 1.96$ TeV. *Phys. Rev. D* **86**, 052010 (2012). [arXiv:1207.7138](#) [hep-ex]
33. V.M. Abazov et al., Measurement of the normalized $Z/\gamma^* \rightarrow \mu^+\mu^-$ transverse momentum distribution in $p\bar{p}$ collisions at $\sqrt{s} = 1.96$ TeV. *Phys. Lett. B* **693**, 522 (2010). [arXiv:1006.0618](#) [hep-ex]
34. V.M. Abazov et al., Precise study of the Z/γ^* Boson transverse momentum distribution in $p\bar{p}$ collisions using a novel technique. *Phys. Rev. Lett.* **106**, 122001 (2011). [arXiv:1010.0262](#) [hep-ex]
35. A. Banfi, S. Redford, M. Vesterinen, P. Waller, T.R. Wyatt, Optimisation of variables for studying dilepton transverse momentum distributions at hadron colliders. *Eur. Phys. J. C* **71**, 1600 (2011). [arXiv:1009.1580](#) [hep-ex]
36. ATLAS Collaboration, The ATLAS Experiment at the CERN Large Hadron Collider, *JINST* **3**, S08003 (2008)
37. B. Abbott et al., Production and integration of the ATLAS Insertable B-Layer. *JINST* **13**, T05008 (2018). [arXiv:1803.00844](#) [physics.ins-det]
38. ATLAS Collaboration, ATLAS Insertable B-Layer Technical Design Report, ATLAS-TDR-19, (2010), <https://cds.cern.ch/record/1291633>, Addendum: ATLAS-TDR-19-ADD-1, (2012), <https://cds.cern.ch/record/1451888>
39. ATLAS Collaboration, Performance of the ATLAS trigger system in 2015. *Eur. Phys. J. C* **77**, 317 (2017). [arXiv:1611.09661](#) [hep-ex]
40. P. Nason, A new method for combining NLO QCD with shower Monte Carlo algorithms. *JHEP* **11**, 040 (2004). [arXiv:hep-ph/0409146](#)
41. S. Frixione, P. Nason, C. Oleari, Matching NLO QCD computations with parton shower simulations: the POWHEG method. *JHEP* **11**, 070 (2007). [arXiv:0709.2092](#) [hep-ph]

42. S. Alioli, P. Nason, C. Oleari, E. Re, A general framework for implementing NLO calculations in shower Monte Carlo programs: the POWHEG BOX. *JHEP* **06**, 043 (2010). [arXiv:1002.2581](#) [hep-ph]
43. S. Alioli, P. Nason, C. Oleari, E. Re, NLO vector-boson production matched with shower in POWHEG. *JHEP* **07**, 060 (2008). [arXiv:0805.4802](#) [hep-ph]
44. H.-L. Lai et al., New parton distributions for collider physics. *Phys. Rev. D* **82**, 074024 (2010). [arXiv:1007.2241](#) [hep-ph]
45. J. Pumplin et al., New Generation of Parton Distributions with Uncertainties from Global QCD Analysis. *JHEP* **07**, 012 (2002). [arXiv:hep-ph/0201195](#)
46. P. Golonka, Z. Was, PHOTOS Monte Carlo: a precision tool for QED corrections in Z and W decays. *Eur. Phys. J. C* **45**, 97 (2006). [arXiv:hep-ph/0506026](#)
47. N. Davidson, T. Przedzinski, Z. Was, PHOTOS Interface in C++: Technical and Physics Documentation. *Comput. Phys. Commun.* **199**, 86 (2016). [arXiv:1011.0937](#) [hep-ph]
48. D.J. Lange, The EvtGen particle decay simulation package. *Nucl. Instrum. Methods A* **462**, 152 (2001)
49. P. Nason, G. Zanderighi, W^+W^- , WZ and ZZ production in the POWHEG-BOX-V2. *Eur. Phys. J. C* **74**, 2702 (2014). [arXiv:1311.1365](#) [hep-ph]
50. S. Frixione, P. Nason, G. Ridolfi, A positive-weight next-to-leading-order Monte Carlo for heavy flavour hadroproduction. *JHEP* **09**, 126 (2007). [arXiv:0707.3088](#) [hep-ph]
51. E. Re, Single-top W_t -channel production matched with parton showers using the POWHEG method. *Eur. Phys. J. C* **71**, 1547 (2011). [arXiv:1009.2450](#) [hep-ph]
52. T. Sjöstrand, S. Mrenna, P.Z. Skands, PYTHIA 6.4 Physics and Manual. *JHEP* **05**, 026 (2006). [arXiv:hep-ph/0603175](#)
53. P.Z. Skands, Tuning Monte Carlo generators: The Perugia tunes. *Phys. Rev. D* **82**, 074018 (2010). [arXiv:1005.3457](#) [hep-ph]
54. ATLAS Collaboration, ATLAS Pythia 8 tunes to 7 TeV data, ATL-PHYS-PUB-2014-021 (2014). <https://cds.cern.ch/record/1966419>
55. R.D. Ball et al., Parton distributions for the LHC Run II. *JHEP* **04**, 040 (2015). [arXiv:1410.8849](#) [hep-ph]
56. R.D. Ball et al., Parton distributions with QED corrections. *Nucl. Phys. B* **877**, 290 (2013). [arXiv:1308.0598](#) [hep-ph]
57. A.D. Martin, W.J. Stirling, R.S. Thorne, G. Watt, Parton distributions for the LHC. *Eur. Phys. J. C* **63**, 189 (2009). [arXiv:0901.0002](#) [hep-ph]
58. ATLAS Collaboration, Summary of ATLAS Pythia 8 tunes, ATL-PHYS-PUB-2012-003 (2012). <https://cds.cern.ch/record/1474107>
59. S. Agostinelli et al., GEANT4 - a simulation toolkit. *Nucl. Instrum. Methods A* **506**, 250 (2003)
60. ATLAS Collaboration, The ATLAS simulation infrastructure. *Eur. Phys. J. C* **70**, 823 (2010). [arXiv:1005.4568](#) [physics.ins-det]
61. ATLAS Collaboration, Muon reconstruction performance of the ATLAS detector in proton–proton collision data at $\sqrt{s} = 13$ TeV. *Eur. Phys. J. C* **76**, 292 (2016). [arXiv:1603.05598](#) [hep-ex]
62. ATLAS Collaboration, Electron reconstruction and identification in the ATLAS experiment using the 2015 and 2016 LHC proton–proton collision data at $\sqrt{s} = 13$ TeV. *Eur. Phys. J. C* **79**, 639 (2019). [arXiv:1902.04655](#) [hep-ex]
63. ATLAS Collaboration, Electron and photon energy calibration with the ATLAS detector using 2015–2016 LHC proton–proton collision data. *JINST* **14**, P03017 (2019). [arXiv:1812.03848](#) [hep-ex]
64. ATLAS Collaboration, Performance of electron and photon triggers in ATLAS during LHC Run 2 (2019). [arXiv:1909.00761](#) [hep-ex]
65. G. D’Agostini, A multidimensional unfolding method based on Bayes’ theorem. *Nucl. Instrum. Meth. Phys. Res. A* **A362**, 487 (1995)
66. G. D’Agostini, Improved iterative Bayesian unfolding (2010). [arXiv:1010.0632](#) [physics.data-an]
67. T. Adye, Unfolding algorithms and tests using RooUnfold (2011). [arXiv:1105.1160](#) [physics.data-an]
68. ATLAS Collaboration, Measurement of the Inelastic Proton–Proton Cross Section at $\sqrt{s} = 13$ TeV with the ATLAS Detector at the LHC. *Phys. Rev. Lett.* **117**, 182002 (2016). [arXiv:1606.02625](#) [hep-ex]
69. A. Buckley et al., LHAPDF6: parton density access in the LHC precision era. *Eur. Phys. J. C* **75**, 132 (2015). [arXiv:1412.7420](#) [hep-ph]
70. ATLAS Collaboration, Luminosity determination in pp collisions at $\sqrt{s} = 13$ TeV using the ATLAS detector at the LHC, ATLAS-CONF-2019-021 (2019). <https://cds.cern.ch/record/2677054>
71. G. Avoni et al., The new LUCID-2 detector for luminosity measurement and monitoring in ATLAS. *JINST* **13**, P07017 (2018)
72. ATLAS Collaboration, Measurements of top-quark pair to Z-boson cross-section ratios at $\sqrt{s} = 13, 8, 7$ TeV with the ATLAS detector. *JHEP* **02**, 117 (2017). [arXiv:1612.03636](#) [hep-ex]
73. L. Lyons, D. Gibaut, P. Clifford, How to combine correlated estimates of a single physical quantity. *Nucl. Instrum. Methods A* **270**, 110 (1988)
74. A. Valassi, Combining correlated measurements of several different physical quantities. *Nucl. Instrum. Methods A* **500**, 391 (2003)
75. R. Nisius, On the combination of correlated estimates of a physics observable. *Eur. Phys. J. C* **74**, 3004 (2014). [arXiv:1402.4016](#) [physics.data-an]
76. ATLAS Collaboration, Measurement of W^\pm and Z-boson production cross sections in pp collisions at $\sqrt{s} = 13$ TeV with the ATLAS detector. *Phys. Lett. B* **759**, 601 (2016). [arXiv:1603.09222](#) [hep-ex]
77. S. Camarda et al., DYTURBO: Fast predictions for Drell–Yan processes (2019). [arXiv:1910.07049](#) [hep-ph]
78. S. Dulat et al., New parton distribution functions from a global analysis of quantum chromodynamics. *Phys. Rev. D* **93**, 033006 (2016). [arXiv:1506.07443](#) [hep-ph]
79. W.F.L. Hollik, Radiative corrections in the standard model and their role for precision tests of the electroweak theory. *Fortsch. Phys.* **38**, 165 (1990)
80. ATLAS Collaboration, Measurement of angular correlations in Drell–Yan lepton pairs to probe Z/γ^* boson transverse momentum at $\sqrt{s} = 7$ TeV with the ATLAS detector. *Phys. Lett. B* **720**, 32 (2013). [arXiv:1211.6899](#) [hep-ex]
81. T. Gleisberg, S. Höche, Comix, a new matrix element generator. *JHEP* **12**, 039 (2008). [arXiv:0808.3674](#) [hep-ph]
82. F. Cascioli, P. Maierhofer, S. Pozzorini, Scattering amplitudes with open loops. *Phys. Rev. Lett.* **108**, 111601 (2012). [arXiv:1111.5206](#) [hep-ph]
83. A. Denner, S. Dittmaier, L. Hofer, Collier: a fortran-based complex one-loop library in extended regularizations. *Comput. Phys. Commun.* **212**, 220 (2017). [arXiv:1604.06792](#) [hep-ph]
84. S. Schumann, F. Krauss, A parton shower algorithm based on Catani–Seymour dipole factorisation. *JHEP* **03**, 038 (2008). [arXiv:0709.1027](#) [hep-ph]
85. J.-C. Winter, F. Krauss, G. Soff, A modified cluster-hadronisation model. *Eur. Phys. J. C* **36**, 381 (2004). [arXiv:hep-ph/0311085](#) [hep-ph]
86. S. Höche, F. Krauss, M. Schönherr, F. Siegert, A critical appraisal of NLO+PS matching methods. *JHEP* **09**, 049 (2012). [arXiv:1111.1220](#) [hep-ph]
87. S. Catani, F. Krauss, R. Kuhn, B.R. Webber, QCD matrix elements + parton showers. *JHEP* **11**, 063 (2001). [arXiv:hep-ph/0109231](#)
88. S. Höche, F. Krauss, S. Schumann, F. Siegert, QCD matrix elements and truncated showers. *JHEP* **05**, 053 (2009). [arXiv:0903.1219](#) [hep-ph]
89. S. Höche, F. Krauss, M. Schönherr, F. Siegert, QCD matrix elements + parton showers: the NLO case. *JHEP* **04**, 027 (2013). [arXiv:1207.5030](#) [hep-ph]

90. E. Bothmann, M. Schönherr, S. Schumann, Reweighting QCD matrix-element and parton-shower calculations. *Eur. Phys. J. C* **76**, 590 (2016). [arXiv:1606.08753](#) [hep-ph]
91. W. Bizon et al., The transverse momentum spectrum of weak gauge bosons at N³LL+NNLO. *Eur. Phys. J. C* **79**, 868 (2019). [arXiv:1905.05171](#) [hep-ph]
92. W. Bizon et al., Fiducial distributions in Higgs and Drell-Yan production at N³LL+NNLO. *JHEP* **12**, 132 (2018). [arXiv:1805.05916](#) [hep-ph]
93. A. Gehrmann-De Ridder, T. Gehrmann, E.W.N. Glover, A. Huss, T.A. Morgan, NNLO QCD corrections for Drell-Yan p_T^Z and ϕ^* observables at the LHC. *JHEP* **11**, 094 (2016). [arXiv:1610.01843](#) [hep-ph]. Erratum: *JHEP* **10** (2018) 126
94. R.D. Ball et al., Parton distributions from high-precision collider data. *Eur. Phys. J. C* **77**, 663 (2017). [arXiv:1706.00428](#) [hep-ph]
95. ATLAS Collaboration, ATLAS Computing Acknowledgements, ATL-GEN-PUB-2016-002. <https://cds.cern.ch/record/2202407>

ATLAS Collaboration

G. Aad¹⁰², B. Abbott¹²⁹, D. C. Abbott¹⁰³, A. Abed Abud³⁶, K. Abeling⁵³, D. K. Abhayasinghe⁹⁴, S. H. Abidi¹⁶⁷, O. S. AbouZeid⁴⁰, N. L. Abraham¹⁵⁶, H. Abramowicz¹⁶¹, H. Abreu¹⁶⁰, Y. Abulaiti⁶, B. S. Acharya^{67a,67b,n}, B. Achkar⁵³, S. Adachi¹⁶³, L. Adam¹⁰⁰, C. Adam Bourdarios⁵, L. Adamczyk^{84a}, L. Adamek¹⁶⁷, J. Adelman¹²¹, M. Adersberger¹¹⁴, A. Adiguzel^{12c}, S. Adorni⁵⁴, T. Adye¹⁴⁴, A. A. Affolder¹⁴⁶, Y. Afik¹⁶⁰, C. Agapopoulou⁶⁵, M. N. Agaras³⁸, A. Aggarwal¹¹⁹, C. Agheorghiesei^{27c}, J. A. Aguilar-Saavedra^{140f,140a,ag}, F. Ahmadov⁸⁰, W. S. Ahmed¹⁰⁴, X. Ai¹⁸, G. Aielli^{74a,74b}, S. Akatsuka⁸⁶, T. P. A. Åkesson⁹⁷, E. Akilli⁵⁴, A. V. Akimov¹¹¹, K. Al Khoury⁶⁵, G. L. Alberghi^{23a,23b}, J. Albert¹⁷⁶, M. J. Alconada Verzini¹⁶¹, S. Alderweireldt³⁶, M. Aleksa³⁶, I. N. Aleksandrov⁸⁰, C. Alexa^{27b}, T. Alexopoulos¹⁰, A. Alfonsi¹²⁰, F. Alfonsi^{23a,23b}, M. Alhroob¹²⁹, B. Ali¹⁴², M. Aliev¹⁶⁶, G. Alimonti^{69a}, S. P. Alkire¹⁴⁸, C. Allaire⁶⁵, B. M. M. Allbrooke¹⁵⁶, B. W. Allen¹³², P. P. Allport²¹, A. Aloisio^{70a,70b}, F. Alonso⁸⁹, C. Alpigiani¹⁴⁸, A. A. Alshehri⁵⁷, E. Alunno Camelia^{74a,74b}, M. Alvarez Estevez⁹⁹, M. G. Alvigi^{70a,70b}, Y. Amaral Coutinho^{81b}, A. Ambler¹⁰⁴, L. Ambroz¹³⁵, C. Amelung²⁶, D. Amidei¹⁰⁶, S. P. Amor Dos Santos^{140a}, S. Amoroso⁴⁶, C. S. Amrouche⁵⁴, F. An⁷⁹, C. Anastopoulos¹⁴⁹, N. Andari¹⁴⁵, T. Andeen¹¹, C. F. Anders^{61b}, J. K. Anders²⁰, A. Andreazza^{69a,69b}, V. Andrei^{61a}, C. R. Anelli¹⁷⁶, S. Angelidakis³⁸, A. Angerami³⁹, A. V. Anisenkov^{122a,122b}, A. Annovi^{72a}, C. Antel⁵⁴, M. T. Anthony¹⁴⁹, E. Antipov¹³⁰, M. Antonelli⁵¹, D. J. A. Antrim¹⁷¹, F. Anulli^{73a}, M. Aoki⁸², J. A. Aparisi Pozo¹⁷⁴, L. Aperio Bella^{15a}, J. P. Araque^{140a}, V. Araujo Ferraz^{81b}, R. Araujo Pereira^{81b}, C. Arcangeletti⁵¹, A. T. H. Arce⁴⁹, F. A. Arduh⁸⁹, J.-F. Arguin¹¹⁰, S. Argyropoulos⁷⁸, J.-H. Arling⁴⁶, A. J. Armbruster³⁶, A. Armstrong¹⁷¹, O. Arnaez¹⁶⁷, H. Arnold¹²⁰, Z. P. Arrubarrena Tame¹¹⁴, G. Artoni¹³⁵, S. Artz¹⁰⁰, S. Asai¹⁶³, T. Asawatavonvanich¹⁶⁵, N. Asbah⁵⁹, E. M. Asimakopoulou¹⁷², L. Asquith¹⁵⁶, J. Assahsah^{35d}, K. Assamagan²⁹, R. Astalos^{28a}, R. J. Atkin^{33a}, M. Atkinson¹⁷³, N. B. Atlay¹⁹, H. Atmani⁶⁵, K. Augsten¹⁴², G. Avolio³⁶, R. Avramidou^{60a}, M. K. Ayoub^{15a}, A. M. Azoulay^{168b}, G. Azuelos^{110,ar}, H. Bachacou¹⁴⁵, K. Bachas^{68a,68b}, M. Backes¹³⁵, F. Backman^{45a,45b}, P. Bagnaia^{73a,73b}, M. Bahmani⁸⁵, H. Bahrasemani¹⁵², A. J. Bailey¹⁷⁴, V. R. Bailey¹⁷³, J. T. Baines¹⁴⁴, M. Bajic⁴⁰, C. Bakalis¹⁰, O. K. Baker¹⁸³, P. J. Bakker¹²⁰, D. Bakshi Gupta⁸, S. Balaji¹⁵⁷, E. M. Baldin^{122a,122b}, P. Balek¹⁸⁰, F. Balli¹⁴⁵, W. K. Balunas¹³⁵, J. Balz¹⁰⁰, E. Banas⁸⁵, A. Bandyopadhyay²⁴, Sw. Banerjee^{181,i}, A. A. E. Bannoura¹⁸², L. Barak¹⁶¹, W. M. Barbe³⁸, E. L. Barberio¹⁰⁵, D. Barberis^{55a,55b}, M. Barbero¹⁰², G. Barbour⁹⁵, T. Barillari¹¹⁵, M.-S. Barisits³⁶, J. Barkeloo¹³², T. Barklow¹⁵³, R. Barnea¹⁶⁰, S. L. Barnes^{60c}, B. M. Barnett¹⁴⁴, R. M. Barnett¹⁸, Z. Barnovska-Blenessy^{60a}, A. Baroncelli^{60a}, G. Barone²⁹, A. J. Barr¹³⁵, L. Barranco Navarro^{45a,45b}, F. Barreiro⁹⁹, J. Barreiro Guimarães da Costa^{15a}, S. Barsov¹³⁸, R. Bartoldus¹⁵³, G. Bartolini¹⁰², A. E. Barton⁹⁰, P. Bartos^{28a}, A. Basalaev⁴⁶, A. Basan¹⁰⁰, A. Bassalat^{65,am}, M. J. Basso¹⁶⁷, R. L. Bates⁵⁷, S. Batlamous^{35e}, J. R. Batley³², B. Batool¹⁵¹, M. Battaglia¹⁴⁶, M. Bause^{73a,73b}, F. Bauer¹⁴⁵, K. T. Bauer¹⁷¹, H. S. Bawa³¹, J. B. Beacham⁴⁹, T. Beau¹³⁶, P. H. Beauchemin¹⁷⁰, F. Becherer⁵², P. Bechtel²⁴, H. C. Beck⁵³, H. P. Beck^{20,r}, K. Becker¹⁷⁸, C. Becot⁴⁶, A. Beddall^{12d}, A. J. Beddall^{12a}, V. A. Bednyakov⁸⁰, M. Bedognetti¹²⁰, C. P. Bee¹⁵⁵, T. A. Beermann¹⁸², M. Begalli^{81b}, M. Begel²⁹, A. Behera¹⁵⁵, J. K. Behr⁴⁶, F. Beisiegel²⁴, A. S. Bell⁹⁵, G. Bella¹⁶¹, L. Bellagamba^{23b}, A. Bellerive³⁴, P. Bellos⁹, K. Beloborodov^{122a,122b}, K. Belotskiy¹¹², N. L. Belyaev¹¹², D. Bencheekroun^{35a}, N. Benekos¹⁰, Y. Benhammou¹⁶¹, D. P. Benjamin⁶, M. Benoit⁵⁴, J. R. Bensinger²⁶, S. Bentvelsen¹²⁰, L. Beresford¹³⁵, M. Beretta⁵¹, D. Berge⁴⁶, E. Bergeas Kuutmann¹⁷², N. Berger⁵, B. Bergmann¹⁴², L. J. Bergsten²⁶, J. Beringer¹⁸, S. Berlendis⁷, G. Bernardi¹³⁶, C. Bernius¹⁵³, F. U. Bernlochner²⁴, T. Berry⁹⁴, P. Berta¹⁰⁰, C. Bertella^{15a}, I. A. Bertram⁹⁰, O. Bessidskaia Bylund¹⁸², N. Besson¹⁴⁵, A. Bethani¹⁰¹, S. Bethke¹¹⁵, A. Betti⁴², A. J. Bevan⁹³, J. Beyer¹¹⁵, D. S. Bhattacharya¹⁷⁷, P. Bhattacharai²⁶, R. Bi¹³⁹, R. M. Bianchi¹³⁹, O. Biebel¹¹⁴, D. Biedermann¹⁹, R. Bielski³⁶, K. Bierwagen¹⁰⁰, N. V. Biesuz^{72a,72b}, M. Biglietti^{75a}, T. R. V. Billoud¹¹⁰, M. Bindi⁵³, A. Bingul^{12d}, C. Bini^{73a,73b}, S. Biondi^{23a,23b}, M. Birman¹⁸⁰, T. Bisanz⁵³, J. P. Biswal¹⁶¹, D. Biswas^{181,i}, A. Bitadze¹⁰¹, C. Bittrich⁴⁸, K. Björke¹³⁴, K. M. Black²⁵, T. Blazek^{28a}, I. Bloch⁴⁶, C. Blocker²⁶, A. Blue⁵⁷, U. Blumenschein⁹³, G. J. Bobbink¹²⁰, V. S. Bobrovnikov^{122a,122b}, S. S. Bocchetta⁹⁷, A. Bocci⁴⁹, D. Boerner⁴⁶,

- D. Bogavac¹⁴, A. G. Bogdanchikov^{122a,122b}, C. Bohm^{45a}, V. Boisvert⁹⁴, P. Bokan^{53,172}, T. Bold^{84a}, A. S. Boldyrev¹¹³, A. E. Bolz^{61b}, M. Bomben¹³⁶, M. Bona⁹³, J. S. Bonilla¹³², M. Boonekamp¹⁴⁵, C. D. Booth⁹⁴, H. M. Borecka-Bielska⁹¹, A. Borisov¹²³, G. Borissov⁹⁰, J. Bortfeldt³⁶, D. Bortoletto¹³⁵, D. Boscherini^{23b}, M. Bosman¹⁴, J. D. Bossio Sola¹⁰⁴, K. Bouaouda^{35a}, J. Boudreau¹³⁹, E. V. Bouhova-Thacker⁹⁰, D. Boumediene³⁸, S. K. Boutle⁵⁷, A. Boveia¹²⁷, J. Boyd³⁶, D. Boye^{33c,an}, I. R. Boyko⁸⁰, A. J. Bozson⁹⁴, J. Bracinik²¹, N. Brahimi¹⁰², G. Brandt¹⁸², O. Brandt³², F. Braren⁴⁶, B. Brau¹⁰³, J. E. Brau¹³², W. D. Breaden Madden⁵⁷, K. Brendlinger⁴⁶, L. Brenner⁴⁶, R. Brenner¹⁷², S. Bressler¹⁸⁰, B. Brickwedde¹⁰⁰, D. L. Briglin²¹, D. Britton⁵⁷, D. Britzger¹¹⁵, I. Brock²⁴, R. Brock¹⁰⁷, G. Brooijmans³⁹, W. K. Brooks^{147c}, E. Brost¹²¹, J. H. Broughton²¹, P. A. Bruckman de Renstrom⁸⁵, D. Bruncko^{28b}, A. Bruni^{23b}, G. Bruni^{23b}, L. S. Bruni¹²⁰, S. Bruno^{74a,74b}, M. Bruschi^{23b}, N. Bruscino^{73a,73b}, P. Bryant³⁷, L. Bryngemark⁹⁷, T. Buanes¹⁷, Q. Buat³⁶, P. Buchholz¹⁵¹, A. G. Buckley⁵⁷, I. A. Budagov⁸⁰, M. K. Bugge¹³⁴, F. Bühner⁵², O. Bulekov¹¹², T. J. Burch¹²¹, S. Burdin⁹¹, C. D. Burgard¹²⁰, A. M. Burger¹³⁰, B. Burghgrave⁸, J. T. P. Burr⁴⁶, C. D. Burton¹¹, J. C. Burzynski¹⁰³, V. Büscher¹⁰⁰, E. Buschmann⁵³, P. J. Bussey⁵⁷, J. M. Butler²⁵, C. M. Buttar⁵⁷, J. M. Butterworth⁹⁵, P. Butti³⁶, W. Buttinger³⁶, C. J. Buxo Vazquez¹⁰⁷, A. Buzatu¹⁵⁸, A. R. Buzykaev^{122a,122b}, G. Cabras^{23a,23b}, S. Cabrera Urbán¹⁷⁴, D. Caforio⁵⁶, H. Cai¹⁷³, V. M. M. Cairo¹⁵³, O. Cakir^{4a}, N. Calace³⁶, P. Calafiura¹⁸, A. Calandri¹⁰², G. Calderini¹³⁶, P. Calfayan⁶⁶, G. Callea⁵⁷, L. P. Caloba^{81b}, A. Caltabiano^{74a,74b}, S. Calvente Lopez⁹⁹, D. Calvet³⁸, S. Calvet³⁸, T. P. Calvet¹⁵⁵, M. Calvetti^{72a,72b}, R. Camacho Toro¹³⁶, S. Camarda³⁶, D. Camarero Munoz⁹⁹, P. Camarri^{74a,74b}, D. Cameron¹³⁴, R. Caminal Armadans¹⁰³, C. Camincher³⁶, S. Campana³⁶, M. Campanelli⁹⁵, A. Camplani⁴⁰, A. Campoverde¹⁵¹, V. Canale^{70a,70b}, A. Canesse¹⁰⁴, M. Cano Bret^{60c}, J. Cantero¹³⁰, T. Cao¹⁶¹, Y. Cao¹⁷³, M. D. M. Capeans Garrido³⁶, M. Capua^{41a,41b}, R. Cardarelli^{74a}, F. Cardillo¹⁴⁹, G. Carducci^{41a,41b}, I. Carli¹⁴³, T. Carli³⁶, G. Carlino^{70a}, B. T. Carlson¹³⁹, L. Carminati^{69a,69b}, R. M. D. Carney^{45a,45b}, S. Caron¹¹⁹, E. Carquin^{147c}, S. Carrá⁴⁶, J. W. S. Carter¹⁶⁷, M. P. Casado^{14,e}, A. F. Casha¹⁶⁷, D. W. Casper¹⁷¹, R. Castelijns¹²⁰, F. L. Castillo¹⁷⁴, L. Castillo Garcia¹⁴, V. Castillo Gimenez¹⁷⁴, N. F. Castro^{140a,140e}, A. Catinaccio³⁶, J. R. Catmore¹³⁴, A. Cattai³⁶, V. Cavaliere²⁹, E. Cavallaro¹⁴, M. Cavalli-Sforza¹⁴, V. Cavasinni^{72a,72b}, E. Celebi^{12b}, L. Cerda Alberich¹⁷⁴, K. Cerny¹³¹, A. S. Cerqueira^{81a}, A. Cerri¹⁵⁶, L. Cerrito^{74a,74b}, F. Cerutti¹⁸, A. Cervelli^{23a,23b}, S. A. Cetin^{12b}, Z. Chadi^{35a}, D. Chakraborty¹²¹, W. S. Chan¹²⁰, W. Y. Chan⁹¹, J. D. Chapman³², B. Chargeishvili^{159b}, D. G. Charlton²¹, T. P. Charman⁹³, C. C. Chau³⁴, S. Che¹²⁷, S. Chekanov⁶, S. V. Chekulaev^{168a}, G. A. Chelkov^{80,aq}, M. A. Chelstowska³⁶, B. Chen⁷⁹, C. Chen^{60a}, C. H. Chen⁷⁹, H. Chen²⁹, J. Chen^{60a}, J. Chen³⁹, J. Chen²⁶, S. Chen¹³⁷, S. J. Chen^{15c}, X. Chen^{15b}, Y.-H. Chen⁴⁶, H. C. Cheng^{63a}, H. J. Cheng^{15a}, A. Cheplakov⁸⁰, E. Cheremushkina¹²³, R. Cherkaoui El Moursli^{35e}, E. Cheu⁷, K. Cheung⁶⁴, T. J. A. Chevaléris¹⁴⁵, L. Chevalier¹⁴⁵, V. Chiarella⁵¹, G. Chiarelli^{72a}, G. Chiodini^{68a}, A. S. Chisholm²¹, A. Chitan^{27b}, I. Chiu¹⁶³, Y. H. Chiu¹⁷⁶, M. V. Chizhov⁸⁰, K. Choi⁶⁶, A. R. Chomont^{73a,73b}, S. Chouridou¹⁶², Y. S. Chow¹²⁰, M. C. Chu^{63a}, X. Chu^{15a,15d}, J. Chudoba¹⁴¹, A. J. Chuinard¹⁰⁴, J. J. Chwastowski⁸⁵, L. Chytka¹³¹, D. Cieri¹¹⁵, K. M. Ciesla⁸⁵, D. Cinca⁴⁷, V. Cindro⁹², I. A. Cioară^{27b}, A. Ciochio¹⁸, F. Ciotto^{70a,70b}, Z. H. Citron^{180j}, M. Citterio^{69a}, D. A. Ciubotaru^{27b}, B. M. Ciungu¹⁶⁷, A. Clark⁵⁴, M. R. Clark³⁹, P. J. Clark⁵⁰, C. Clement^{45a,45b}, Y. Coadou¹⁰², M. Cobal^{67a,67c}, A. Coccaro^{55b}, J. Cochran⁷⁹, H. Cohen¹⁶¹, A. E. C. Coimbra³⁶, L. Colasurdo¹¹⁹, B. Cole³⁹, A. P. Colijn¹²⁰, J. Collot⁵⁸, P. Conde Muiño^{140a,140h}, S. H. Connell^{33c}, I. A. Connelly⁵⁷, S. Constantinescu^{27b}, F. Conventi^{70a,as}, A. M. Cooper-Sarkar¹³⁵, F. Cormier¹⁷⁵, K. J. R. Cormier¹⁶⁷, L. D. Corpe⁹⁵, M. Corradi^{73a,73b}, E. E. Corrigan⁹⁷, F. Corriveau^{104,ae}, A. Cortes-Gonzalez³⁶, M. J. Costa¹⁷⁴, F. Costanza⁵, D. Costanzo¹⁴⁹, G. Cowan⁹⁴, J. W. Cowley³², J. Crane¹⁰¹, K. Cranmer¹²⁵, S. J. Crawley⁵⁷, R. A. Creager¹³⁷, S. Crépe-Renaudin⁵⁸, F. Crescioli¹³⁶, M. Cristinziani²⁴, V. Croft¹⁷⁰, G. Crosetti^{41a,41b}, A. Cueto⁵, T. Cuhadar Donszelmann¹⁴⁹, A. R. Cukierman¹⁵³, W. R. Cunningham⁵⁷, S. Czekierda⁸⁵, P. Czodrowski³⁶, M. J. Da Cunha Sargedass De Sousa^{60b}, J. V. Da Fonseca Pinto^{81b}, C. Da Via¹⁰¹, W. Dabrowski^{84a}, F. Dachs³⁶, T. Dado^{28a}, S. Dahbi^{35e}, T. Dai¹⁰⁶, C. Dallapiccola¹⁰³, M. Dam⁴⁰, G. D'amen²⁹, V. D'Amico^{75a,75b}, J. Damp¹⁰⁰, J. R. Dandoy¹³⁷, M. F. Daneri³⁰, N. P. Dang^{181,i}, N. S. Dann¹⁰¹, M. Danninger¹⁷⁵, V. Dao³⁶, G. Darbo^{55b}, O. Dartsis⁵, A. Dattagupta¹³², T. Daubney⁴⁶, S. D'Auria^{69a,69b}, C. David^{168b}, T. Davidek¹⁴³, D. R. Davis⁴⁹, I. Dawson¹⁴⁹, K. De⁸, R. De Asmundis^{70a}, M. De Beurs¹²⁰, S. De Castro^{23a,23b}, S. De Cecco^{73a,73b}, N. De Groot¹¹⁹, P. de Jong¹²⁰, H. De la Torre¹⁰⁷, A. De Maria^{15c}, D. De Pedis^{73a}, A. De Salvo^{73a}, U. De Sanctis^{74a,74b}, M. De Santis^{74a,74b}, A. De Santo¹⁵⁶, K. De Vasconcelos Corga¹⁰², J. B. De Vivie De Regie⁶⁵, C. Debenedetti¹⁴⁶, D. V. Dedovich⁸⁰, A. M. Deiana⁴², J. Del Peso⁹⁹, Y. Delabat Diaz⁴⁶, D. Delgove⁶⁵, F. Deliot^{145,q}, C. M. Delitzsch⁷, M. Della Pietra^{70a,70b}, D. Della Volpe⁵⁴, A. Dell'Acqua³⁶, L. Dell'Asta^{74a,74b}, M. Delmastro⁵, C. Delporte⁶⁵, P. A. Delsart⁵⁸, D. A. DeMarco¹⁶⁷, S. Demers¹⁸³, M. Demichev⁸⁰, G. Demontigny¹¹⁰, S. P. Denisov¹²³, L. D'Eramo¹³⁶, D. Derendarz⁸⁵, J. E. Derkaoui^{35d}, F. Derue¹³⁶, P. Dervan⁹¹, K. Desch²⁴, C. Deterre⁴⁶, K. Dette¹⁶⁷, C. Deutsch²⁴, M. R. Devesa³⁰, P. O. Deviveiros³⁶, A. Dewhurst¹⁴⁴, F. A. Di Bello⁵⁴, A. Di Ciaccio^{74a,74b}, L. Di Ciaccio⁵, W. K. Di Clemente¹³⁷, C. Di Donato^{70a,70b}, A. Di Girolamo³⁶, G. Di Gregorio^{72a,72b}, B. Di Micco^{75a,75b}, R. Di Nardo^{75a,75b}, K. F. Di Petrillo⁵⁹, R. Di Sipio¹⁶⁷, D. Di Valentino³⁴, C. Diaconu¹⁰², F. A. Dias⁴⁰, T. Dias Do Vale^{140a}, M. A. Diaz^{147a}, J. Dickinson¹⁸, E. B. Diehl¹⁰⁶

J. Dietrich¹⁹, S. Díez Cornell⁴⁶, A. Dimitrievska¹⁸, W. Ding^{15b}, J. Dingfelder²⁴, F. Dittus³⁶, F. Djama¹⁰², T. Djobava^{159b}, J. I. Djuvsland¹⁷, M. A. B. Do Vale^{81c}, M. Dobre^{27b}, D. Dodsworth²⁶, C. Doglioni⁹⁷, J. Dolejsi¹⁴³, Z. Dolezal¹⁴³, M. Donadelli^{81d}, B. Dong^{60c}, J. Donini³⁸, A. D'Onofrio^{15c}, M. D'Onofrio⁹¹, J. Dopke¹⁴⁴, A. Doria^{70a}, M. T. Dova⁸⁹, A. T. Doyle⁵⁷, E. Drechsler¹⁵², E. Dreyer¹⁵², T. Dreyer⁵³, A. S. Drobac¹⁷⁰, D. Du^{60b}, Y. Duan^{60b}, F. Dubinin¹¹¹, M. Dubovsky^{28a}, A. Dubreuil⁵⁴, E. Duchovni¹⁸⁰, G. Duckeck¹¹⁴, A. Ducourthial¹³⁶, O. A. Ducu¹¹⁰, D. Duda¹¹⁵, A. Dudarev³⁶, A. C. Dudder¹⁰⁰, E. M. Duffield¹⁸, L. Dufflot⁶⁵, M. Dührssen³⁶, C. Dülzen¹⁸², M. Dumancic¹⁸⁰, A. E. Dumitriu^{27b}, A. K. Duncan⁵⁷, M. Dunford^{61a}, A. Duperrin¹⁰², H. Duran Yildiz^{4a}, M. Düren⁵⁶, A. Durglishvili^{159b}, D. Duschinger⁴⁸, B. Dutta⁴⁶, D. Duvnjak¹, G. I. Dyckes¹³⁷, M. Dyndal³⁶, S. Dysch¹⁰¹, B. S. Dziedzic⁸⁵, K. M. Ecker¹¹⁵, R. C. Edgar¹⁰⁶, M. G. Eggleston⁴⁹, T. Eifert⁸, G. Eigen¹⁷, K. Einsweiler¹⁸, T. Ekelof¹⁷², H. El Jarrari^{35e}, R. El Kosseifi¹⁰², V. Ellajosyula¹⁷², M. Ellert¹⁷², F. Ellinghaus¹⁸², A. A. Elliot⁹³, N. Ellis³⁶, J. Elmsheuser²⁹, M. Elsing³⁶, D. Emelianov¹⁴⁴, A. Emerman³⁹, Y. Enari¹⁶³, M. B. Epland⁴⁹, J. Erdmann⁴⁷, A. Ereditato²⁰, M. Errenst³⁶, M. Escalier⁶⁵, C. Escobar¹⁷⁴, O. Estrada Pastor¹⁷⁴, E. Etzion¹⁶¹, H. Evans⁶⁶, A. Ezhilov¹³⁸, F. Fabbri⁵⁷, L. Fabbri^{23a,23b}, V. Fabiani¹¹⁹, G. Facini⁹⁵, R. M. Faisca Rodrigues Pereira^{140a}, R. M. Fakhruddinov¹²³, S. Falciano^{73a}, P. J. Falke⁵, S. Falke⁵, J. Faltova¹⁴³, Y. Fang^{15a}, Y. Fang^{15a}, G. Fanourakis⁴⁴, M. Fanti^{69a,69b}, M. Faraj^{67a,67c,t}, A. Farbin⁸, A. Farilla^{75a}, E. M. Farina^{71a,71b}, T. Farooque¹⁰⁷, S. Farrell¹⁸, S. M. Farrington⁵⁰, P. Farthouat³⁶, F. Fassi^{35e}, P. Fassnacht³⁶, D. Fassouliotis⁹, M. Faucci Giannelli⁵⁰, W. J. Fawcett³², L. Fayard⁶⁵, O. L. Fedin^{138,o}, W. Fedorko¹⁷⁵, A. Fehr²⁰, M. Feickert¹⁷³, L. Feligioni¹⁰², A. Fell¹⁴⁹, C. Feng^{60b}, M. Feng⁴⁹, M. J. Fenton⁵⁷, A. B. Fenyuk¹²³, S. W. Ferguson⁴³, J. Ferrando⁴⁶, A. Ferrante¹⁷³, A. Ferrari¹⁷², P. Ferrari¹²⁰, R. Ferrari^{71a}, D. E. Ferreira de Lima^{61b}, A. Ferrer¹⁷⁴, D. Ferrere⁵⁴, C. Ferretti¹⁰⁶, F. Fiedler¹⁰⁰, A. Filipčič⁹², F. Filthaut¹¹⁹, K. D. Finelli²⁵, M. C. N. Fiolhais^{140a,140c,a}, L. Fiorini¹⁷⁴, F. Fischer¹¹⁴, W. C. Fisher¹⁰⁷, I. Fleck¹⁵¹, P. Fleischmann¹⁰⁶, R. R. M. Fletcher¹³⁷, T. Flick¹⁸², B. M. Flierl¹¹⁴, L. Flores¹³⁷, L. R. Flores Castillo^{63a}, F. M. Follega^{76a,76b}, N. Fomin¹⁷, J. H. Foo¹⁶⁷, G. T. Forcolin^{76a,76b}, A. Formica¹⁴⁵, F. A. Förster¹⁴, A. C. Forti¹⁰¹, A. G. Foster²¹, M. G. Foti¹³⁵, D. Fournier⁶⁵, H. Fox⁹⁰, P. Francavilla^{72a,72b}, S. Francescato^{73a,73b}, M. Franchini^{23a,23b}, S. Franchino^{61a}, D. Francis³⁶, L. Franconi²⁰, M. Franklin⁵⁹, A. N. Fray⁹³, P. M. Freeman²¹, B. Freund¹¹⁰, W. S. Freund^{81b}, E. M. Freundlich⁴⁷, D. C. Frizzell¹²⁹, D. Froidevaux³⁶, J. A. Frost¹³⁵, C. Fukunaga¹⁶⁴, E. Fullana Torregrosa¹⁷⁴, E. Fumagalli^{55a,55b}, T. Fusayasu¹¹⁶, J. Fuster¹⁷⁴, A. Gabrielli^{23a,23b}, A. Gabrielli¹⁸, S. Gadatsch⁵⁴, P. Gadow¹¹⁵, G. Gagliardi^{55a,55b}, L. G. Gagnon¹¹⁰, C. Galea^{27b}, B. Galhardo^{140a}, G. E. Gallardo¹³⁵, E. J. Gallas¹³⁵, B. J. Gallop¹⁴⁴, G. Galster⁴⁰, R. Gamboa Goni⁹³, K. K. Gan¹²⁷, S. Ganguly¹⁸⁰, J. Gao^{60a}, Y. Gao⁵⁰, Y. S. Gao^{31,l}, C. García¹⁷⁴, J. E. García Navarro¹⁷⁴, J. A. García Pascual^{15a}, C. Garcia-Argos⁵², M. Garcia-Sciveres¹⁸, R. W. Gardner³⁷, N. Garelli¹⁵³, S. Gargiulo⁵², C. A. Garner¹⁶⁷, V. Garonne¹³⁴, S. J. Gasiorowski¹⁴⁸, P. Gaspar^{81b}, A. Gaudiello^{55a,55b}, G. Gaudio^{71a}, I. L. Gavrilenko¹¹¹, A. Gavrilyuk¹²⁴, C. Gay¹⁷⁵, G. Gaycken⁴⁶, E. N. Gazis¹⁰, A. A. Geanta^{27b}, C. M. Gee¹⁴⁶, C. N. P. Gee¹⁴⁴, J. Geisen⁵³, M. Geisen¹⁰⁰, C. Gemme^{55b}, M. H. Genest⁵⁸, C. Geng¹⁰⁶, S. Gentile^{73a,73b}, S. George⁹⁴, T. Gerasis⁴⁴, L. O. Gerlach⁵³, P. Gessinger-Befurt¹⁰⁰, G. Gessner⁴⁷, S. Ghasemi¹⁵¹, M. Ghasemi Bostanabad¹⁷⁶, M. Ghneimat¹⁵¹, A. Ghosh⁶⁵, A. Ghosh⁷⁸, B. Giacobbe^{23b}, S. Giagu^{73a,73b}, N. Giangiacomi^{23a,23b}, P. Giannetti^{72a}, A. Giannini^{70a,70b}, G. Giannini¹⁴, S. M. Gibson⁹⁴, M. Gignac¹⁴⁶, D. Gillberg³⁴, G. Gilles¹⁸², D. M. Gingrich^{3,ar}, M. P. Giordani^{67a,67c}, P. F. Giraud¹⁴⁵, G. Giugliarelli^{67a,67c}, D. Giugni^{69a}, F. Giuli^{74a,74b}, S. Gkaitatzis¹⁶², I. Gkialas^{9,g}, E. L. Gkougkousis¹⁴, P. Gkoutoumis¹⁰, L. K. Gladilin¹¹³, C. Glasman⁹⁹, J. Glatzer¹⁴, P. C. F. Glaysheer⁴⁶, A. Glazov⁴⁶, G. R. Gledhill¹³², M. Goblirsch-Kolb²⁶, D. Godin¹¹⁰, S. Goldfarb¹⁰⁵, T. Golling⁵⁴, D. Golubkov¹²³, A. Gomes^{140a,140b}, R. Goncalves Gama⁵³, R. Gonçalves^{140a}, G. Gonella⁵², L. Gonella²¹, A. Gongadze⁸⁰, F. Gonnella²¹, J. L. Gonski³⁹, S. González de la Hoz¹⁷⁴, S. Gonzalez-Sevilla⁵⁴, G. R. Gonzalvo Rodriguez¹⁷⁴, L. Goossens³⁶, N. A. Gorasia²¹, P. A. Gorbounov¹²⁴, H. A. Gordon²⁹, B. Gorini³⁶, E. Gorini^{68a,68b}, A. Gorišek⁹², A. T. Goshaw⁴⁹, M. I. Gostkin⁸⁰, C. A. Gottardo¹¹⁹, M. Gouighri^{35b}, A. G. Goussiou¹⁴⁸, N. Govender^{33c}, C. Goy⁵, E. Gozani¹⁶⁰, I. Grabowska-Bold^{84a}, E. C. Graham⁹¹, J. Gramling¹⁷¹, E. Gramstad¹³⁴, S. Grancagnolo¹⁹, M. Grandi¹⁵⁶, V. Gratchev¹³⁸, P. M. Gravila^{27f}, F. G. Gravili^{68a,68b}, C. Gray⁵⁷, H. M. Gray¹⁸, C. Grefe²⁴, K. Gregersen⁹⁷, I. M. Gregor⁴⁶, P. Grenier¹⁵³, K. Grevtsov⁴⁶, C. Grieco¹⁴, N. A. Grieser¹²⁹, A. A. Grillo¹⁴⁶, K. Grimm^{31,k}, S. Grinstein^{14,z}, J.-F. Grivaz⁶⁵, S. Groh¹⁰⁰, E. Gross¹⁸⁰, J. Grosse-Knetter⁵³, Z. J. Grout⁹⁵, C. Grud¹⁰⁶, A. Grummer¹¹⁸, L. Guan¹⁰⁶, W. Guan¹⁸¹, C. Gubbels¹⁷⁵, J. Guenther³⁶, A. Guerguichon⁶⁵, J. G. R. Guerrero Rojas¹⁷⁴, F. Guescini¹¹⁵, D. Guest¹⁷¹, R. Gugel⁵², T. Guillemin⁵, S. Guindon³⁶, U. Gul⁵⁷, J. Guo^{60c}, W. Guo¹⁰⁶, Y. Guo^{60a,s}, Z. Guo¹⁰², R. Gupta⁴⁶, S. Gurbuz^{12c}, G. Gustavino¹²⁹, M. Guth⁵², P. Gutierrez¹²⁹, C. Gutschow⁹⁵, C. Guyot¹⁴⁵, C. Gwenlan¹³⁵, C. B. Gwilliam⁹¹, A. Haas¹²⁵, C. Haber¹⁸, H. K. Hadavand⁸, A. Hadeef^{60a}, S. Hageböck³⁶, M. Haleem¹⁷⁷, J. Haley¹³⁰, G. Halladjian¹⁰⁷, G. D. Hallowell¹⁰², K. Hamacher¹⁸², P. Hamal¹³¹, K. Hamano¹⁷⁶, H. Hamdaoui^{35e}, M. Hamer²⁴, G. N. Hamity⁵⁰, K. Han^{60a,y}, L. Han^{60a}, S. Han^{15a}, Y. F. Han¹⁶⁷, K. Hanagaki^{82,w}, M. Hance¹⁴⁶, D. M. Handl¹¹⁴, B. Haney¹³⁷, R. Hankache¹³⁶, E. Hansen⁹⁷, J. B. Hansen⁴⁰, J. D. Hansen⁴⁰, M. C. Hansen²⁴, P. H. Hansen⁴⁰, E. C. Hanson¹⁰¹, K. Hara¹⁶⁹, T. Harenberg¹⁸², S. Harkusha¹⁰⁸, P. F. Harrison¹⁷⁸, N. M. Hartmann¹¹⁴, Y. Hasegawa¹⁵⁰, A. Hasib⁵⁰, S. Hassani¹⁴⁵, S. Haug²⁰, R. Hauser¹⁰⁷, L. B. Havener³⁹

M. Havranek¹⁴², C. M. Hawkes²¹, R. J. Hawkins³⁶, D. Hayden¹⁰⁷, C. Hayes¹⁰⁶, R. L. Hayes¹⁷⁵, C. P. Hays¹³⁵, J. M. Hays⁹³, H. S. Hayward⁹¹, S. J. Haywood¹⁴⁴, F. He^{60a}, M. P. Heath⁵⁰, V. Hedberg⁹⁷, L. Heelan⁸, S. Heer²⁴, K. K. Heidegger⁵², W. D. Heidorn⁷⁹, J. Heilman³⁴, S. Heim⁴⁶, T. Heim¹⁸, B. Heinemann^{46,ao}, J. J. Heinrich¹³², L. Heinrich³⁶, J. Hejbal¹⁴¹, L. Helary^{61b}, A. Held¹⁷⁵, S. Hellesund¹³⁴, C. M. Helling¹⁴⁶, S. Hellman^{45a,45b}, C. Helsen³⁶, R. C. W. Henderson⁹⁰, Y. Heng¹⁸¹, L. Henkelmann^{61a}, S. Henkelmann¹⁷⁵, A. M. Henriques Correia³⁶, H. Herde²⁶, V. Herget¹⁷⁷, Y. Hernández Jiménez^{33e}, H. Herr¹⁰⁰, M. G. Herrmann¹¹⁴, T. Herrmann⁴⁸, G. Herten⁵², R. Hertenberger¹¹⁴, L. Hervas³⁶, T. C. Herwig¹³⁷, G. G. Hesketh⁹⁵, N. P. Hessey^{168a}, A. Higashida¹⁶³, S. Higashino⁸², E. Higón-Rodríguez¹⁷⁴, K. Hildebrand³⁷, J. C. Hill³², K. K. Hill²⁹, K. H. Hiller⁴⁶, S. J. Hillier²¹, M. Hils⁴⁸, I. Hinchliffe¹⁸, F. Hinterkeuser²⁴, M. Hirose¹³³, S. Hirose⁵², D. Hirschbuehl¹⁸², B. Hiti⁹², O. Hladik¹⁴¹, D. R. Hlaluku^{33e}, X. Hoad⁵⁰, J. Hobbs¹⁵⁵, N. Hod¹⁸⁰, M. C. Hodgkinson¹⁴⁹, A. Hoecker³⁶, D. Hohn⁵², D. Hohov⁶⁵, T. Holm²⁴, T. R. Holmes³⁷, M. Holzbock¹¹⁴, L. B. A. H. Hommels³², S. Honda¹⁶⁹, T. M. Hong¹³⁹, J. C. Honig⁵², A. Hönle¹¹⁵, B. H. Hooberman¹⁷³, W. H. Hopkins⁶, Y. Horii¹¹⁷, P. Horn⁴⁸, L. A. Horyn³⁷, S. Hou¹⁵⁸, A. Hoummada^{35a}, J. Howarth¹⁰¹, J. Hoya⁸⁹, M. Hrabovsky¹³¹, J. Hrdinka⁷⁷, I. Hristova¹⁹, J. Hrivnac⁶⁵, A. Hrynevich¹⁰⁹, T. Hryn'ova⁵, P. J. Hsu⁶⁴, S.-C. Hsu¹⁴⁸, Q. Hu²⁹, S. Hu^{60c}, Y. F. Hu^{15a,15d}, D. P. Huang⁹⁵, Y. Huang^{60a}, Y. Huang^{15a}, Z. Hubacek¹⁴², F. Hubaut¹⁰², M. Huebner²⁴, F. Huegging²⁴, T. B. Huffman¹³⁵, M. Huhtinen³⁶, R. F. H. Hunter³⁴, P. Huo¹⁵⁵, N. Huseynov^{80,af}, J. Huston¹⁰⁷, J. Huth⁵⁹, R. Hyneman¹⁰⁶, S. Hyrych^{28a}, G. Iacobucci⁵⁴, G. Iakovidis²⁹, I. Ibragimov¹⁵¹, L. Iconomidou-Fayard⁶⁵, P. Iengo³⁶, R. Ignazzi⁴⁰, O. Igonkina^{120,ab,*}, R. Iguchi¹⁶³, T. Iizawa⁵⁴, Y. Ikegami⁸², M. Ikeno⁸², D. Iliadis¹⁶², N. Ilic^{119,167,ae}, F. Iltzsche⁴⁸, G. Introzzi^{71a,71b}, M. Iodice^{75a}, K. Iordanidou^{168a}, V. Ippolito^{73a,73b}, M. F. Isacson¹⁷², M. Ishino¹⁶³, W. Islam¹³⁰, C. Issever^{19,46}, S. Istin¹⁶⁰, F. Ito¹⁶⁹, J. M. Iturbe Ponce^{63a}, R. Iuppa^{76a,76b}, A. Ivina¹⁸⁰, H. Iwasaki⁸², J. M. Izen⁴³, V. Izzo^{70a}, P. Jacka¹⁴¹, P. Jackson¹, R. M. Jacobs²⁴, B. P. Jaeger¹⁵², V. Jain², G. Jäkel¹⁸², K. B. Jakobi¹⁰⁰, K. Jakobs⁵², T. Jakoubek¹⁴¹, J. Jamieson⁵⁷, K. W. Janas^{84a}, R. Jansky⁵⁴, J. Janssen²⁴, M. Janus⁵³, P. A. Janus^{84a}, G. Jarlskog⁹⁷, N. Javadov^{80,af}, T. Javůrek³⁶, M. Javurkova¹⁰³, F. Jeanneau¹⁴⁵, L. Jeanty¹³², J. Jejelava^{159a}, A. Jelinskas¹⁷⁸, P. Jenni^{52,b}, J. Jeong⁴⁶, N. Jeong⁴⁶, S. Jézéquel⁵, H. Ji¹⁸¹, J. Jia¹⁵⁵, H. Jiang⁷⁹, Y. Jiang^{60a}, Z. Jiang^{153,p}, S. Jiggins⁵², F. A. Jimenez Morales³⁸, J. Jimenez Pena¹¹⁵, S. Jin^{15c}, A. Jinaru^{27b}, O. Jinnouchi¹⁶⁵, H. Jivan^{33e}, P. Johansson¹⁴⁹, K. A. Johns⁷, C. A. Johnson⁶⁶, K. Jon-And^{45a,45b}, R. W. L. Jones⁹⁰, S. D. Jones¹⁵⁶, S. Jones⁷, T. J. Jones⁹¹, J. Jongmanns^{61a}, P. M. Jorge^{140a}, J. Jovicevic³⁶, X. Ju¹⁸, J. J. Junggeburth¹¹⁵, A. Juste Rozas^{14,z}, A. Kaczmarska⁸⁵, M. Kado^{73a,73b}, H. Kagan¹²⁷, M. Kagan¹⁵³, A. Kahn³⁹, C. Kahra¹⁰⁰, T. Kajji¹⁷⁹, E. Kajomovitz¹⁶⁰, C. W. Kalderon⁹⁷, A. Kaluza¹⁰⁰, A. Kamenshchikov¹²³, M. Kaneda¹⁶³, N. J. Kang¹⁴⁶, L. Kanji⁹², Y. Kano¹¹⁷, V. A. Kantserov¹¹², J. Kanzaki⁸², L. S. Kaplan¹⁸¹, D. Kar^{33e}, K. Karava¹³⁵, M. J. Kareem^{168b}, S. N. Karpov⁸⁰, Z. M. Karpova⁸⁰, V. Kartvelishvili⁹⁰, A. N. Karyukhin¹²³, L. Kashif¹⁸¹, R. D. Kass¹²⁷, A. Kastanas^{45a,45b}, C. Kato^{60c,60d}, J. Katzy⁴⁶, K. Kawade¹⁵⁰, K. Kawagoe⁸⁸, T. Kawaguchi¹¹⁷, T. Kawamoto¹⁴⁵, G. Kawamura⁵³, E. F. Kay¹⁷⁶, V. F. Kazanin^{122a,122b}, R. Keeler¹⁷⁶, R. Kehoe⁴², J. S. Keller³⁴, E. Kellermann⁹⁷, D. Kelsey¹⁵⁶, J. J. Kempster²¹, J. Kendrick²¹, K. E. Kennedy³⁹, O. Kepka¹⁴¹, S. Kersten¹⁸², B. P. Kerševan⁹², S. Ketabchi Haghighat¹⁶⁷, M. Khader¹⁷³, F. Khalil-Zada¹³, M. Khandoga¹⁴⁵, A. Khanov¹³⁰, A. G. Kharlamov^{122a,122b}, T. Kharlamova^{122a,122b}, E. E. Khoda¹⁷⁵, A. Khodinov¹⁶⁶, T. J. Khoo⁵⁴, E. Khramov⁸⁰, J. Khubua^{159b}, S. Kido⁸³, M. Kiehn⁵⁴, C. R. Kilby⁹⁴, Y. K. Kim³⁷, N. Kimura⁹⁵, O. M. Kind¹⁹, B. T. King^{91,*}, D. Kirchmeier⁴⁸, J. Kirk¹⁴⁴, A. E. Kiryunin¹¹⁵, T. Kishimoto¹⁶³, D. P. Kisliuk¹⁶⁷, V. Kitali⁴⁶, O. Kivernyk⁵, T. Klapdor-Kleingrothaus⁵², M. Klassen^{61a}, M. H. Klein¹⁰⁶, M. Klein⁹¹, U. Klein⁹¹, K. Kleinknecht¹⁰⁰, P. Klimek¹²¹, A. Klimentov²⁹, T. Klingl²⁴, T. Klioutchnikova³⁶, F. F. Klitzner¹¹⁴, P. Kluit¹²⁰, S. Kluth¹¹⁵, E. Kneringer⁷⁷, E. B. F. G. Knoops¹⁰², A. Knue⁵², D. Kobayashi⁸⁸, T. Kobayashi¹⁶³, M. Kobel⁴⁸, M. Kocian¹⁵³, P. Kodys¹⁴³, P. T. Koenig²⁴, T. Koffas³⁴, N. M. Köhler³⁶, T. Koi¹⁵³, M. Kolb¹⁴⁵, I. Koletsou⁵, T. Komarek¹³¹, T. Kondo⁸², K. Köneke⁵², A. X. Y. Kong¹, A. C. König¹¹⁹, T. Kono¹²⁶, R. Konoplich^{125,aj}, V. Konstantinides⁹⁵, N. Konstantinidis⁹⁵, B. Konya⁹⁷, R. Kopeliansky⁶⁶, S. Koperny^{84a}, K. Korcyl⁸⁵, K. Kordas¹⁶², G. Koren¹⁶¹, A. Korn⁹⁵, I. Korolkov¹⁴, E. V. Korolkova¹⁴⁹, N. Korotkova¹¹³, O. Kortner¹¹⁵, S. Kortner¹¹⁵, T. Kosek¹⁴³, V. V. Kostyukhin^{149,166}, A. Kotskechagia⁶⁵, A. Kotwal⁴⁹, A. Koulouris¹⁰, A. Kourkoumeli-Charalampidi^{71a,71b}, C. Kourkoumelis⁹, E. Kourlitis¹⁴⁹, V. Kouskoura²⁹, A. B. Kowalewska⁸⁵, R. Kowalewski¹⁷⁶, C. Kozakai¹⁶³, W. Kozanecki¹⁴⁵, A. S. Kozhin¹²³, V. A. Kramarenko¹¹³, G. Kramberger⁹², D. Krasnopevtsev^{60a}, M. W. Krasny¹³⁶, A. Krasznahorkay³⁶, D. Krauss¹¹⁵, J. A. Kremer^{84a}, J. Kretzschmar⁹¹, P. Krieger¹⁶⁷, F. Krieter¹¹⁴, A. Krishnan^{61b}, K. Krizka¹⁸, K. Kroeninger⁴⁷, H. Kroha¹¹⁵, J. Kroll¹⁴¹, J. Kroll¹³⁷, K. S. Krowpman¹⁰⁷, J. Krstic¹⁶, U. Kruchonak⁸⁰, H. Krüger²⁴, N. Krumnack⁷⁹, M. C. Kruse⁴⁹, J. A. Krzysiak⁸⁵, T. Kubota¹⁰⁵, O. Kuchinskaia¹⁶⁶, S. Kuday^{4b}, J. T. Kuechler⁴⁶, S. Kuehn³⁶, A. Kugel^{61a}, T. Kuhl⁴⁶, V. Kukhtin⁸⁰, R. Kukla¹⁰², Y. Kulchitsky^{108,ah}, S. Kuleshov^{147c}, Y. P. Kulinich¹⁷³, M. Kuna⁵⁸, T. Kunigo⁸⁶, A. Kupco¹⁴¹, T. Kupfer⁴⁷, O. Kuprash⁵², H. Kurashige⁸³, L. L. Kurchaninov^{168a}, Y. A. Kurochkin¹⁰⁸, A. Kurova¹¹², M. G. Kurth^{15a,15d}, E. S. Kuwertz³⁶, M. Kuze¹⁶⁵, A. K. Kvam¹⁴⁸, J. Kvita¹³¹, T. Kwan¹⁰⁴, A. La Rosa¹¹⁵, L. La Rotonda^{41a,41b}, F. La Ruffa^{41a,41b}, C. Lacasta¹⁷⁴, F. Lacava^{73a,73b}, D. P. J. Lack¹⁰¹, H. Lacker¹⁹, D. Lacour¹³⁶, E. Ladygin⁸⁰, R. Lafaye⁵, B. Laforge¹³⁶, T. Lagouri^{33e}, S. Lai⁵³, I. K. Lakomic^{84a},

S. Lammers⁶⁶, W. Lampl⁷, C. Lampoudis¹⁶², E. Lançon²⁹, U. Landgraf⁵², M. P. J. Landon⁹³, M. C. Lanfermann⁵⁴, V. S. Lang⁴⁶, J. C. Lange⁵³, R. J. Langenberg¹⁰³, A. J. Lankford¹⁷¹, F. Lanni²⁹, K. Lantzsch²⁴, A. Lanza^{71a}, A. Lapertosa^{55a,55b}, S. Laplace¹³⁶, J. F. Laporte¹⁴⁵, T. Lari^{69a}, F. Lasagni Manghi^{23b,23a}, M. Lassnig³⁶, T. S. Lau^{63a}, A. Laudrain⁶⁵, A. Laurier³⁴, M. Lavorgna^{70a,70b}, S. D. Lawlor⁹⁴, M. Lazzaroni^{69a,69b}, B. Le¹⁰⁵, E. Le Guirriec¹⁰², M. LeBlanc⁷, T. LeCompte⁶, F. Ledroit-Guillon⁵⁸, A. C. A. Lee⁹⁵, C. A. Lee²⁹, G. R. Lee¹⁷, L. Lee⁵⁹, S. C. Lee¹⁵⁸, S. J. Lee³⁴, S. Lee⁷⁹, B. Lefebvre^{168a}, H. P. Lefebvre⁹⁴, M. Lefebvre¹⁷⁶, C. Leggett¹⁸, K. Lehmann¹⁵², N. Lehmann¹⁸², G. Lehmann Miotto³⁶, W. A. Leight⁴⁶, A. Leisos^{162,x}, M. A. L. Leite^{81d}, C. E. Leitgeb¹¹⁴, R. Leitner¹⁴³, D. Lellouch^{180,*}, K. J. C. Leney⁴², T. Lenz²⁴, R. Leone⁷, S. Leone^{72a}, C. Leonidopoulos⁵⁰, A. Leopold¹³⁶, C. Leroy¹¹⁰, R. Les¹⁶⁷, C. G. Lester³², M. Levchenko¹³⁸, J. Levêque⁵, D. Levin¹⁰⁶, L. J. Levinson¹⁸⁰, D. J. Lewis²¹, B. Li^{15b}, B. Li¹⁰⁶, C.-Q. Li^{60a}, F. Li^{60c}, H. Li^{60a}, H. Li^{60b}, J. Li^{60c}, K. Li¹⁵³, L. Li^{60c}, M. Li^{15a,15d}, Q. Li^{15a,15d}, Q. Y. Li^{60a}, S. Li^{60c,60d}, X. Li⁴⁶, Y. Li⁴⁶, Z. Li^{60b}, Z. Liang^{15a}, B. Liberti^{74a}, A. Liblong¹⁶⁷, K. Lie^{63c}, S. Lim²⁹, C. Y. Lin³², K. Lin¹⁰⁷, T. H. Lin¹⁰⁰, R. A. Linck⁶⁶, J. H. Lindon²¹, A. L. Lioni⁵⁴, E. Lipeles¹³⁷, A. Lipniacka¹⁷, T. M. Liss^{173,ap}, A. Lister¹⁷⁵, J. D. Little⁸, B. Liu⁷⁹, B. L. Liu⁶, H. B. Liu²⁹, H. Liu¹⁰⁶, J. B. Liu^{60a}, J. K. K. Liu³⁷, K. Liu¹³⁶, M. Liu^{60a}, P. Liu¹⁸, Y. Liu^{15a,15d}, Y. L. Liu¹⁰⁶, Y. W. Liu^{60a}, M. Livan^{71a,71b}, A. Lleres⁵⁸, J. Llorente Merino¹⁵², S. L. Lloyd⁹³, C. Y. Lo^{63b}, F. Lo Sterzo⁴², E. M. Lobodzinska⁴⁶, P. Loch⁷, S. Loffredo^{74a,74b}, T. Lohse¹⁹, K. Lohwasser¹⁴⁹, M. Lokajicek¹⁴¹, J. D. Long¹⁷³, R. E. Long⁹⁰, L. Longo³⁶, K. A. Looper¹²⁷, J. A. Lopez^{147c}, I. Lopez Paz¹⁰¹, A. Lopez Solis¹⁴⁹, J. Lorenz¹¹⁴, N. Lorenzo Martinez⁵, A. M. Lory¹¹⁴, M. Losada²², P. J. Lösel¹¹⁴, A. Lösle⁵², X. Lou⁴⁶, X. Lou^{15a}, A. Lounis⁶⁵, J. Love⁶, P. A. Love⁹⁰, J. J. Lozano Bahilo¹⁷⁴, M. Lu^{60a}, Y. J. Lu⁶⁴, H. J. Lubatti¹⁴⁸, C. Luci^{73a,73b}, A. Lucotte⁵⁸, C. Luedtke⁵², F. Luehring⁶⁶, I. Luise¹³⁶, L. Luminari^{73a}, B. Lund-Jensen¹⁵⁴, M. S. Lutz¹⁰³, D. Lynn²⁹, H. Lyons⁹¹, R. Lysak¹⁴¹, E. Lytken⁹⁷, F. Lyu^{15a}, V. Lyubushkin⁸⁰, T. Lyubushkina⁸⁰, H. Ma²⁹, L. L. Ma^{60b}, Y. Ma^{60b}, G. Maccarrone⁵¹, A. Macchiolo¹¹⁵, C. M. Macdonald¹⁴⁹, J. Machado Miguens¹³⁷, D. Madaffari¹⁷⁴, R. Madar³⁸, W. F. Mader⁴⁸, M. Madugoda Ralalage Don¹³⁰, N. Madysa⁴⁸, J. Maeda⁸³, T. Maeno²⁹, M. Maerker⁴⁸, A. S. Maevskiy¹¹³, V. Magerl⁵², N. Magini⁷⁹, D. J. Mahon³⁹, C. Maidantchik^{81b}, T. Maier¹¹⁴, A. Maio^{140a,140b,140d}, K. Maj^{84a}, O. Majersky^{28a}, S. Majewski¹³², Y. Makida⁸², N. Makovec⁶⁵, B. Malaescu¹³⁶, Pa. Malecki⁸⁵, V. P. Maleev¹³⁸, F. Malek⁵⁸, U. Mallik⁷⁸, D. Malon⁶, C. Malone³², S. Maltezos¹⁰, S. Malyukov⁸⁰, J. Mamuzic¹⁷⁴, G. Mancini⁵¹, I. Mandić⁹², L. Manhaes de Andrade Filho^{81a}, I. M. Maniatis¹⁶², J. Manjarres Ramos⁴⁸, K. H. Mankinen⁹⁷, A. Mann¹¹⁴, A. Manousos⁷⁷, B. Mansoulie¹⁴⁵, I. Manthos¹⁶², S. Manzoni¹²⁰, A. Marantis¹⁶², G. Marceca³⁰, L. Marchese¹³⁵, G. Marchiori¹³⁶, M. Marcisovsky¹⁴¹, L. Marcoccia^{74a,74b}, C. Marcon⁹⁷, C. A. Marin Tobon³⁶, M. Marjanovic¹²⁹, Z. Marshall¹⁸, M. U. F. Martensson¹⁷², S. Marti-Garcia¹⁷⁴, C. B. Martin¹²⁷, T. A. Martin¹⁷⁸, V. J. Martin⁵⁰, B. Martin di t Latour¹⁷, L. Martinelli^{75a,75b}, M. Martinez^{14,z}, V. I. Martinez Outschoorn¹⁰³, S. Martin-Haugh¹⁴⁴, V. S. Martoiu^{27b}, A. C. Martyniuk⁹⁵, A. Marzin³⁶, S. R. Maschek¹¹⁵, L. Masetti¹⁰⁰, T. Mashimo¹⁶³, R. Mashinistov¹¹¹, J. Masik¹⁰¹, A. L. Maslennikov^{122a,122b}, L. Massa^{23a,23b}, P. Massarotti^{70a,70b}, P. Mastrandrea^{72a,72b}, A. Mastroberardino^{41a,41b}, T. Masubuchi¹⁶³, D. Matakias¹⁰, A. Matic¹¹⁴, N. Matsuzawa¹⁶³, P. Mättig²⁴, J. Maurer^{27b}, B. Maček⁹², D. A. Maximov^{122a,122b}, R. Mazini¹⁵⁸, I. Maznas¹⁶², S. M. Mazza¹⁴⁶, S. P. Mc Kee¹⁰⁶, T. G. McCarthy¹¹⁵, W. P. McCormack¹⁸, E. F. McDonald¹⁰⁵, J. A. Mcfayden³⁶, G. Mchedlidze^{159b}, M. A. McKay⁴², K. D. McLean¹⁷⁶, S. J. McMahon¹⁴⁴, P. C. McNamara¹⁰⁵, C. J. McNicol¹⁷⁸, R. A. McPherson^{176,ae}, J. E. Mdhluli^{33e}, Z. A. Meadows¹⁰³, S. Meehan³⁶, T. Megy⁵², S. Mehlhase¹¹⁴, A. Mehta⁹¹, T. Meideck⁵⁸, B. Meirose⁴³, D. Melini¹⁶⁰, B. R. Mellado Garcia^{33e}, J. D. Mellenthin⁵³, M. Melo^{28a}, F. Meloni⁴⁶, A. Melzer²⁴, S. B. Menary¹⁰¹, E. D. Mendes Gouveia^{140a,140e}, L. Meng³⁶, X. T. Meng¹⁰⁶, S. Menke¹¹⁵, E. Meoni^{41a,41b}, S. Mergelmeyer¹⁹, S. A. M. Merkt¹³⁹, C. Merlassino¹³⁵, P. Mermod⁵⁴, L. Merola^{70a,70b}, C. Meroni^{69a}, G. Merz¹⁰⁶, O. Meshkov^{113,111}, J. K. R. Meshreki¹⁵¹, A. Messina^{73a,73b}, J. Metcalfe⁶, A. S. Mete¹⁷¹, C. Meyer⁶⁶, J.-P. Meyer¹⁴⁵, H. Meyer Zu Theenhausen^{61a}, F. Miano¹⁵⁶, M. Michetti¹⁹, R. P. Middleton¹⁴⁴, L. Mijović⁵⁰, G. Mikenberg¹⁸⁰, M. Mikesikova¹⁴¹, M. Mikuž⁹², H. Mildner¹⁴⁹, M. Milesi¹⁰⁵, A. Milic¹⁶⁷, D. A. Millar⁹³, D. W. Miller³⁷, A. I. Milov¹⁸⁰, D. A. Milstead^{45a,45b}, R. A. Mina¹⁵³, A. A. Minaenko¹²³, M. Miñano Moya¹⁷⁴, I. A. Minashvili^{159b}, A. I. Mincer¹²⁵, B. Mindur^{84a}, M. Mineev⁸⁰, Y. Minegishi¹⁶³, L. M. Mir¹⁴, A. Mirto^{68a,68b}, K. P. Mistry¹³⁷, T. Mitani¹⁷⁹, J. Mitrevski¹¹⁴, V. A. Mitsou¹⁷⁴, M. Mittal^{60c}, O. Miu¹⁶⁷, A. Miucci²⁰, P. S. Miyagawa¹⁴⁹, A. Mizukami⁸², J. U. Mjörnmark⁹⁷, T. Mkrtchyan^{61a}, M. Mlynarikova¹⁴³, T. Moa^{45a,45b}, K. Mochizuki¹¹⁰, P. Mogg⁵², S. Mohapatra³⁹, R. Moles-Valls²⁴, M. C. Mondragon¹⁰⁷, K. Mönig⁴⁶, J. Monk⁴⁰, E. Monnier¹⁰², A. Montalbano¹⁵², J. Montejo Berlingen³⁶, M. Montella⁹⁵, F. Monticelli⁸⁹, S. Monzani^{69a}, N. Morange⁶⁵, D. Moreno²², M. Moreno Llacer¹⁷⁴, C. Moreno Martinez¹⁴, P. Morettini^{55b}, M. Morgenstern¹²⁰, S. Morgenstern⁴⁸, D. Mori¹⁵², M. Morii⁵⁹, M. Morinaga¹⁷⁹, V. Morisbak¹³⁴, A. K. Morley³⁶, G. Mornacchi³⁶, A. P. Morris⁹⁵, L. Morvaj¹⁵⁵, P. Moschovakos³⁶, B. Moser¹²⁰, M. Mosidze^{159b}, T. Moskalets¹⁴⁵, H. J. Moss¹⁴⁹, J. Moss^{31,m}, E. J. W. Moyse¹⁰³, S. Muanza¹⁰², J. Mueller¹³⁹, R. S. P. Mueller¹¹⁴, D. Muenstermann⁹⁰, G. A. Mullier⁹⁷, D. P. Mungo^{69a,69b}, J. L. Munoz Martinez¹⁴, F. J. Munoz Sanchez¹⁰¹, P. Murin^{28b}, W. J. Murray^{178,144}, A. Murrone^{69a,69b}, M. Muškinja¹⁸, C. Mwewa^{33a}, A. G. Myagkov^{123,ak}, A. A. Myers¹³⁹, J. Myers¹³², M. Myska¹⁴²,

B. P. Nachman¹⁸, O. Nackenhorst⁴⁷, A. Nag Nag⁴⁸, K. Nagai¹³⁵, K. Nagano⁸², Y. Nagasaka⁶², J. L. Nagle²⁹, E. Nagy¹⁰², A. M. Nairz³⁶, Y. Nakahama¹¹⁷, K. Nakamura⁸², T. Nakamura¹⁶³, I. Nakano¹²⁸, H. Nanjo¹³³, F. Napolitano^{61a}, R. F. Naranjo Garcia⁴⁶, R. Narayan⁴², I. Naryshkin¹³⁸, T. Naumann⁴⁶, G. Navarro²², P. Y. Nechaeva¹¹¹, F. Nechansky⁴⁶, T. J. Neep²¹, A. Negri^{71a,71b}, M. Negrini^{23b}, C. Nellist⁵³, M. E. Nelson^{45a,45b}, S. Nemecek¹⁴¹, P. Nemethy¹²⁵, M. Nessi^{36,d}, M. S. Neubauer¹⁷³, M. Neumann¹⁸², R. Newhouse¹⁷⁵, P. R. Newman²¹, C. W. Ng¹³⁹, Y. S. Ng¹⁹, Y. W. Y. Ng¹⁷¹, B. Ngair^{35e}, H. D. N. Nguyen¹⁰², T. Nguyen Manh¹¹⁰, E. Nibigira³⁸, R. B. Nickerson¹³⁵, R. Nicolaidou¹⁴⁵, D. S. Nielsen⁴⁰, J. Nielsen¹⁴⁶, N. Nikiforou¹¹, V. Nikolaenko^{123,ak}, I. Nikolic-Audit¹³⁶, K. Nikolopoulos²¹, P. Nilsson²⁹, H. R. Nindhito⁵⁴, Y. Ninomiya⁸², A. Nisati^{73a}, N. Nishu^{60c}, R. Nisius¹¹⁵, I. Nitsche⁴⁷, T. Nitta¹⁷⁹, T. Nobe¹⁶³, Y. Noguchi⁸⁶, I. Nomidis¹³⁶, M. A. Nomura²⁹, M. Nordberg³⁶, N. Norjoharuddeen¹³⁵, T. Novak⁹², O. Novgorodova⁴⁸, R. Novotny¹⁴², L. Nozka¹³¹, K. Ntekas¹⁷¹, E. Nurse⁹⁵, F. G. Oakham^{34,ar}, H. Oberlack¹¹⁵, J. Ocariz¹³⁶, A. Ochi⁸³, I. Ochoa³⁹, J. P. Ochoa-Ricoux^{147a}, K. O'Connor²⁶, S. Oda⁸⁸, S. Odaka⁸², S. Oerdek⁵³, A. Ogrodnik^{84a}, A. Oh¹⁰¹, S. H. Oh⁴⁹, C. C. Ohm¹⁵⁴, H. Oide¹⁶⁵, M. L. Ojeda¹⁶⁷, H. Okawa¹⁶⁹, Y. Okazaki⁸⁶, M. W. O'Keefe⁹¹, Y. Okumura¹⁶³, T. Okuyama⁸², A. Olariu^{27b}, L. F. Oleiro Seabra^{140a}, S. A. Olivares Pino^{147a}, D. Oliveira Damazio²⁹, J. L. Oliver¹, M. J. R. Olsson¹⁷¹, A. Olszewski⁸⁵, J. Olszowska⁸⁵, D. C. O'Neil¹⁵², A. P. O'Neill¹³⁵, A. Onofre^{140a,140e}, P. U. E. Onyisi¹¹, H. Oppen¹³⁴, M. J. Oreglia³⁷, G. E. Orellana⁸⁹, D. Orestano^{75a,75b}, N. Orlando¹⁴, R. S. Orr¹⁶⁷, V. O'Shea⁵⁷, R. Ospanov^{60a}, G. Otero y Garzon³⁰, H. Otono⁸⁸, P. S. Ott^{61a}, M. Ouchrif^{35d}, J. Ouellette²⁹, F. Ould-Saada¹³⁴, A. Ouraou¹⁴⁵, Q. Ouyang^{15a}, M. Owen⁵⁷, R. E. Owen²¹, V. E. Ozcan^{12c}, N. Ozturk⁸, J. Pacalt¹³¹, H. A. Pacey³², K. Pachal⁴⁹, A. Pacheco Pages¹⁴, C. Padilla Aranda¹⁴, S. Pagan Griso¹⁸, M. Paganini¹⁸³, G. Palacino⁶⁶, S. Palazzo⁵⁰, S. Palestini³⁶, M. Palka^{84b}, D. Pallin³⁸, I. Panagoulas¹⁰, C. E. Pandini³⁶, J. G. Panduro Vazquez⁹⁴, P. Pani⁴⁶, G. Panizzo^{67a,67c}, L. Paolozzi⁵⁴, C. Papadatos¹¹⁰, K. Papageorgiou^{9,g}, S. Parajuli⁴³, A. Paramonov⁶, D. Paredes Hernandez^{63b}, S. R. Paredes Saenz¹³⁵, B. Parida¹⁶⁶, T. H. Park¹⁶⁷, A. J. Parker³¹, M. A. Parker³², F. Parodi^{55a,55b}, E. W. Parrish¹²¹, J. A. Parsons³⁹, U. Parzefall⁵², L. Pascual Dominguez¹³⁶, V. R. Pascuzzi¹⁶⁷, J. M. P. Pasner¹⁴⁶, F. Pasquali¹²⁰, E. Pasqualucci^{73a}, S. Passaggio^{55b}, F. Pastore⁹⁴, P. Pasuwan^{45a,45b}, S. Pataria¹⁰⁰, J. R. Pater¹⁰¹, A. Pathak^{181,i}, J. Patton⁹¹, T. Pauly³⁶, J. Pearkes¹⁵³, B. Pearson¹¹⁵, M. Pedersen¹³⁴, L. Pedraza Diaz¹¹⁹, R. Pedro^{140a}, T. Peiffer⁵³, S. V. Peleganchuk^{122a,122b}, O. Penc¹⁴¹, H. Peng^{60a}, B. S. Peralva^{81a}, M. M. Perego⁶⁵, A. P. Pereira Peixoto^{140a}, D. V. Perepelitsa²⁹, F. Peri¹⁹, L. Perini^{69a,69b}, H. Pernegger³⁶, S. Perrella^{140a}, A. Perrevoort¹²⁰, K. Peters⁴⁶, R. F. Y. Peters¹⁰¹, B. A. Petersen³⁶, T. C. Petersen⁴⁰, E. Petit¹⁰², A. Petridis¹, C. Petridou¹⁶², P. Petroff⁶⁵, M. Petrov¹³⁵, F. Petrucci^{75a,75b}, M. Pettee¹⁸³, N. E. Pettersson¹⁰³, K. Petukhova¹⁴³, A. Peyaud¹⁴⁵, R. Pezoa^{147c}, L. Pezzotti^{71a,71b}, T. Pham¹⁰⁵, F. H. Phillips¹⁰⁷, P. W. Phillips¹⁴⁴, M. W. Phipps¹⁷³, G. Piacquadio¹⁵⁵, E. Pianori¹⁸, A. Picazio¹⁰³, R. H. Pickles¹⁰¹, R. Piegai³⁰, D. Pietreanu^{27b}, J. E. Pilcher³⁷, A. D. Pilkington¹⁰¹, M. Pinamonti^{67a,67c}, J. L. Pinfold³, M. Pitt¹⁶¹, L. Pizzimento^{74a,74b}, M.-A. Pleier²⁹, V. Pleskot¹⁴³, E. Plotnikova⁸⁰, P. Podberesko^{122a,122b}, R. Poettgen⁹⁷, R. Poggi⁵⁴, L. Poggioli⁶⁵, I. Pogrebnyak¹⁰⁷, D. Pohl²⁴, I. Pokharel⁵³, G. Polesello^{71a}, A. Poley¹⁸, A. Policicchio^{73a,73b}, R. Polifka¹⁴³, A. Polini^{23b}, C. S. Pollard⁴⁶, V. Polychronakos²⁹, D. Ponomarenko¹¹², L. Pontecorvo³⁶, S. Popa^{27a}, G. A. Popeneciu^{27d}, L. Portales⁵, D. M. Portillo Quintero⁵⁸, S. Pospisil¹⁴², K. Potamianos⁴⁶, I. N. Potrap⁸⁰, C. J. Potter³², H. Potti¹¹, T. Poulsen⁹⁷, J. Poveda³⁶, T. D. Powell¹⁴⁹, G. Pownall⁴⁶, M. E. Pozo Astigarraga³⁶, P. Pralavorio¹⁰², S. Prell⁷⁹, D. Price¹⁰¹, M. Primavera^{68a}, S. Prince¹⁰⁴, M. L. Proffitt¹⁴⁸, N. Proklova¹¹², K. Prokofiev^{63c}, F. Prokoshin⁸⁰, S. Protopopescu²⁹, J. Proudfoot⁶, M. Przybycien^{84a}, D. Pudza¹³⁸, A. Puri¹⁷³, P. Puzo⁶⁵, J. Qian¹⁰⁶, Y. Qin¹⁰¹, A. Quadt⁵³, M. Queitsch-Maitland³⁶, A. Qureshi¹, M. Racko^{28a}, F. Ragusa^{69a,69b}, G. Rahal⁹⁸, J. A. Raine⁵⁴, S. Rajagopalan²⁹, A. Ramirez Morales⁹³, K. Ran^{15a,15d}, T. Rashid⁶⁵, S. Raspopov⁵, D. M. Rauch⁴⁶, F. Rauscher¹¹⁴, S. Rave¹⁰⁰, B. Ravina¹⁴⁹, I. Ravinovich¹⁸⁰, J. H. Rawling¹⁰¹, M. Raymond³⁶, A. L. Read¹³⁴, N. P. Readioff⁵⁸, M. Reale^{68a,68b}, D. M. Rebuffi^{71a,71b}, A. Redelbach¹⁷⁷, G. Redlinger²⁹, K. Reeves⁴³, L. Rehnisch¹⁹, J. Reichert¹³⁷, D. Reikher¹⁶¹, A. Reiss¹⁰⁰, A. Rej¹⁵¹, C. Rembser³⁶, M. Renda^{27b}, M. Rescigno^{73a}, S. Resconi^{69a}, E. D. Resseguie¹³⁷, S. Rettie¹⁷⁵, B. Reynolds¹²⁷, E. Reynolds²¹, O. L. Rezanova^{122a,122b}, P. Reznicek¹⁴³, E. Ricci^{76a,76b}, R. Richter¹¹⁵, S. Richter⁴⁶, E. Richter-Was^{84b}, O. Ricken²⁴, M. Ridet¹³⁶, P. Rieck¹¹⁵, O. Rifki⁴⁶, M. Rijssenbeek¹⁵⁵, A. Rimoldi^{71a,71b}, M. Rimoldi⁴⁶, L. Rinaldi^{23b}, G. Ripellino¹⁵⁴, I. Riu¹⁴, J. C. Rivera Vergara¹⁷⁶, F. Rizatdinova¹³⁰, E. Rizvi⁹³, C. Rizzi³⁶, R. T. Roberts¹⁰¹, S. H. Robertson^{104,ae}, M. Robin⁴⁶, D. Robinson³², J. E. M. Robinson⁴⁶, C. M. Robles Gajardo^{147c}, M. Robles Manzano¹⁰⁰, A. Robson⁵⁷, A. Rocchi^{74a,74b}, E. Rocco¹⁰⁰, C. Roda^{72a,72b}, S. Rodriguez Bosca¹⁷⁴, A. Rodriguez Perez¹⁴, D. Rodriguez Rodriguez¹⁷⁴, A. M. Rodríguez Vera^{168b}, S. Roe³⁶, O. Røhne¹³⁴, R. Röhrig¹¹⁵, R. A. Rojas^{147c}, B. Roland⁵², C. P. A. Roland⁶⁶, J. Roloff²⁹, A. Romaniouk¹¹², M. Romano^{23a,23b}, N. Rompotis⁹¹, M. Ronzani¹²⁵, L. Roos¹³⁶, S. Rosati^{73a}, G. Rosin¹⁰³, B. J. Rosser¹³⁷, E. Rossi⁴⁶, E. Rossi^{75a,75b}, E. Rossi^{70a,70b}, L. P. Rossi^{55b}, L. Rossini^{69a,69b}, R. Rosten¹⁴, M. Rotaru^{27b}, J. Rothberg¹⁴⁸, B. Rottler⁵², D. Rousseau⁶⁵, G. Rovelli^{71a,71b}, A. Roy¹¹, D. Roy^{33e}, A. Rozanov¹⁰², Y. Rozen¹⁶⁰, X. Ruan^{33e}, F. Rühr⁵², A. Ruiz-Martinez¹⁷⁴, A. Rummeler³⁶, Z. Rurikova⁵², N. A. Rusakovich⁸⁰, H. L. Russell¹⁰⁴, L. Rustige^{38,47}, J. P. Rutherford⁷, E. M. Rüttinger¹⁴⁹, M. Rybar³⁹

G. Rybkin⁶⁵, E. B. Rye¹³⁴, A. Ryzhov¹²³, J. A. Sabater Iglesias⁴⁶, P. Sabatini⁵³, G. Sabato¹²⁰, S. Sacerdoti⁶⁵, H. F.-W. Sadrozinski¹⁴⁶, R. Sadykov⁸⁰, F. Safai Tehrani^{73a}, B. Safarzadeh Samani¹⁵⁶, M. Safdari¹⁵³, P. Saha¹²¹, S. Saha¹⁰⁴, M. Sahinsoy^{61a}, A. Sahu¹⁸², M. Saimpert⁴⁶, M. Saito¹⁶³, T. Saito¹⁶³, H. Sakamoto¹⁶³, A. Sakharov^{125,aj}, D. Salamani⁵⁴, G. Salamanna^{75a,75b}, J. E. Salazar Loyola^{147c}, A. Salnikov¹⁵³, J. Salt¹⁷⁴, D. Salvatore^{41a,41b}, F. Salvatore¹⁵⁶, A. Salvucci^{63a,63b,63c}, A. Salzburger³⁶, J. Samarati³⁶, D. Sammel⁵², D. Sampsonidis¹⁶², D. Sampsonidou¹⁶², J. Sánchez¹⁷⁴, A. Sanchez Pineda^{67a,36,67c}, H. Sandaker¹³⁴, C. O. Sander⁴⁶, I. G. Sanderswood⁹⁰, M. Sandhoff¹⁸², C. Sandoval²², D. P. C. Sankey¹⁴⁴, M. Sannino^{55a,55b}, Y. Sano¹¹⁷, A. Sansoni⁵¹, C. Santoni³⁸, H. Santos^{140a,140b}, S. N. Santpur¹⁸, A. Santra¹⁷⁴, A. Saponov⁸⁰, J. G. Saraiva^{140a,140d}, O. Sasaki⁸², K. Sato¹⁶⁹, F. Sauerburger⁵², E. Sauvan⁵, P. Savard^{167,ar}, R. Sawada¹⁶³, C. Sawyer¹⁴⁴, L. Sawyer^{96,ai}, C. Sbarra^{23b}, A. Sbrizzi^{23a}, T. Scanlon⁹⁵, J. Schaarschmidt¹⁴⁸, P. Schacht¹¹⁵, B. M. Schachtner¹¹⁴, D. Schaefer³⁷, L. Schaefer¹³⁷, J. Schaeffer¹⁰⁰, S. Schaepe³⁶, U. Schäfer¹⁰⁰, A. C. Schaffer⁶⁵, D. Schaile¹¹⁴, R. D. Schamberger¹⁵⁵, N. Scharmberg¹⁰¹, V. A. Schegelsky¹³⁸, D. Scheirich¹⁴³, F. Schenck¹⁹, M. Schernau¹⁷¹, C. Schiavi^{55a,55b}, S. Schier¹⁴⁶, L. K. Schildgen²⁴, Z. M. Schillaci²⁶, E. J. Schioppa³⁶, M. Schioppa^{41a,41b}, K. E. Schleicher⁵², S. Schlenker³⁶, K. R. Schmidt-Sommerfeld¹¹⁵, K. Schmieden³⁶, C. Schmitt¹⁰⁰, S. Schmitt⁴⁶, S. Schmitz¹⁰⁰, J. C. Schmoeckel⁴⁶, U. Schnoor⁵², L. Schoeffel¹⁴⁵, A. Schoening^{61b}, P. G. Scholer⁵², E. Schopf¹³⁵, M. Schott¹⁰⁰, J. F. P. Schouwenberg¹¹⁹, J. Schovancova³⁶, S. Schramm⁵⁴, F. Schroeder¹⁸², A. Schulte¹⁰⁰, H.-C. Schultz-Coulon^{61a}, M. Schumacher⁵², B. A. Schumm¹⁴⁶, Ph. Schune¹⁴⁵, A. Schwartzman¹⁵³, T. A. Schwarz¹⁰⁶, Ph. Schwemling¹⁴⁵, R. Schwienhorst¹⁰⁷, A. Sciandra¹⁴⁶, G. Sciolla²⁶, M. Scodeggio⁴⁶, M. Scornajenghi^{41a,41b}, F. Scuri^{72a}, F. Scutti¹⁰⁵, L. M. Scyboz¹¹⁵, C. D. Sebastiani^{73a,73b}, P. Seema¹⁹, S. C. Seidel¹¹⁸, A. Seiden¹⁴⁶, B. D. Seidlitz²⁹, T. Seiss³⁷, J. M. Seixas^{81b}, G. Sekhniaidze^{70a}, K. Sekhon¹⁰⁶, S. J. Sekula⁴², N. Semprini-Cesari^{23a,23b}, S. Sen⁴⁹, C. Serfon⁷⁷, L. Serin⁶⁵, L. Serkin^{67a,67b}, M. Sessa^{60a}, H. Severini¹²⁹, S. Sevova¹⁵³, T. Šfiligoj⁹², F. Sforza^{55a,55b}, A. Sfyrila⁵⁴, E. Shabalina⁵³, J. D. Shahinian¹⁴⁶, N. W. Shaikh^{45a,45b}, D. Shaked Renous¹⁸⁰, L. Y. Shan^{15a}, J. T. Shank²⁵, M. Shapiro¹⁸, A. Sharma¹³⁵, A. S. Sharma¹, P. B. Shatalov¹²⁴, K. Shaw¹⁵⁶, S. M. Shaw¹⁰¹, M. Shehade¹⁸⁰, Y. Shen¹²⁹, A. D. Sherman²⁵, P. Sherwood⁹⁵, L. Shi¹⁵⁸, S. Shimizu⁸², C. O. Shimmin¹⁸³, Y. Shimogama¹⁷⁹, M. Shimojima¹¹⁶, I. P. J. Shipsey¹³⁵, S. Shirabe¹⁶⁵, M. Shiyakova^{80,ac}, J. Shlomi¹⁸⁰, A. Shmeleva¹¹¹, M. J. Shochet³⁷, J. Shojaii¹⁰⁵, D. R. Shope¹²⁹, S. Shrestha¹²⁷, E. M. Shrif^{33e}, E. Shulga¹⁸⁰, P. Sicho¹⁴¹, A. M. Sickles¹⁷³, P. E. Sidebo¹⁵⁴, E. Sideras Haddad^{33e}, O. Sidiropoulou³⁶, A. Sidoti^{23a,23b}, F. Siegert⁴⁸, Dj. Sijacki¹⁶, M. Jr. Silva¹⁸¹, M. V. Silva Oliveira^{81a}, S. B. Silverstein^{45a}, S. Simion⁶⁵, R. Simoniello¹⁰⁰, S. Simsek^{12b}, P. Sinervo¹⁶⁷, V. Sinetckii¹¹³, N. B. Sinev¹³², S. Singh¹⁵², M. Sioli^{23a,23b}, I. Siral¹³², S. Yu. Sivoklov¹¹³, J. Sjölin^{45a,45b}, E. Skorda⁹⁷, P. Skubic¹²⁹, M. Slawinska⁸⁵, K. Sliwa¹⁷⁰, R. Slovak¹⁴³, V. Smakhtin¹⁸⁰, B. H. Smart¹⁴⁴, J. Smiesko^{28a}, N. Smirnov¹¹², S. Yu. Smirnov¹¹², Y. Smirnov¹¹², L. N. Smirnova^{113,u}, O. Smirnova⁹⁷, J. W. Smith⁵³, M. Smizanska⁹⁰, K. Smolek¹⁴², A. Smykiewicz⁸⁵, A. A. Snesarev¹¹¹, H. L. Snoek¹²⁰, I. M. Snyder¹³², S. Snyder²⁹, R. Sobie^{176,ac}, A. Soffer¹⁶¹, A. Sogaard⁵⁰, F. Sohns⁵³, C. A. Solans Sanchez³⁶, E. Yu. Soldatov¹¹², U. Soldevila¹⁷⁴, A. A. Solodkov¹²³, A. Soloshenko⁸⁰, O. V. Solovyanov¹²³, V. Solovye¹³⁸, P. Sommer¹⁴⁹, H. Son¹⁷⁰, W. Song¹⁴⁴, W. Y. Song^{168b}, A. Sopczak¹⁴², A. L. Sopio⁹⁵, F. Sopkova^{28b}, C. L. Sotiropoulou^{72a,72b}, S. Sottocornola^{71a,71b}, R. Soualah^{67a,67c,f}, A. M. Soukharev^{122a,122b}, D. South⁴⁶, S. Spagnolo^{68a,68b}, M. Spalla¹¹⁵, M. Spangenberg¹⁷⁸, F. Spanò⁹⁴, D. Sperlich⁵², T. M. Spieker^{61a}, G. Spigo³⁶, M. Spina¹⁵⁶, D. P. Spiteri⁵⁷, M. Spousta¹⁴³, A. Stabile^{69a,69b}, B. L. Stamas¹²¹, R. Stamen^{61a}, M. Stamenkovic¹²⁰, E. Stanecka⁸⁵, B. Stanislaus¹³⁵, M. M. Stanitzki⁴⁶, M. Stankaityte¹³⁵, B. Stapf¹²⁰, E. A. Starchenko¹²³, G. H. Stark¹⁴⁶, J. Stark⁵⁸, S. H. Stark⁴⁰, P. Staroba¹⁴¹, P. Starovoitov^{61a}, S. Stärz¹⁰⁴, R. Staszewski⁸⁵, G. Stavropoulos⁴⁴, M. Stegler⁴⁶, P. Steinberg²⁹, A. L. Steinhebel¹³², B. Stelzer¹⁵², H. J. Stelzer¹³⁹, O. Stelzer-Chilton^{168a}, H. Stenzel⁵⁶, T. J. Stevenson¹⁵⁶, G. A. Stewart³⁶, M. C. Stockton³⁶, G. Stoica^{27b}, M. Stolarski^{140a}, S. Stonjek¹¹⁵, A. Straessner⁴⁸, J. Strandberg¹⁵⁴, S. Strandberg^{45a,45b}, M. Strauss¹²⁹, P. Strizenec^{28b}, R. Ströhmer¹⁷⁷, D. M. Strom¹³², R. Stroynowski⁴², A. Strubig⁵⁰, S. A. Stucci²⁹, B. Stugu¹⁷, J. Stupak¹²⁹, N. A. Styles⁴⁶, D. Su¹⁵³, S. Suchek^{61a}, V. V. Sulin¹¹¹, M. J. Sullivan⁹¹, D. M. S. Sultan⁵⁴, S. Sultansoy^{4c}, T. Sumida⁸⁶, S. Sun¹⁰⁶, X. Sun³, K. Suruliz¹⁵⁶, C. J. E. Suster¹⁵⁷, M. R. Sutton¹⁵⁶, S. Suzuki⁸², M. Svatos¹⁴¹, M. Swiatlowski³⁷, S. P. Swift², T. Swirski¹⁷⁷, A. Sydorenko¹⁰⁰, I. Sykora^{28a}, M. Sykora¹⁴³, T. Sykora¹⁴³, D. Ta¹⁰⁰, K. Tackmann^{46,aa}, J. Taenzer¹⁶¹, A. Taffard¹⁷¹, R. Tafirout^{168a}, H. Takai²⁹, R. Takashima⁸⁷, K. Takeda⁸³, T. Takeshita¹⁵⁰, E. P. Takeva⁵⁰, Y. Takubo⁸², M. Talby¹⁰², A. A. Talyshev^{122a,122b}, N. M. Tamir¹⁶¹, J. Tanaka¹⁶³, M. Tanaka¹⁶⁵, R. Tanaka⁶⁵, S. Tapia Araya¹⁷³, S. Tapprogge¹⁰⁰, A. Tarek Abouelfadl Mohamed¹³⁶, S. Tarem¹⁶⁰, K. Tariq^{60b}, G. Tarna^{27b,c}, G. F. Tartarelli^{69a}, P. Tas¹⁴³, M. Tasevsky¹⁴¹, T. Tashiro⁸⁶, E. Tassi^{41a,41b}, A. Tavares Delgado^{140a}, Y. Tayalati^{35e}, A. J. Taylor⁵⁰, G. N. Taylor¹⁰⁵, W. Taylor^{168b}, A. S. Tee⁹⁰, R. Teixeira De Lima¹⁵³, P. Teixeira-Dias⁹⁴, H. Ten Kate³⁶, J. J. Teoh¹²⁰, S. Terada⁸², K. Terashi¹⁶³, J. Terron⁹⁹, S. Terzo¹⁴, M. Testa⁵¹, R. J. Teuscher^{167,ac}, S. J. Thais¹⁸³, T. Theveneaux-Pelzer⁴⁶, F. Thiele⁴⁰, D. W. Thomas⁹⁴, J. O. Thomas⁴², J. P. Thomas²¹, P. D. Thompson²¹, L. A. Thomsen¹⁸³, E. Thomson¹³⁷, E. J. Thorpe⁹³, R. E. Ticse Torres⁵³, V. O. Tikhomirov^{111,al}, Yu. A. Tikhonov^{122a,122b}, S. Timoshenko¹¹², P. Tipton¹⁸³, S. Tisserant¹⁰², K. Todome^{23a,23b}, S. Todorova-Nova⁵,

S. Todt⁴⁸, J. Tojo⁸⁸, S. Tokár^{28a}, K. Tokushuku⁸², E. Tolley¹²⁷, K. G. Tomiwa^{33e}, M. Tomoto¹¹⁷, L. Tompkins^{153,p}, B. Tong⁵⁹, P. Tornambe¹⁰³, E. Torrence¹³², H. Torres⁴⁸, E. Torró Pastor¹⁴⁸, C. Tosiri¹³⁵, J. Toth^{102,ad}, D. R. Tovey¹⁴⁹, A. Traeet¹⁷, C. J. Treado¹²⁵, T. Trefzger¹⁷⁷, F. Tresoldi¹⁵⁶, A. Tricoli²⁹, I. M. Trigger^{168a}, S. Trincas-Duvold¹³⁶, D. T. Trischuk¹⁷⁵, W. Trischuk¹⁶⁷, B. Trocme⁵⁸, A. Trofymov¹⁴⁵, C. Troncon^{69a}, M. Trovatelli¹⁷⁶, F. Trovato¹⁵⁶, L. Truong^{33c}, M. Trzebinski⁸⁵, A. Trzupek⁸⁵, F. Tsai⁴⁶, J. C.-L. Tseng¹³⁵, P. V. Tsiarshka^{108,ah}, A. Tsirigotis^{162,x}, V. Tsiskaridze¹⁵⁵, E. G. Tskhadadze^{159a}, M. Tsopoulou¹⁶², I. I. Tsukerman¹²⁴, V. Tsulaia¹⁸, S. Tsuno⁸², D. Tsybychev¹⁵⁵, Y. Tu^{63b}, A. Tudorache^{27b}, V. Tudorache^{27b}, T. T. Tulbure^{27a}, A. N. Tuna⁵⁹, S. Turchikhin⁸⁰, D. Turgeman¹⁸⁰, I. Turk Cakir^{4b,v}, R. J. Turner²¹, R. T. Turra^{69a}, P. M. Tuts³⁹, S. Tzamarias¹⁶², E. Tzovara¹⁰⁰, G. Uccielli⁴⁷, K. Uchida¹⁶³, I. Ueda⁸², F. Ukegawa¹⁶⁹, G. Unal³⁶, A. Undrus²⁹, G. Unel¹⁷¹, F. C. Ungaro¹⁰⁵, Y. Unno⁸², K. Uno¹⁶³, J. Urban^{28b}, P. Urquijo¹⁰⁵, G. Usai⁸, Z. Uysal^{12d}, V. Vacek¹⁴², B. Vachon¹⁰⁴, K. O. H. Vadla¹³⁴, A. Vaidya⁹⁵, C. Valderanis¹¹⁴, E. Valdes Santurio^{45a,45b}, M. Valente⁵⁴, S. Valentinetti^{23a,23b}, A. Valero¹⁷⁴, L. Valéry⁴⁶, R. A. Vallance²¹, A. Vallier³⁶, J. A. Valls Ferrer¹⁷⁴, T. R. Van Daalen¹⁴, P. Van Gemmeren⁶, I. Van Vulpen¹²⁰, M. Vanadia^{74a,74b}, W. Vandelli³⁶, M. Vandenbroucke¹⁴⁵, E. R. Vandewall¹³⁰, A. Vaniachine¹⁶⁶, D. Vannicola^{73a,73b}, R. Vari^{73a}, E. W. Varnes⁷, C. Varni^{55a,55b}, T. Varol¹⁵⁸, D. Varouchas⁶⁵, K. E. Varvell¹⁵⁷, M. E. Vasile^{27b}, G. A. Vazquez¹⁷⁶, F. Vazeille³⁸, D. Vazquez Furelos¹⁴, T. Vazquez Schroeder³⁶, J. Veatch⁵³, V. Vecchio^{75a,75b}, M. J. Veen¹²⁰, L. M. Veloce¹⁶⁷, F. Veloso^{140a,140c}, S. Veneziano^{73a}, A. Ventura^{68a,68b}, N. Venturi³⁶, A. Verbytskyi¹¹⁵, V. Vercesi^{71a}, M. Verducci^{72a,72b}, C. M. Vergel Infante⁷⁹, C. Vergis²⁴, W. Verkerke¹²⁰, A. T. Vermeulen¹²⁰, J. C. Vermeulen¹²⁰, M. C. Vetterli^{152,ar}, N. Viaux Maira^{147c}, M. Vicente Barreto Pinto⁵⁴, T. Vickey¹⁴⁹, O. E. Vickey Boeriu¹⁴⁹, G. H. A. Viehhauser¹³⁵, L. Vignani^{61b}, M. Villa^{23a,23b}, M. Villaplana Perez³, E. Vilucchi⁵¹, M. G. Vinciter³⁴, G. S. Virdee²¹, A. Vishwakarma⁴⁶, C. Vittori^{23a,23b}, I. Vivarelli¹⁵⁶, M. Vogel¹⁸², P. Vokac¹⁴², S. E. von Buddenbrock^{33e}, E. Von Toerne²⁴, V. Vorobel¹⁴³, K. Vorobev¹¹², M. Vos¹⁷⁴, J. H. Vossebeld⁹¹, M. Vozak¹⁰¹, N. Vranjes¹⁶, M. Vranjes Milosavljevic¹⁶, V. Vrba¹⁴², M. Vreeswijk¹²⁰, R. Vuillemet³⁶, I. Vukotic³⁷, P. Wagner²⁴, W. Wagner¹⁸², J. Wagner-Kuhr¹¹⁴, S. Wahdan¹⁸², H. Wahlberg⁸⁹, V. M. Walbrecht¹¹⁵, J. Walder⁹⁰, R. Walker¹¹⁴, S. D. Walker⁹⁴, W. Walkowiak¹⁵¹, V. Wallangen^{45a,45b}, A. M. Wang⁵⁹, A. Z. Wang¹⁸¹, C. Wang^{60c}, F. Wang¹⁸¹, H. Wang¹⁸, H. Wang³, J. Wang^{63a}, J. Wang^{61b}, P. Wang⁴², Q. Wang¹²⁹, R.-J. Wang¹⁰⁰, R. Wang^{60a}, R. Wang⁶, S. M. Wang¹⁵⁸, W. T. Wang^{60a}, W. Wang^{15c}, W. X. Wang^{60a}, Y. Wang^{60a}, Z. Wang^{60c}, C. Wanotayaroj⁴⁶, A. Warburton¹⁰⁴, C. P. Ward³², D. R. Wardrope⁹⁵, N. Warrack⁵⁷, A. Washbrook⁵⁰, A. T. Watson²¹, M. F. Watson²¹, G. Watts¹⁴⁸, B. M. Waugh⁹⁵, A. F. Webb¹¹, S. Webb¹⁰⁰, C. Weber¹⁸³, M. S. Weber²⁰, S. A. Weber³⁴, S. M. Weber^{61a}, A. R. Weidberg¹³⁵, J. Weingarten⁴⁷, M. Weirich¹⁰⁰, C. Weiser⁵², P. S. Wells³⁶, T. Wenaus²⁹, T. Wengler³⁶, S. Wenig³⁶, N. Wermes²⁴, M. D. Werner⁷⁹, M. Wessels^{61a}, T. D. Weston²⁰, K. Whalen¹³², N. L. Whallon¹⁴⁸, A. M. Wharton⁹⁰, A. S. White¹⁰⁶, A. White⁸, M. J. White¹, D. Whiteson¹⁷¹, B. W. Whitmore⁹⁰, W. Wiedenmann¹⁸¹, C. Wiel⁴⁸, M. WIELERS¹⁴⁴, N. Wieseotte¹⁰⁰, C. Wiglesworth⁴⁰, L. A. M. Wiik-Fuchs⁵², H. G. Wilkens³⁶, L. J. Wilkins⁹⁴, H. H. Williams¹³⁷, S. Williams³², C. Willis¹⁰⁷, S. Willocq¹⁰³, J. A. Wilson²¹, I. Wingerter-Seez⁵, E. Winkels¹⁵⁶, F. Winklmeier¹³², O. J. Winston¹⁵⁶, B. T. Winter⁵², M. Wittgen¹⁵³, M. Wobisch⁹⁶, A. Wolf¹⁰⁰, T. M. H. Wolf¹²⁰, R. Wolff¹⁰², R. Wölker¹³⁵, J. Wollrath⁵², M. W. Wolter⁸⁵, H. Wolters^{140a,140c}, V. W. S. Wong¹⁷⁵, N. L. Woods¹⁴⁶, S. D. Worm²¹, B. K. Wosiek⁸⁵, K. W. Woźniak⁸⁵, K. Wraight⁵⁷, S. L. Wu¹⁸¹, X. Wu⁵⁴, Y. Wu^{60a}, T. R. Wyatt¹⁰¹, B. M. Wynne⁵⁰, S. Xella⁴⁰, Z. Xi¹⁰⁶, L. Xia¹⁷⁸, X. Xiao¹⁰⁶, I. Xiotidis¹⁵⁶, D. Xu^{15a}, H. Xu^{60a}, L. Xu²⁹, T. Xu¹⁴⁵, W. Xu¹⁰⁶, Z. Xu^{60b}, Z. Xu¹⁵³, B. Yabsley¹⁵⁷, S. Yacoub^{33a}, K. Yajima¹³³, D. P. Yallup⁹⁵, N. Yamaguchi⁸⁸, Y. Yamaguchi¹⁶⁵, A. Yamamoto⁸², M. Yamatani¹⁶³, T. Yamazaki¹⁶³, Y. Yamazaki⁸³, Z. Yan²⁵, H. J. Yang^{60c,60d}, H. T. Yang¹⁸, S. Yang^{60a}, X. Yang^{58,60b}, Y. Yang¹⁶³, W.-M. Yao¹⁸, Y. C. Yap⁴⁶, Y. Yasu⁸², E. Yatsenko^{60c,60d}, H. Ye^{15c}, J. Ye⁴², S. Ye²⁹, I. Yeletsikh⁸⁰, M. R. Yexley⁹⁰, E. Yigitbasi²⁵, K. Yorita¹⁷⁹, K. Yoshihara¹³⁷, C. J. S. Young³⁶, C. Young¹⁵³, J. Yu⁷⁹, R. Yuan^{60b,h}, X. Yue^{61a}, S. P. Y. Yuen²⁴, M. Zaazoua^{35e}, B. Zabinski⁸⁵, G. Zacharis¹⁰, E. Zaffaroni⁵⁴, J. Zahreddine¹³⁶, A. M. Zaitsev^{123,ak}, T. Zakareishvili^{159b}, N. Zakharchuk³⁴, S. Zambito⁵⁹, D. Zanzi³⁶, D. R. Zaripovas⁵⁷, S. V. Zeibner⁴⁷, C. Zeitnitz¹⁸², G. Zemaityte¹³⁵, J. C. Zeng¹⁷³, O. Zenin¹²³, T. Ženiš^{28a}, D. Zerwas⁶⁵, M. Zgubič¹³⁵, B. Zhang^{15c}, D. F. Zhang^{15b}, G. Zhang^{15b}, H. Zhang^{15c}, J. Zhang⁶, L. Zhang^{15c}, L. Zhang^{60a}, M. Zhang¹⁷³, R. Zhang¹⁸¹, S. Zhang¹⁰⁶, X. Zhang^{60b}, Y. Zhang^{15a,15d}, Z. Zhang^{63a}, Z. Zhang⁶⁵, P. Zhao⁴⁹, Y. Zhao^{60b}, Z. Zhao^{60a}, A. Zhemchugov⁸⁰, Z. Zheng¹⁰⁶, D. Zhong¹⁷³, B. Zhou¹⁰⁶, C. Zhou¹⁸¹, M. S. Zhou^{15a,15d}, M. Zhou¹⁵⁵, N. Zhou^{60c}, Y. Zhou⁷, C. G. Zhu^{60b}, C. Zhu^{15a,15d}, H. L. Zhu^{60a}, H. Zhu^{15a}, J. Zhu¹⁰⁶, Y. Zhu^{60a}, X. Zhuang^{15a}, K. Zhukov¹¹¹, V. Zhulanov^{122a,122b}, D. Zieminska⁶⁶, N. I. Zimine⁸⁰, S. Zimmermann⁵², Z. Zinonos¹¹⁵, M. Ziolkowski¹⁵¹, L. Živković¹⁶, G. Zobernig¹⁸¹, A. Zoccoli^{23a,23b}, K. Zoch⁵³, T. G. Zorbas¹⁴⁹, R. Zou³⁷, L. Zwalinski³⁶

¹ Department of Physics, University of Adelaide, Adelaide, Australia

² Physics Department, SUNY Albany, Albany, NY, USA

³ Department of Physics, University of Alberta, Edmonton, AB, Canada

- ⁴ (a)Department of Physics, Ankara University, Ankara, Turkey; (b)Istanbul Aydin University, Istanbul, Turkey; (c)Division of Physics, TOBB University of Economics and Technology, Ankara, Turkey
- ⁵ LAPP, Université Grenoble Alpes, Université Savoie Mont Blanc, CNRS/IN2P3, Annecy, France
- ⁶ High Energy Physics Division, Argonne National Laboratory, Argonne, IL, USA
- ⁷ Department of Physics, University of Arizona, Tucson, AZ, USA
- ⁸ Department of Physics, University of Texas at Arlington, Arlington, TX, USA
- ⁹ Physics Department, National and Kapodistrian University of Athens, Athens, Greece
- ¹⁰ Physics Department, National Technical University of Athens, Zografou, Greece
- ¹¹ Department of Physics, University of Texas at Austin, Austin, TX, USA
- ¹² (a)Bahcesehir University, Faculty of Engineering and Natural Sciences, Istanbul, Turkey; (b)Istanbul Bilgi University, Faculty of Engineering and Natural Sciences, Istanbul, Turkey; (c)Department of Physics, Bogazici University, Istanbul, Turkey; (d)Department of Physics Engineering, Gaziantep University, Gaziantep, Turkey
- ¹³ Institute of Physics, Azerbaijan Academy of Sciences, Baku, Azerbaijan
- ¹⁴ Institut de Física d'Altes Energies (IFAE), Barcelona Institute of Science and Technology, Barcelona, Spain
- ¹⁵ (a)Institute of High Energy Physics, Chinese Academy of Sciences, Beijing, China; (b)Physics Department, Tsinghua University, Beijing, China; (c)Department of Physics, Nanjing University, Nanjing, China; (d)University of Chinese Academy of Science (UCAS), Beijing, China
- ¹⁶ Institute of Physics, University of Belgrade, Belgrade, Serbia
- ¹⁷ Department for Physics and Technology, University of Bergen, Bergen, Norway
- ¹⁸ Physics Division, Lawrence Berkeley National Laboratory and University of California, Berkeley, CA, USA
- ¹⁹ Institut für Physik, Humboldt Universität zu Berlin, Berlin, Germany
- ²⁰ Albert Einstein Center for Fundamental Physics and Laboratory for High Energy Physics, University of Bern, Bern, Switzerland
- ²¹ School of Physics and Astronomy, University of Birmingham, Birmingham, UK
- ²² Facultad de Ciencias y Centro de Investigaciones, Universidad Antonio Nariño, Bogota, Colombia
- ²³ (a)Dipartimento di Fisica, INFN Bologna and Università di Bologna, Fisica, Italy; (b)INFN Sezione di Bologna, Bologna, Italy
- ²⁴ Physikalisches Institut, Universität Bonn, Bonn, Germany
- ²⁵ Department of Physics, Boston University, Boston, MA, USA
- ²⁶ Department of Physics, Brandeis University, Waltham, MA, USA
- ²⁷ (a)Transilvania University of Brasov, Brasov, Romania; (b)Horia Hulubei National Institute of Physics and Nuclear Engineering, Bucharest, Romania; (c)Department of Physics, Alexandru Ioan Cuza University of Iasi, Iasi, Romania; (d)National Institute for Research and Development of Isotopic and Molecular Technologies, Physics Department, Cluj-Napoca, Romania; (e)University Politehnica Bucharest, Bucharest, Romania; (f)West University in Timisoara, Timisoara, Romania
- ²⁸ (a)Faculty of Mathematics, Physics and Informatics, Comenius University, Bratislava, Slovak Republic; (b)Department of Subnuclear Physics, Institute of Experimental Physics of the Slovak Academy of Sciences, Kosice, Slovak Republic
- ²⁹ Physics Department, Brookhaven National Laboratory, Upton, NY, USA
- ³⁰ Departamento de Física, Universidad de Buenos Aires, Buenos Aires, Argentina
- ³¹ California State University, CA, USA
- ³² Cavendish Laboratory, University of Cambridge, Cambridge, UK
- ³³ (a)Department of Physics, University of Cape Town, Cape Town, South Africa; (b)iThemba Labs, Western Cape, South Africa; (c)Department of Mechanical Engineering Science, University of Johannesburg, Johannesburg, South Africa; (d)University of South Africa, Department of Physics, Pretoria, South Africa; (e)School of Physics, University of the Witwatersrand, Johannesburg, South Africa
- ³⁴ Department of Physics, Carleton University, Ottawa, ON, Canada
- ³⁵ (a)Faculté des Sciences Ain Chock, Réseau Universitaire de Physique des Hautes Energies - Université Hassan II, Casablanca, Morocco; (b)Faculté des Sciences, Université Ibn-Tofail, Kénitra, Morocco; (c)Faculté des Sciences Semlalia, Université Cadi Ayyad, LPHEA-Marrakech, Morocco; (d)Faculté des Sciences, Université Mohamed Premier and LPTPM, Oujda, Morocco; (e)Faculté des sciences, Université Mohammed V, Rabat, Morocco
- ³⁶ CERN, Geneva, Switzerland
- ³⁷ Enrico Fermi Institute, University of Chicago, Chicago, IL, USA
- ³⁸ LPC, Université Clermont Auvergne, CNRS/IN2P3, Clermont-Ferrand, France

- ³⁹ Nevis Laboratory, Columbia University, Irvington, NY, USA
- ⁴⁰ Niels Bohr Institute, University of Copenhagen, Copenhagen, Denmark
- ⁴¹ (a)Dipartimento di Fisica, Università della Calabria, Rende, Italy; (b)INFN Gruppo Collegato di Cosenza, Laboratori Nazionali di Frascati, Italy
- ⁴² Physics Department, Southern Methodist University, Dallas, TX, USA
- ⁴³ Physics Department, University of Texas at Dallas, Richardson, TX, USA
- ⁴⁴ National Centre for Scientific Research “Demokritos”, Agia Paraskevi, Greece
- ⁴⁵ (a)Department of Physics, Stockholm University, Stockholm, Sweden; (b)Oskar Klein Centre, Stockholm, Sweden
- ⁴⁶ Deutsches Elektronen-Synchrotron DESY, Hamburg and Zeuthen, Germany
- ⁴⁷ Lehrstuhl für Experimentelle Physik IV, Technische Universität Dortmund, Dortmund, Germany
- ⁴⁸ Institut für Kern- und Teilchenphysik, Technische Universität Dresden, Dresden, Germany
- ⁴⁹ Department of Physics, Duke University, Durham, NC, USA
- ⁵⁰ SUPA - School of Physics and Astronomy, University of Edinburgh, Edinburgh, UK
- ⁵¹ INFN e Laboratori Nazionali di Frascati, Frascati, Italy
- ⁵² Physikalisches Institut, Albert-Ludwigs-Universität Freiburg, Freiburg, Germany
- ⁵³ II. Physikalisches Institut, Georg-August-Universität Göttingen, Göttingen, Germany
- ⁵⁴ Département de Physique Nucléaire et Corpusculaire, Université de Genève, Geneva, Switzerland
- ⁵⁵ (a)Dipartimento di Fisica, Università di Genova, Genova, Italy; (b)INFN Sezione di Genova, Genova, Italy
- ⁵⁶ II. Physikalisches Institut, Justus-Liebig-Universität Giessen, Giessen, Germany
- ⁵⁷ SUPA - School of Physics and Astronomy, University of Glasgow, Glasgow, UK
- ⁵⁸ LPSC, Université Grenoble Alpes, CNRS/IN2P3, Grenoble INP, Grenoble, France
- ⁵⁹ Laboratory for Particle Physics and Cosmology, Harvard University, Cambridge, MA, USA
- ⁶⁰ (a)Department of Modern Physics and State Key Laboratory of Particle Detection and Electronics, University of Science and Technology of China, Hefei, China; (b)Institute of Frontier and Interdisciplinary Science and Key Laboratory of Particle Physics and Particle Irradiation (MOE), Shandong University, Qingdao, China; (c)School of Physics and Astronomy, Shanghai Jiao Tong University, KLPPAC-MoE, SKLPPC, Shanghai, China; (d)Tsung-Dao Lee Institute, Shanghai, China
- ⁶¹ (a)Kirchhoff-Institut für Physik, Ruprecht-Karls-Universität Heidelberg, Heidelberg, Germany; (b)Physikalisches Institut, Ruprecht-Karls-Universität Heidelberg, Heidelberg, Germany
- ⁶² Faculty of Applied Information Science, Hiroshima Institute of Technology, Hiroshima, Japan
- ⁶³ (a)Department of Physics, Chinese University of Hong Kong, Shatin, N.T., Hong Kong, China; (b)Department of Physics, University of Hong Kong, Hong Kong, China; (c)Department of Physics and Institute for Advanced Study, Hong Kong University of Science and Technology, Clear Water Bay, Kowloon, Hong Kong, China
- ⁶⁴ Department of Physics, National Tsing Hua University, Hsinchu, Taiwan
- ⁶⁵ IJCLab, Université Paris-Saclay, CNRS/IN2P3, 91405 Orsay, France
- ⁶⁶ Department of Physics, Indiana University, Bloomington, IN, USA
- ⁶⁷ (a)INFN Gruppo Collegato di Udine, Sezione di Trieste, Udine, Italy; (b)ICTP, Trieste, Italy; (c)Dipartimento Politecnico di Ingegneria e Architettura, Università di Udine, Udine, Italy
- ⁶⁸ (a)INFN Sezione di Lecce, Lecce, Italy; (b)Dipartimento di Matematica e Fisica, Università del Salento, Lecce, Italy
- ⁶⁹ (a)INFN Sezione di Milano, Milan, Italy; (b)Dipartimento di Fisica, Università di Milano, Milan, Italy
- ⁷⁰ (a)INFN Sezione di Napoli, Naples, Italy; (b)Dipartimento di Fisica, Università di Napoli, Naples, Italy
- ⁷¹ (a)INFN Sezione di Pavia, Pavia, Italy; (b)Dipartimento di Fisica, Università di Pavia, Pavia, Italy
- ⁷² (a)INFN Sezione di Pisa, Pisa, Italy; (b)Dipartimento di Fisica E. Fermi, Università di Pisa, Pisa, Italy
- ⁷³ (a)INFN Sezione di Roma, Rome, Italy; (b)Dipartimento di Fisica, Sapienza Università di Roma, Rome, Italy
- ⁷⁴ (a)INFN Sezione di Roma Tor Vergata, Rome, Italy; (b)Dipartimento di Fisica, Università di Roma Tor Vergata, Rome, Italy
- ⁷⁵ (a)INFN Sezione di Roma Tre, Rome, Italy; (b)Dipartimento di Matematica e Fisica, Università Roma Tre, Rome, Italy
- ⁷⁶ (a)INFN-TIFPA, Rome, Italy; (b)Università degli Studi di Trento, Trento, Italy
- ⁷⁷ Institut für Astro- und Teilchenphysik, Leopold-Franzens-Universität, Innsbruck, Austria
- ⁷⁸ University of Iowa, Iowa City, IA, USA
- ⁷⁹ Department of Physics and Astronomy, Iowa State University, Ames, IA, USA
- ⁸⁰ Joint Institute for Nuclear Research, Dubna, Russia

- 81 (a) Departamento de Engenharia Elétrica, Universidade Federal de Juiz de Fora (UFJF), Juiz de Fora, Brazil
; (b) Universidade Federal do Rio De Janeiro COPPE/EE/IF, Rio de Janeiro, Brazil; (c) Universidade Federal de São João del Rei (UFSJ), São João del Rei, Brazil; (d) Instituto de Física, Universidade de São Paulo, São Paulo, Brazil
- 82 KEK, High Energy Accelerator Research Organization, Tsukuba, Japan
- 83 Graduate School of Science, Kobe University, Kobe, Japan
- 84 (a) AGH University of Science and Technology, Faculty of Physics and Applied Computer Science, Krakow, Poland
; (b) Marian Smoluchowski Institute of Physics, Jagiellonian University, Krakow, Poland
- 85 Institute of Nuclear Physics Polish Academy of Sciences, Krakow, Poland
- 86 Faculty of Science, Kyoto University, Kyoto, Japan
- 87 Kyoto University of Education, Kyoto, Japan
- 88 Research Center for Advanced Particle Physics and Department of Physics, Kyushu University, Fukuoka, Japan
- 89 Instituto de Física La Plata, Universidad Nacional de La Plata and CONICET, La Plata, Argentina
- 90 Physics Department, Lancaster University, Lancaster, UK
- 91 Oliver Lodge Laboratory, University of Liverpool, Liverpool, UK
- 92 Department of Experimental Particle Physics, Jožef Stefan Institute and Department of Physics, University of Ljubljana, Ljubljana, Slovenia
- 93 School of Physics and Astronomy, Queen Mary University of London, London, UK
- 94 Department of Physics, Royal Holloway University of London, Egham, UK
- 95 Department of Physics and Astronomy, University College London, London, UK
- 96 Louisiana Tech University, Ruston, LA, USA
- 97 Fysiska institutionen, Lunds universitet, Lund, Sweden
- 98 Centre de Calcul de l'Institut National de Physique Nucléaire et de Physique des Particules (IN2P3), Villeurbanne, France
- 99 Departamento de Física Teórica C-15 and CIAFF, Universidad Autónoma de Madrid, Madrid, Spain
- 100 Institut für Physik, Universität Mainz, Mainz, Germany
- 101 School of Physics and Astronomy, University of Manchester, Manchester, UK
- 102 CPPM, Aix-Marseille Université, CNRS/IN2P3, Marseille, France
- 103 Department of Physics, University of Massachusetts, Amherst, MA, USA
- 104 Department of Physics, McGill University, Montreal, QC, Canada
- 105 School of Physics, University of Melbourne, Victoria, Australia
- 106 Department of Physics, University of Michigan, Ann Arbor, MI, USA
- 107 Department of Physics and Astronomy, Michigan State University, East Lansing, MI, USA
- 108 B.I. Stepanov Institute of Physics, National Academy of Sciences of Belarus, Minsk, Belarus
- 109 Research Institute for Nuclear Problems of Byelorussian State University, Minsk, Belarus
- 110 Group of Particle Physics, University of Montreal, Montreal, QC, Canada
- 111 P.N. Lebedev Physical Institute of the Russian Academy of Sciences, Moscow, Russia
- 112 National Research Nuclear University MEPhI, Moscow, Russia
- 113 D.V. Skobeltsyn Institute of Nuclear Physics, M.V. Lomonosov Moscow State University, Moscow, Russia
- 114 Fakultät für Physik, Ludwig-Maximilians-Universität München, Munich, Germany
- 115 Max-Planck-Institut für Physik (Werner-Heisenberg-Institut), Munich, Germany
- 116 Nagasaki Institute of Applied Science, Nagasaki, Japan
- 117 Graduate School of Science and Kobayashi-Maskawa Institute, Nagoya University, Nagoya, Japan
- 118 Department of Physics and Astronomy, University of New Mexico, Albuquerque, NM, USA
- 119 Institute for Mathematics, Astrophysics and Particle Physics, Radboud University Nijmegen/Nikhef, Nijmegen, The Netherlands
- 120 Nikhef National Institute for Subatomic Physics and University of Amsterdam, Amsterdam, The Netherlands
- 121 Department of Physics, Northern Illinois University, DeKalb, IL, USA
- 122 (a) Budker Institute of Nuclear Physics and NSU, SB RAS, Novosibirsk, Russia; (b) Novosibirsk State University Novosibirsk, Novosibirsk, Russia
- 123 Institute for High Energy Physics of the National Research Centre Kurchatov Institute, Protvino, Russia
- 124 Institute for Theoretical and Experimental Physics named by A.I. Alikhanov of National Research Centre "Kurchatov Institute", Moscow, Russia
- 125 Department of Physics, New York University, New York, NY, USA

- 126 Ochanomizu University, Otsuka, Bunkyo-ku, Tokyo, Japan
- 127 Ohio State University, Columbus, OH, USA
- 128 Faculty of Science, Okayama University, Okayama, Japan
- 129 Homer L. Dodge Department of Physics and Astronomy, University of Oklahoma, Norman, OK, USA
- 130 Department of Physics, Oklahoma State University, Stillwater, OK, USA
- 131 Palacký University, RCPTM, Joint Laboratory of Optics, Olomouc, Czech Republic
- 132 Center for High Energy Physics, University of Oregon, Eugene, OR, USA
- 133 Graduate School of Science, Osaka University, Osaka, Japan
- 134 Department of Physics, University of Oslo, Oslo, Norway
- 135 Department of Physics, Oxford University, Oxford, UK
- 136 LPNHE, Sorbonne Université, Université de Paris, CNRS/IN2P3, Paris, France
- 137 Department of Physics, University of Pennsylvania, Philadelphia, PA, USA
- 138 Konstantinov Nuclear Physics Institute of National Research Centre “Kurchatov Institute”, PNPI, St. Petersburg, Russia
- 139 Department of Physics and Astronomy, University of Pittsburgh, Pittsburgh, PA, USA
- 140 (a) Laboratório de Instrumentação e Física Experimental de Partículas - LIP, Lisbon, Portugal; (b) Departamento de Física, Faculdade de Ciências, Universidade de Lisboa, Lisbon, Portugal; (c) Departamento de Física, Universidade de Coimbra, Coimbra, Portugal; (d) Centro de Física Nuclear da Universidade de Lisboa, Lisboa, Portugal; (e) Departamento de Física, Universidade do Minho, Braga, Portugal; (f) Departamento de Física Teórica y del Cosmos, Universidad de Granada, Granada (Spain), Portugal; (g) Dep Física and CEFITEC of Faculdade de Ciências e Tecnologia, Universidade Nova de Lisboa, Caparica, Portugal; (h) Instituto Superior Técnico, Universidade de Lisboa, Lisboa, Portugal
- 141 Institute of Physics of the Czech Academy of Sciences, Prague, Czech Republic
- 142 Czech Technical University in Prague, Prague, Czech Republic
- 143 Charles University, Faculty of Mathematics and Physics, Prague, Czech Republic
- 144 Particle Physics Department, Rutherford Appleton Laboratory, Didcot, UK
- 145 IRFU, CEA, Université Paris-Saclay, Gif-sur-Yvette, France
- 146 Santa Cruz Institute for Particle Physics, University of California Santa Cruz, Santa Cruz, CA, USA
- 147 (a) Departamento de Física, Pontificia Universidad Católica de Chile, Santiago, Chile; (b) Universidad Andres Bello, Department of Physics, Santiago, Chile; (c) Departamento de Física, Universidad Técnica Federico Santa María, Valparaíso, Chile
- 148 Department of Physics, University of Washington, Seattle, WA, USA
- 149 Department of Physics and Astronomy, University of Sheffield, Sheffield, UK
- 150 Department of Physics, Shinshu University, Nagano, Japan
- 151 Department Physik, Universität Siegen, Siegen, Germany
- 152 Department of Physics, Simon Fraser University, Burnaby, BC, Canada
- 153 SLAC National Accelerator Laboratory, Stanford, CA, USA
- 154 Physics Department, Royal Institute of Technology, Stockholm, Sweden
- 155 Departments of Physics and Astronomy, Stony Brook University, Stony Brook, NY, USA
- 156 Department of Physics and Astronomy, University of Sussex, Brighton, UK
- 157 School of Physics, University of Sydney, Sydney, Australia
- 158 Institute of Physics, Academia Sinica, Taipei, Taiwan
- 159 (a) E. Andronikashvili Institute of Physics, Iv. Javakhishvili Tbilisi State University, Tbilisi, Georgia; (b) High Energy Physics Institute, Tbilisi State University, Tbilisi, Georgia
- 160 Department of Physics, Technion, Israel Institute of Technology, Haifa, Israel
- 161 Raymond and Beverly Sackler School of Physics and Astronomy, Tel Aviv University, Tel Aviv, Israel
- 162 Department of Physics, Aristotle University of Thessaloniki, Thessaloniki, Greece
- 163 International Center for Elementary Particle Physics and Department of Physics, University of Tokyo, Tokyo, Japan
- 164 Graduate School of Science and Technology, Tokyo Metropolitan University, Tokyo, Japan
- 165 Department of Physics, Tokyo Institute of Technology, Tokyo, Japan
- 166 Tomsk State University, Tomsk, Russia
- 167 Department of Physics, University of Toronto, Toronto, ON, Canada
- 168 (a) TRIUMF, Vancouver, BC, Canada; (b) Department of Physics and Astronomy, York University, Toronto, ON, Canada
- 169 Division of Physics and Tomonaga Center for the History of the Universe, Faculty of Pure and Applied Sciences, University of Tsukuba, Tsukuba, Japan

- ¹⁷⁰ Department of Physics and Astronomy, Tufts University, Medford, MA, USA
 - ¹⁷¹ Department of Physics and Astronomy, University of California Irvine, Irvine, CA, USA
 - ¹⁷² Department of Physics and Astronomy, University of Uppsala, Uppsala, Sweden
 - ¹⁷³ Department of Physics, University of Illinois, Urbana, IL, USA
 - ¹⁷⁴ Instituto de Física Corpuscular (IFIC), Centro Mixto Universidad de Valencia - CSIC, Valencia, Spain
 - ¹⁷⁵ Department of Physics, University of British Columbia, Vancouver, BC, Canada
 - ¹⁷⁶ Department of Physics and Astronomy, University of Victoria, Victoria, BC, Canada
 - ¹⁷⁷ Fakultät für Physik und Astronomie, Julius-Maximilians-Universität Würzburg, Würzburg, Germany
 - ¹⁷⁸ Department of Physics, University of Warwick, Coventry, UK
 - ¹⁷⁹ Waseda University, Tokyo, Japan
 - ¹⁸⁰ Department of Particle Physics, Weizmann Institute of Science, Rehovot, Israel
 - ¹⁸¹ Department of Physics, University of Wisconsin, Madison, WI, USA
 - ¹⁸² Fakultät für Mathematik und Naturwissenschaften, Fachgruppe Physik, Bergische Universität Wuppertal, Wuppertal, Germany
 - ¹⁸³ Department of Physics, Yale University, New Haven, CT, USA
- ^a Also at Borough of Manhattan Community College, City University of New York, New York NY, USA
 - ^b Also at CERN, Geneva, Switzerland
 - ^c Also at CPPM, Aix-Marseille Université, CNRS/IN2P3, Marseille, France
 - ^d Also at Département de Physique Nucléaire et Corpusculaire, Université de Genève, Genève, Switzerland
 - ^e Also at Departament de Física de la Universitat Autònoma de Barcelona, Barcelona, Spain
 - ^f Also at Department of Applied Physics and Astronomy, University of Sharjah, Sharjah, United Arab Emirates
 - ^g Also at Department of Financial and Management Engineering, University of the Aegean, Chios, Greece
 - ^h Also at Department of Physics and Astronomy, Michigan State University, East Lansing MI, USA
 - ⁱ Also at Department of Physics and Astronomy, University of Louisville, Louisville, KY, USA
 - ^j Also at Department of Physics, Ben Gurion University of the Negev, Beer Sheva, Israel
 - ^k Also at Department of Physics, California State University, East Bay, USA
 - ^l Also at Department of Physics, California State University, Fresno, USA
 - ^m Also at Department of Physics, California State University, Sacramento, USA
 - ⁿ Also at Department of Physics, King's College London, London, UK
 - ^o Also at Department of Physics, St. Petersburg State Polytechnical University, St. Petersburg, Russia
 - ^p Also at Department of Physics, Stanford University, Stanford CA, USA
 - ^q Also at Department of Physics, University of Adelaide, Adelaide, Australia
 - ^r Also at Department of Physics, University of Fribourg, Fribourg, Switzerland
 - ^s Also at Department of Physics, University of Michigan, Ann Arbor MI, USA
 - ^t Also at Dipartimento di Matematica, Informatica e Fisica, Università di Udine, Udine, Italy
 - ^u Also at Faculty of Physics, M.V. Lomonosov Moscow State University, Moscow, Russia
 - ^v Also at Giresun University, Faculty of Engineering, Giresun, Turkey
 - ^w Also at Graduate School of Science, Osaka University, Osaka, Japan
 - ^x Also at Hellenic Open University, Patras, Greece
 - ^y Also at IJCLab, Université Paris-Saclay, CNRS/IN2P3, 91405, Orsay, France
 - ^z Also at Institutio Catalana de Recerca i Estudis Avancats, ICREA, Barcelona, Spain
 - ^{aa} Also at Institut für Experimentalphysik, Universität Hamburg, Hamburg, Germany
 - ^{ab} Also at Institute for Mathematics, Astrophysics and Particle Physics, Radboud University Nijmegen/Nikhef, Nijmegen, Netherlands
 - ^{ac} Also at Institute for Nuclear Research and Nuclear Energy (INRNE) of the Bulgarian Academy of Sciences, Sofia, Bulgaria
 - ^{ad} Also at Institute for Particle and Nuclear Physics, Wigner Research Centre for Physics, Budapest, Hungary
 - ^{ae} Also at Institute of Particle Physics (IPP), Vancouver, Canada
 - ^{af} Also at Institute of Physics, Azerbaijan Academy of Sciences, Baku, Azerbaijan
 - ^{ag} Also at Instituto de Física Teórica, IFT-UAM/CSIC, Madrid, Spain
 - ^{ah} Also at Joint Institute for Nuclear Research, Dubna, Russia
 - ^{ai} Also at Louisiana Tech University, Ruston LA, USA

^{aj} Also at Manhattan College, New York NY, USA

^{ak} Also at Moscow Institute of Physics and Technology State University, Dolgoprudny, Russia

^{al} Also at National Research Nuclear University MEPhI, Moscow, Russia

^{am} Also at Physics Department, An-Najah National University, Nablus, Palestine

^{an} Also at Physics Dept, University of South Africa, Pretoria, South Africa

^{ao} Also at Physikalisches Institut, Albert-Ludwigs-Universität Freiburg, Freiburg, Germany

^{ap} Also at The City College of New York, New York NY, USA

^{aq} Also at Tomsk State University, Tomsk, and Moscow Institute of Physics and Technology State University, Dolgoprudny, Russia

^{ar} Also at TRIUMF, Vancouver BC, Canada

^{as} Also at Università di Napoli Parthenope, Napoli, Italy

*Deceased